A New View of Particle Physics with Gravity and Accelerating Expansion as Emergent Properties of Quantum Mechanics and Massive Spin 2 Gravitons as Dark Matter giving Galaxies their MOND-like behaviour

Julian Williams.   <jjawilliams@xtra.co.nz>

Abstract

This paper explores ideas for new physics at both quantum and cosmological levels. It begins with proposals for building the fundamental particles from infinite superpositions that fit the SM, apart from infinitesimal differences, with possibly profound consequences including the possibility of both massive and infinitesimal mass spin 2 gravitons. All fundamental particles have at least an infinitesimal mass always proportional to the inverse horizon radius times the the Hubble flow velocity. The symmetry breaking of the SM remains essentially valid because, with masses almost zero and nearly light velocity, helicity is virtually fixed. Cosmic wavelength (k_{min}) gravitons vastly outnumber all other particles and the invariant action they require comes from the expansion of space inside the horizon. When mass is distributed evenly as dust, gravitons have uniform spatial density. To maintain k_{min} action density invariance, the metric changes around mass concentrations in agreement with Einstein's equations, apart from infinitesimal differences at small cosmic radii, becoming very significant at large radii. Over large regions of space this difference makes the values of the Einstein tensor components in the Freidman equations average zero. Space is always flat, and Quantum Mechanics (QM) controls the expansion of space regardless of Omega, with or without inflation. The scale factors in the radiation era, and the start of the matter era, are similar to Lambda-CDM cosmology. Massive spin 2 gravitons have galactic radii Compton wavelengths and spherically symmetric wavefunctions with inverse radius squared mass density, just as the proposed dark matter properties that give galaxies their observed behaviour. The rate at which massive gravitons form inside the cosmic horizon is related to the clustering of matter into galaxies and controls both the scale factor and accelerating space expansion.

Contents

1 Introduction

Th**e** current formulation of the Standard Model (SM) of particle physics was finalised in the mid-1970s. However, although extremely successful in providing testable experimental predictions and currently the best description we have of the subatomic world, the theory still leaves a significant number of phenomena unexplained. In the last forty years or so there have been a number of theories seeking to move physics beyond the SM, including supersymmetry and string theory. However, none of the particles predicted by supersymmetry have yet been found, despite a decade of work at CERN's Large Hadron Collider (LHC), and string theory, widely considered the most likely path for including gravity in the SM, is not yet supported by any direct empirical evidence. Further, dark matter has yet to be directly detected, and dark energy remains elusive. In contrast to these disappointments however, the ATLAS and CMS experiments at CERN's LHC announced in 2012 that they had each observed a new particle in the mass region around 126 GeV; a particle consistent with the Higgs boson predicted by the SM.

String theory has been strongly criticised over its inability to make testable predictions [1-6]. However, along with the multiverse theory, it has generated intense and important debate over the scientific standing of non-testable theories in physics. In 2009 Dawid, a theoretical physicist turned philosopher, noted substantial conflict between supporters and critics of string theory in assessing its status and success [7]. Dawid argued that this disagreement could best be understood in terms of a paradigmatic rift between the two sides over their understandings of theory assessment. Critics on the one hand believed that "it is a core principle that scientific theories must face continuous *empirical testing* [emphasis added] to avoid going astray" (p988). In contrast, supporters of string theory placed importance on *theoretical criteria* for theory assessment. In an interview several years later Dawid [8] suggested this emergence of non-empirical theory assessment, or post-empirical science, represented a Kuhnian paradigm shift in physics and that it would become increasingly important due to the difficulties associated with experimentally testing new theories. In *Nature*, Ellis and Silk in 2014 [9] made an appeal to "Defend the integrity of physics." They expressed concern that when faced with the difficulties of applying fundamental theories to the observed universe, some researchers had begun explicitly advocating a change to how theories should be assessed, viz., if deemed sufficiently elegant and explanatory, experimental testing was unnecessary. Ellis and Silk disagreed, insisting that empirical testability is a necessary condition for a theory to be considered scientific, and concurred with Hossenfelder [10] that the concept of post-empirical science was an oxymoron.

Another important issue relating to the testability of theories in physics has been highlighted recently by the astrophysicist David Merritt [11]. In regard to the lambda cold dark matter model (ΛCDM), which contains Einstein's theory of gravity, Merritt notes that dark matter, dark energy and inflation were all added to the theory in response to observations that would falsify it, i.e. they are ad hoc, or auxiliary hypotheses. Further, he argues that they are conventionalist hypotheses in that they add no empirical content and hence are unfalsifiable in the sense defined by the philosopher Karl Popper. Popper had set specific criteria for preserving falsifiability (or testability) when such "conventionalist stratagems" are employed,

i.e., the modified theory had to make some new, testable predictions, and at least some of the new predictions should be verified. Further, Popper's student Imre Lakatos, tested and refined these criteria to distinguish between "progressive" and "degenerating" research programs. A progressive research program is one in which "its theoretical growth anticipates its empirical growth, that is, as long as it keeps predicting novel facts with some success." The ΛCDM, according to Merritt, fails to meet such requirements as the auxiliary hypotheses (dark matter, dark energy and inflation) have yet to be confirmed, and the ΛCDM is notably lacking in successful predictions. Steinhardt [12] one of the founders of inflationary cosmology, now also views that theory untestable and has become one of its sharpest critics. The failure to progress significantly beyond the SM during the past four decades, the increasing prominence of highly theoretical, mathematically elegant but difficult to test or untestable theories, and threats to undermine testability as a sine qua non for a theory to be considered scientific, all appear responsible for a succession of popular books expressing concern at the current state of physics [1-5]. In her recently published *Lost in Math: How Beauty Leads Physics Astray,* Hossenfelder [3] contends that the search for beauty has led physicists astray, giving wonderful mathematics but bad science; belief that the best theories are beautiful, natural and elegant has resulted in theories that are untestable. Lamenting the lack of a major breakthrough in the foundations of physics during the last forty years, she advocates physicists need to rethink their methods. In reviewing her book Wilczec [13] contends that Hossenfelder presents an overly pessimistic view, but concedes that "the malaise expressed...is not baseless and is widely shared among physicists" (p57).

In view of these concerns over the current state of physics we offer an alternative approach, but one which still uses very simple basic principles of quantum mechanics (QM) and special relativity (SR). Apart from infinitesimal differences it is (almost) consistent with the SM. It suggests the possibility of massive spin 2 gravitons emitted by baryons, with galactic radii Compton wavelength spherically symmetric wavefunctions, causing similar effects in the metric as dark matter. It proposes that the acompanying massive gravitons control both the scale factor and cosmic acceleration.

We contend our theory is both simple and capable of making testable predictions; at the cosmological level, if not the quantum level. It is, however, radical in its proposals and implications. Consequently, it will require a significant shift in thinking, not only in regard to the fundamental particles, but also the evolution of the cosmos. Such a shift, however, may facilitate progress beyond the SM and/or the ΛCDM.

Because these proposed ideas are so radical, we start with some preliminary explanatory notes. Part 1 of the paper follows and includes the forming of fundamental particles from infinite superpositions (section 2), their properties (section 3), and high energy superposition cutoffs (section 4). Part 2 looks at the cosmological consequences of these infinite superpositions. We end with a discussion about the overall implications of this paper, particularly the possibility of massive virtual gravitons forming galaxy halos consistent with the counter intuitive behaviour of QM, and the slightly different way of looking at the warping of spacetime which could lead to a QM expansion model as an alternative to the ΛCDM.

1.1 List of Some Abbreviations, Acronyms and Symbols Used in the Text

ΛCDM The Lambda Cold Dark Matter Model of Cosmology.
CMB   Cosmic Microwave Background.
EM   Electromagnetic.
FLRW   Friedmann-Lemaitre-Robertson-Walker metrics.
GR   General Relativity.
ICM   Intracluster Medium.
MOND   Modified Newtonian Dynamics.
SM   Standard Model.
SR   Special Relativity.
QCD   Quantum Chromodynamics
QED   Quantum Electrodynamics
QM   Quantum Mechanics.

N, n & s. Integers $n = 3, 4, 5, 6$ & 7 are used in $\psi_{nk} = C_{nk} r^3 \exp(-n^2 k^2 r^2 / 18) Y(\theta, \varphi)$ virtual primary $(l = 3)$ wavefunctions at wavenumber k. Their probability is $\left[\dfrac{sN \cdot dk}{k} \right]$, where s is spin, and $N = 1$ for all massive $s = 1/2$ fermions, as well as $s = 1$ and $s = 2$ massive bosons.

$N = 2$ for all spin 1 and spin 2 infinitesimal mass bosons.

χ_C is the primary to secondary coupling ratio $= \alpha_3^{-1}$ at the Planck energy superposition cutoff.

$k_{\min}$ is the wavenumber of the maximum cosmic wavelength but cuts off exponentially.

R_{OH} is the observable horizon radius.

$\Upsilon = k_{\min} R_{OH}$ radians.

$\rho_{Gk\min}$ is the normal three dimensional density of $k_{\min}$ gravitons

$K_{Gk\min}$ is the $k_{\min}$ graviton invariant as in $\rho_{Gk\min} = K_{Gk\min} dk_{\min}$ where $K_{Gk\min} \approx 0.458 \alpha_G$.

$\lambda_{k\min}$ The maximum or $k_{\min}$ wavelength.

m_G is the symbol used for massive gravitons.

α_{MG} is the coupling constant between Planck masses for massive gravitons.

$\alpha_G \approx 0.004$ is the graviton coupling constant between Planck masses used in our models.

α with no subscript is the usual electromagnetic coupling constant.

ρ_U is the average density of both baryonic and massive graviton mass/energy in the universe.

$T'_{\mu\upsilon}$ is the infinitesimally modified Einstein tensor where $T'_{\mu\upsilon} = T_{\mu\upsilon}(\text{Local}) - T_{\mu\upsilon}(\text{Cosmos})$.

$T_{\mu\upsilon}(\text{Cosmos})$ is the Einstein tensor averaged over the whole universe.

$\Omega = 1$ in the ΛCDM at critical density for flatness.

1.2 Preliminary Explanatory Notes

1.2.1 Summary flow chart

This paper starts with the assumption that all "fundamental particles" are built from combinations of "virtual preons". There are three preons, coloured red, green and blue, and their antiparticles. All preons are *spin zero* and electrically charged.

Different groups of 8 preons (with no weak charge) couple to the electromagnetic and 8 colour ground state fields, forming $l = 3$ spatially dependant wave functions. Infinite superpositions of these wave functions form all the spin ½ & spin 1 standard model particles, as well as spin 2 gravitons. The frequencies of these wavefunctions start at $k_{min} \approx (\text{Horizon radius})^{-1} \longrightarrow$ up to Planck scale maximum.

Cosmic wavelength zero point densities are very limited. Because spin zero preons are born with zero momentum and infinite wavelength they can couple to modes anywhere inside the extra space generated by the expanding Hubble flow horizon.

High frequency coupling is to local ground state fields where the available densities are plentiful.

Low frequency coupling controls the average universe density $\rho_U \propto \dfrac{1}{R_{OH}^2 V'}$ in Planck units, where R_{OH} is the observable horizon radius, V' is the Hubble flow velocity.

When mass is distributed evenly as a dust there is a uniform density of k_{min} gravitons throughout a horizon radius sphere, space and spacetime is flat everywhere. If any of this mass is moved to a central location it increases the spatial density of k_{min} gravitons surrounding it, distorting spacetime locally, and restoring density in agreement with Einstein's equations, but with infinitesimal differences effective at cosmic radii: $G_{\mu\nu} = R_{\mu\nu} - \dfrac{1}{2} g_{\mu\nu} R = \dfrac{8\pi G}{c^4}\left[T_{\mu\nu}(\text{Local}) - T_{\mu\nu}(\text{Cosmos}) \right] = \dfrac{8\pi G}{c^4} T'_{\mu\nu}.$ In large regions of space the average values of $T'_{\mu\nu} \equiv 0 \equiv G_{\mu\nu}$. Space is flat and the Freidman equation components average zero. QM controls the expansion of space regardless of Ω. with or without inflation. Writing the scale factor as $a(t) \propto t^p$; in the radiation era $p = 1/2$, the horizon velocity $V = 2$; the matter era starts at $p = 2/3$ and $V = 3$, all as in current cosmology when $\Omega = 1$.

Massive spin 2 gravitons are emitted by baryons with a mass that is always $\approx 10^6$ times the mass of infinitesimal mass gravitons and always proportional to the inverse horizon radius. They currently have galactic radii Compton wavelengths and spherically symmetric wavefunctions mimicking dark matter $\rho \propto r^{-2}$ radial density behaviour. They give galaxies their observed MOND-like behaviour, and control both the scale factor and acceleration of spatial expansion. The domain in which GR is true, is retricted to the spatial location in which it is applied.

1.2.2 General relativity as an initial guide

GR informs us that all forms of mass, energy and pressure are sources of the gravitational field. Thus to create gravitational fields, all spin ½ leptons & quarks, spin 1 gluons, photons, $W^{\pm} \& Z^0$ particles etc. emit virtual gravitons, except possibly gravitons themselves (section 6.2.6), as gravitational energy is not part of the Einstein tensor.

The starting point of this paper assumes there is a common thread uniting these fundamental particles making this possible. Equations are developed that unite the amplitudes of the colour and electromagnetic coupling constants with that of gravity. The precision required by quantum mechanics for half integral and integral angular momentum allows gravity to be included, despite the vast disparity in magnitude between gravity and the other two. This combination of colour, electromagnetic and gravitational amplitudes in the same equation is possible because of a radically different approach taken in this paper: an approach using infinite superpositions of positive and negative integral $\hbar$ angular momentum virtual wavefunctions for spin ½, spin 1 and spin 2 particles. The result is almost identical to the SM, with infinitesimal but important differences. The total angular momentum can be summed over all wavenumbers k; from $k = 0$ to some cutoff value k_{cutoff}. We will assume (as with many unification theories) that the cutoff for these infinite superpositions is somewhere near Planck scale. Firstly, imagine a universe where the gravitational constant $G \to 0$. As $G \to 0$, the Planck length $L_P \to 0$, the Planck energy $E_P \to \infty$ and $k_{cutoff} \to \infty$ also. If we sum the angular momentum of these infinite superpositions when $G \to 0$ (i.e. from $k = 0$ to $k_{cutoff} \to \infty$) we get precisely half integral or integral $\hbar$ for the fundamental spin ½, spin 1 & spin 2 particles in appropriate m states. If we now put $G > 0$ the infinitesimal effect of including gravity can be balanced by an equal but opposite effect due to the non-infinite cutoff value in k. A near Planck scale superposition cutoff requires gravity to be included to get precisely half integral or integral $\hbar$. (Section 4.2)

These infinite superpositions have another very relevant property relating to the fact that all experiments indicate that fundamental particles such as electrons can behave as point particles. Each wavefunction with wavenumber k, which we label as ψ_k, has a maximum radial probability at $r \approx 1/k$ and they all look the same (Figure 1.1.1). Every wavefunction ψ_k of these infinite superpositions, interacts only with virtual photons (for example) of the same k; if superpositions representing say an electron are probed with such photons (that interact only with wavefunction ψ_k) the resolution possible is of the same order as the dimensions of ψ_k, both have $r \approx 1/k$. The higher the energy of the probing particle the smaller the ψ_k it interacts with; the resolution of an observing photon can never be fine enough to see any ψ_k dimensions. Even if this energy approaches the Planck value, with a matching ψ_k radius near the Planck length it is still not possible to resolve it. This behaviour is consistent with the quantum mechanical properties of point particles.

$\dfrac{4\pi}{k}R*R \uparrow$

$kr \rightarrow$
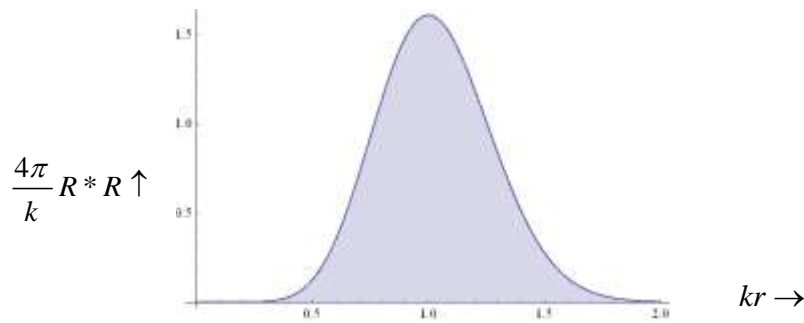
Figure 1.1.1 Radial probability of the dominant $n = 6$ mode of a spin ½ wavefunction ψ_{6k}.

1.2.3 Primary and secondary interactions

Supposing that superpositions can in fact build the fundamental spin ½, spin 1, and spin 2 particles, then what builds the superpositions? Answering that question requires dividing all interactions into two categories: primary and secondary.

Secondary interactions are those we are familiar with, and are covered by the SM; but with the addition of gravity, which is not included in the SM. They take place between the fundamental spin ½, spin 1 and spin 2 particles formed from infinite superpositions. They are the quantum electrodynamics/quantum chromodynamics (QED)/(QCD) etc, interactions of all real world experiments.

Primary interactions we conjecture on the other hand, are those that build virtual infinite superpositions. The base states of virtual infinite superpositions only last for time $\Delta T \leq \hbar / 2\Delta E$, and the primary interactions that build them are completely hidden to the real world of experiments. Infinite superpositions cannot be decomposed into their base states, in the same way as base states of fundamental particles can be observed. The quantum world is always hidden until observation, even if we know base state probabilities. But virtual infinite superpositions are always hidden, and only fundamental particles can be observed.

Primary interactions are extremely simple. They are only one way; zero-point fields act on the particle, but the particle cannot act on, or influence, zero point fields. (Its invariance is guaranteed by Heisenberg's uncertainty principle.) In contrast, secondary interactions involve all the excited modes above the ground state and are two way. These excited field modes both act on the particle which in turn acts back on the field. Quantum field theory (QFT) is all about these complicated two way interactions. Lagrangians are ideal for these two way interactions, predicting symmetries and conservations. However, Lagrangians are less relevant in primary interactions: the natural invariance of the ground state carries through into symmetries and conservation laws. In view of this, our proposals depart from the current practice of basing new theories on Lagrangians. In this regard, while acknowledging their enormous predictive power, Penrose [6] expresses unease with this modern trend, arguing against relying too strongly on Lagrangians in searches for improved fundamental theories (p 491). History tells us progress can be inhibited by assuming that what has worked so well up to now must always be so. Newton reigned supreme for almost two centuries until superseded by Einstein.

The first half of this paper is about these primary interactions, and the superpositions they build representing the fundamental spin ½, spin 1 and spin 2 particles. Primary interactions are between spin zero particles borrowed from a Higgs type scalar field, and the zero-point vector fields. In the 1970's models were proposed with preons as common building blocks of leptons and quarks [14-17]. In contrast with the virtual particles in this paper, some of these earlier models used real spin ½ building blocks. However, real substructure has difficulties with large masses if compressed into the small volumes required to approach point particle behaviour. It was probably because of this high mass/small volume problem that these earlier preon proposals fell out of favour. On the other hand our proposed virtual substructure borrows energy from zero point fields where the mass contribution at high k values can be cancelled (section 3.2.1). As in earlier models this paper also calls the common building blocks preons, but here the preons are both virtual and spin zero. They also now build all spin ½ leptons and quarks, spin 1 gluons, photons, W & Z particles, plus spin 2 gravitons, in contrast to only the leptons and quarks in the earlier models. (SeeTable 2.2.1) As these preons have zero spin they possess no weak charge. Primary interactions (section 2.2.1) can take place only with the zero point colour, electromagnetic and gravitational fields. The three primary coupling constants for each of these three zero-point fields are different from, but related to, secondary coupling constants.

The behaviour of primary coupling is also entirely different from secondary coupling. Secondary coupling strengths vary (or run) with wavenumber k (the electromagnetic increasing with k and colour decreasing with k). In contrast, we conjecture primary coupling strengths (or constants) do not run. In this paper virtual preons are continually born with mass out of a Higgs type scalar field, existing only for time $\Delta t \leq \hbar / 2E$. At their birth, they interact while still bare with zero point vector fields; at this instant of birth $t = 0$. The primary coupling constants consequently are fixed for all k; there is no time for charge cancelling or reinforcing, which in secondary interactions forms around the bare charge progressively after its birth. The equations work only if this is true, and they also work only if the primary colour coupling constant is one. (Sections 2.2.2). The ratio between the primary and secondary colour coupling constants labelled χ_C is thus (if primary colour coupling is one) the inverse of the secondary (or usual α_3^{-1} of QCD) colour coupling constant at the superposition cutoff at Planck Energy. (Sections 3.3 & 4.2.2) To enable the primary coupling to colour, electromagnetic and gravitational zero point fields, preons need colour, electric charge and mass. There are three preons, red, green & blue with positive electric charge, and their three anticounterparts. Their mass borrowed from some type of scalar Higg's field, or the time component of zero-point fields must always be non-zero. This is discussed further in section 1.2.4. As there are eight gluon fields, superpositions are built with eight virtual preons for each virtual wavefunction ψ_k. The nett sum of these eight electric charges is $0, \pm 2, \pm 4, \pm 6$, and never $> \pm 6$. This leads to the usual $0, \pm 1/3, \pm 2/3, \pm 1$ electric charge seen in the real world. Various combinations of these eight preons in appropriate superpositions can build leptons and quarks, colour changing and neutral gluons, neutral photons, neutral massive Z^0 photons and the charged massive $W^{\pm}$ photons. (Table 2.2.1)

11

1.2.4 Photons, gluons and gravitons with infinitesimal mass ($\approx 10^{-34} eV$).

Einstein taught us that regardless of how fast a particle with mass moves, a ray of light always passes it at the same velocity c. The SM builds on this principle with one group of particles travelling at less than c, and another group at c: massive and massless, with a clear division between them. In the SM the neutrino family was included in the massless group.

However, towards the end of last century evidence slowly emerged that this was not true, and the family of three neutrinos must have masses somewhere in the electron volt range. There is no explanation for this in the SM.

Due to their very low mass, and normal emitted energies, neutrinos invariably travel at virtually the velocity of light c. Photons also have always been included in the massless group traveling precisely at velocity c, except in the case of the massive $W^{\pm} \& Z^0$. Massless virtual photons have an infinite range, which has always been seen as an absolute requirement of the electromagnetic field. On the other hand, this paper requires some rest frame (even if this frame can move at virtually c) in which to build all the fundamental particles. Table 6.2.1 suggests photons, gluons and gravitons have $\approx 10^{-34} eV$ mass with a range of approximately the inverse of the causally connected horizon radius, and velocities sufficiently close to that of light their helicity remains essentially fixed. This allows some form of Higgs mechanism to increase this infinitesimal mass to the various values in the massive set. (These infinitesimal masses are also in line with some recent proposals [18,19] where gravitons have a mass of $< 10^{-33} eV$ to explain accelerating expansion.)

The virtual wavefunction we use is $\psi_{nk} = C_{nk} r^3 \exp(-n^2 k^2 r^2 / 18) Y(\theta, \varphi)$, an $l = 3$ wavefunction. This virtual $l = 3$ property is normally hidden. In the same way as scattering experiments on spin 0 pions show spin 0 properties, and not the properties of the two cancelling spin ½ component particles, this $l = 3$ property of the virtual components of superpositions is not visible in the real world. Scattering experiments can exhibit only the spin properties of the resulting particle. The individual angular momentum vectors $|\mathbf{L}| = 2\sqrt{3}\hbar$ of the infinite superposition all sum to a resulting: $|\mathbf{L}_{Total}| = (\sqrt{3}/2)\hbar$, $\sqrt{2}\hbar$ or $\sqrt{6}\hbar$ for spin ½, spin 1 or spin 2 respectively, in a similar way to two spin ½ particles forming spin 0 or spin 1 states. We also use the fact that the angle to the z axis of the angular momentum vector for $s = 1/2, m = \pm 1/2$ is identical to $l = 3, m = \pm 2$.

The wavefunction $\psi_{nk} = C_{nk} r^3 \exp(-n^2 k^2 r^2 / 18) Y(\theta, \varphi)$ has eigenvalues $\mathbf{P}_{nk}^2 = n^2 \hbar^2 k^2$ with $|\mathbf{P}_{nk}| = n\hbar k$, suggesting it borrows n parallel $|\hbar \mathbf{k}|$ quanta from zero point vector fields provided n is integral. We can see this by letting $k \to \infty$ allowing energy $E \to n\hbar\omega$ by absorbing n quanta $\hbar\omega$ from the zero point vector fields (section 2.3.2). As spin 3 needs at least three spin 1 particles to create it, the lowest integral number n can be is 3. The virtual $l = 3$ property can however be used to derive the magnetic moment of a charged spin ½, $m = \pm 1/2$ state as a function of n. Section 3.5 shows $g = 2$ Dirac electrons need an average (over integral n states) of $\bar{n} \approx 6.0135$.

Three member superpositions $\psi_k = \sum c_n \psi_{nk}$ with $n = 5, 6, \& 7$ achieve this, creating Dirac spin ½ states. We also find that $n = 6$ is the dominant member and each superposition ψ_k

needs at least three members to make all the equations consistent for Dirac particles. Secondary interactions at any wavenumber k can occur with ψ_k if integers n change by ± 1, thus changing the eigenvalues $|\mathbf{P}| = n\hbar k$ by $\pm \hbar k$ where this can be only a temporary rearrangement of the triplets of values of n. This is true, whether the interaction is with leptons, quarks, photons, gluons, W & Z particles, or gravitons. (Section 3.3)

1.2.5 Superposition wavefunctions require only squared vector potentials

The wavefunction $\psi_{nk} = C_{nk} r^3 \exp(-n^2 k^2 r^2 / 18) Y(\theta, \varphi)$ requires an invariant in all coordinates spherically symmetric squared vector potential to create it: $Q^2 A^2 = n^4 \hbar^2 k^4 r^2 / 81$. There are no linear potential terms in contrast with secondary interactions. The primary interaction operator is $\hat{P}^2 = -\hbar^2 \nabla^2 + Q^2 A^2$, with no linear potential terms included and Q simply represents a collective symbol for all the effective charges concerned. As an example, the dominant $n = 6$ wavefunction of a spin ½ Dirac ψ_k requires a squared vector potential of $Q^2 A^2 = n^4 \hbar^2 k^4 r^2 / 81 = 16 \hbar^2 k^4 r^2$ (section 2.3.1). Primary coupling between the eight virtual preons and the colour, electromagnetic and gravitational zero-point fields produces a vector potential squared value for all infinite superpositions which can be expressed as:

$$Q^2 A^2 = \frac{\left[8 + 8\sqrt{\alpha_{EMP}} + im_0 \sqrt{G_p / (2s\hbar c)} \right]^2 (\hbar^2 k^4 r^2)}{3\pi (sN)(1+\varepsilon)} \left[\frac{(sN)(1+\varepsilon)dk}{k} \right]$$

(Where the length of the complex vector is simply squared here.) The significance of the cancelling top and bottom factors (sN) is explained in section 2.1.2. Also the cancelling $(1+\varepsilon)$ factors are due to gravity and explained in section 4.2. The primary colour coupling amplitude is conjectured to be 1 to each of the eight preons, and $\sqrt{\alpha_{EMP}}$ the primary electromagnetic coupling. This equation applies regardless of the individual preon colour or electric charge signs, whether positive or negative (section 2.2.3). The primary gravitational coupling is to the particle mass m_0. The primary gravitational constant is G_P divided by $\hbar c$ to put it in the same form as the other two coupling constants. The magnitude of the total angular momentum vector of the infinite superposition is $|\mathbf{L}_{Total}| = \sqrt{s(s+1)}$. This $Q^2 A^2$ without the gravity term generates superpositions with probability $(N \cdot s)dk / k$, where s is the superposition spin, $N = 1$ for massive spin ½ fermion & massive boson superpositions, but $N = 2$ for infinitesimal mass boson superpositions (Table 4.3.1 section 6 and its subsections cover this more fully). Section 4.2 includes gravity raising the superposition probability to $(1+\varepsilon)(N \cdot s)dk / k$ where the infinitesimal ε (not to be confused with infinitesimal mass) is $\varepsilon \approx 2m_0^2 / Spin \approx 7 \times 10^{-45}$ for electrons, and $\varepsilon \approx 10^{-34}$ for a Z^0 in Planck units $\hbar = c = G = 1$. The ψ_k superpositions require at least three integral n members. The following three member superpositions fit the SM best (see Table 4.3.1).

Spin ½ massive $N = 1$ fermion superpositions $\psi_k = \sum_{n=5,6,7} c_n \psi_{nk}$.

Spin 1 massive $N = 1$ boson superpositions $\psi_k = \sum_{n=4,5,6} c_n \psi_{nk}$.

13

Spins 1 & 2 infinitesimal mass $N = 2$ boson superpositions $\qquad \psi_k = \sum_{n=3,4,5} c_n \psi_{nk}$.

Below are infinite superpositions $\left|\psi_{\infty,s,m}\right\rangle$ for only spins ½ & 1. The symbol ∞ refers to the infinite sum, s the spin of the resulting real particle, m its angular momentum state, and ss a spherically symmetric state. Section 3.1.3 explains this format. Also, square cutoffs in wavenumber k are used here for simplicity. Infinitesimal mass superpositions are introduced in section 6.2. (Complex number factors are not included here for clarity.)

Massive $\qquad N = 1$ Spin $\frac{1}{2}$, $\left|\psi_{\infty,1/2,m}\right\rangle = \sum_{n=5,6,7} c_n \int_0^{k(cutoff)} \left[\frac{\left|\psi_{nk,ss}\right\rangle}{\gamma_{nk}} + \beta_{nk}\left|\psi_{nk,4m}\right\rangle) \right] \sqrt{\frac{1+\varepsilon}{2k}} dk$ $\qquad$ (1.1. 1)

Infinitesimal mass $N = 2$ Spin 1, $\left|\psi_{\infty,1,m}\right\rangle = \sum_{n=3,4,5} c_n \int_0^{k(cutoff)} \left[\frac{\left|\psi_{nk,ss}\right\rangle}{\gamma_{nk}} + \beta_{nk}\left|\psi_{nk,2m}\right\rangle \right] \sqrt{\frac{2(1+\varepsilon)}{k}} dk$

In these infinite superpositions the probability that the wavefunction is spherically symmetric is always $\gamma_{nk}^{-2} = 1 - \beta_{nk}^2$ and the probability that it is an m state is β_{nk}^2, where β_{nk} is the magnitude of the velocity of the centre of momentum frame (see Figure 3.1.1), which is where the primary interactions that generate each ψ_{nk} take place. This is similar to the superposition of time and spatially polarized virtual photons in QED. For example, spin ½ has probabilities of $\gamma_{nk}^{-2} = 1 - \beta_{nk}^2$ spherically symmetric ψ_{nk} wavefunctions, and $\beta_{nk}^2 \times (\psi_{nk}, m = \pm 2)$ wavefunctions. Each ψ_k is normalized to one but the infinite superpositions $\psi_{\infty,s,m}$ are not normalized, diverging logarithmically with k; the same logarithmic divergence that applies to virtual photon emission. (Real wavefunctions must be normalized to one as they refer to finding a real particle somewhere, but this need not apply here.) Section 3.1 finds that $m = +2$ virtual wavefunctions have β_{nk}^2 probability of leaving an $m = -2$ debt. Integrating over all k produces a total angular momentum for a spin ½ state of $\hbar / 2$. (The procedures for spin 1 & spin 2 particles are covered in section 3.2.2.)

The first half of this paper is about the primary interactions between spin zero preons and spin one quanta that build the fundamental particles. The SM is about the secondary interactions between them. (The weak force is only between spin ½ particles and thus a secondary interaction. It cannot be involved in primary interactions.) Apart from infinitesimal effects, such as infinitesimal masses, the properties of fundamental particles covered in this paper should be consistent with their SM counterparts. All $N = 1$ & $N = 2$ superpositions as in Table 4.3.1 are conjectured to cutoff at Planck energy E_P. If this is so, both colour and electromagnetic interaction energies must cutoff at $E_P / \langle n \rangle \approx 2.03 \times 10^{18} GeV$., or $\approx 1/6$ of the Planck energy. (The expectation value $\langle n \rangle$ is ≈ 6.0135 for spin ½ leptons and quarks Eq. (3.5.16)). The electromagnetic and colour coupling constants at this cutoff are consistent with SM predictions assuming three families of fermions and one Higgs field. (See Figure 4.1.1 & Figure 4.1.2).

Part 1

Fundamental Particles as Infinite Superpositions

2   Building Infinite Virtual Superpositions

2.1   The Possibility of Infinite Superpositions

2.1.1   **Early ideas**

After World War II there was still much confusion about QED. In 1947 at the Long Island Conference the results of the Lamb shift experiment were announced **[21].** This conference was perhaps the starting point for the development of modern QED: perhaps the pinnacle of accurate theory supported by experiment. QED is also about what we have called secondary interactions. (See 1.2.3.) Part 1 of this paper is about the much simpler primary interactions and we start it with an oversimplified semi-classical way of explaining the Lamb shift. We are going to imagine that the Lamb shift involves primary interactions when, in fact, it doesn't. It is a real world secondary interaction experiment, and therefore our illustration is not the correct QED way of handling this phenomenon. Picturing it as a primary interaction however, with zero point fields, may help illustrate the possibility of connections between fundamental particles and infinite virtual superpositions. Hopefully this is in a similar manner to the way Bohr's original simple semi-classical explanation of quantized atomic energy levels played such a large part in the eventual development of full three dimensional wavefunction solutions of atoms, and quantum mechanics.

The density of transverse modes of waves at frequency ω is $\omega^2 d\omega / \pi^2 c^3$ and the zero point energy for each of these modes is $\hbar\omega / 2$. The electrostatic and magnetic energy densities in electromagnetic waves are equal, thus for electromagnetic zero point fields:

The total average field energy $\dfrac{\varepsilon_0 E^2}{2} + \dfrac{\varepsilon_0 c^2 B^2}{2} = \dfrac{\hbar\omega}{2}\left[\dfrac{\omega^2 d\omega}{\pi^2 c^3}\right]$ or $\overline{\varepsilon_0 E^2} = \overline{\varepsilon_0 c^2 B^2} = \dfrac{\hbar\omega^4}{2\pi^2 c^3}\dfrac{d\omega}{\omega}.$

For a fundamental charge e using $\alpha = e^2 / 4\pi\varepsilon_0 \hbar c,$ and provided $\beta << 1,$ this gives an

$$\text{average force squared of} \quad \overline{F^2} = \overline{e^2 E^2} = \dfrac{2\alpha}{\pi}\dfrac{\hbar^2 \omega^4}{c^2}\dfrac{d\omega}{\omega} \qquad (2.1.1)$$

Thinking semi-classically, for an electron of rest mass m this can generate simple harmonic motion of amplitude r, where $F^2 = m^2 \omega^4 r^2$ (if $\beta << 1$). Solving for r^2 (where r^2 is superimposed on the normal quantum mechanical electron orbit, $\lambdabar_C = \hbar / mc$ is the Compton

wavelength, and $k = \omega / c$): $\qquad r^2 = \dfrac{\hbar^2}{m^2 c^2}\dfrac{2\alpha}{\pi}\dfrac{d\omega}{\omega} \quad = \quad \left[\lambdabar_C^2\right].\left[\dfrac{2\alpha}{\pi}\dfrac{dk}{k}\right]$

Integrating r^2 (as directions are random): $r^2{}_{Total} = \lambdabar_C^2 \dfrac{2\alpha}{\pi}\displaystyle\int_{k\min}^{k\max}\dfrac{dk}{k} = \lambdabar_C^2 \dfrac{2\alpha}{\pi}\log(k_{\max} / k_{\min}).$

The minimum and maximum values for k can be chosen to fit atomic orbits, and a root mean square value for r can be found. Combining this with the small probability that the electron will be found in the nucleus, this small root mean square deviation shifts the average potential by approximately the Lamb shift. This can also be thought of as simple harmonic motion of amplitude $\approx \lambda_C$, occurring with probability $(2\alpha/\pi)dk/k$. It can also be interpreted as the electron recoiling by $\approx \lambda_C$, (provided $\beta_{\text{Recoil}} << 1$) in random directions due to virtual photon emission with a probability of $(2\alpha/\pi)dk/k$.

2.1.2 Dividing probabilities into the product of two component parts

This probability $(2\alpha/\pi)dk/k$ can be thought of as the product of two terms $A \& B$, where A includes the electromagnetic coupling constant α, B includes dk/k, and $AB = (2\alpha/\pi)dk/k$. This suggests that this same behaviour is possible if we have an appropriate superposition of virtual wavefunctions occurring with probability B, which emits virtual photons with probability A (by changing eigenvalues $|\mathbf{p}_{nk}| = n\hbar k$ by $n = \pm 1$). For example, if a virtual superposition occurs with probability $B = (N \cdot s)dk/k$, and has a virtual photon emission probability for each member of these superpositions of $A = (N \cdot s)^{-1}(2\alpha/\pi)$, then the overall virtual photon emission probability remains as above at $AB = (2\alpha/\pi)dk/k$. This applies equally whether it is virtual gluon/photon/W&Z/graviton etc. emission. Provided A includes the appropriate coupling constant this same logic applies regardless of the type of boson emitted. As is usual to get integral or half integral total angular momentum $2s$ has to be integral and section 6.2 argues that N must also be integral. (This paragraph is simplified to illustrate the principle and will later be modified in section 3.3.)

In section 1.2.5 we said that these wavefunctions are built with squared vector potentials. If superpositions of them are to represent real particles they must be able to exist anywhere. This is possible only if they are generated by invariant fields. The only fields uniform in space-time are the zero point fields and looking at the electromagnetic field first we can use section 2.1.1 above. Consider a vector $\mathbf{r}$ from some central origin O and a magnetic field vector $\mathbf{B}$ through origin O, then the vector potential at point $\mathbf{r}$ is $\mathbf{A} = (\mathbf{B} \times \mathbf{r})/2$ and the vector potential squared is $A^2 = (B^2 r^2 \sin^2 \theta)/4$ where the angle between vectors $\mathbf{B} \& \mathbf{r}$ is θ.

$$\text{As } \sin^2 \theta \text{ averages 2/3 over a sphere: } \overline{A^2} = B^2 r^2 / 6 \tag{2.1.2}$$

This requires the source of these fields to be spherically symmetric, where B^2 here is the magnetic field squared at any point due to the invariant cubic intensity of zero point electromagnetic fields, also as in section 2.1.1. This is only true at higher frequencies, and we will find later that at cosmic wavelengths we need a similarly invariant spherically symmetric source redshifted from the receding spherical horizon. Putting Eqs.   (2.1.1) and (2.1.2) together the vector potential squared is

$$\overline{e^2 A^2} = \frac{e^2 B^2 r^2}{6} = \frac{\alpha}{3\pi}\frac{\hbar^2 \omega^4 r^2}{c^4}\frac{d\omega}{\omega} = \frac{\alpha}{3\pi}\hbar^2 k^4 r^2 \frac{dk}{k} \tag{2.1.3}$$

16

As in section 2.1.2 we can divide this into two parts, noting the inclusion of spin s and integer N in the numerator and denominator:

$$\overline{e^2 A^2} = \left[\frac{\alpha}{3\pi sN} \hbar^2 k^4 r^2 \right] \cdot \left[\frac{sN \cdot dk}{k} \right] \tag{2.1.4}$$

But here a vector potential squared term $\left[\dfrac{\alpha}{3\pi sN} \hbar^2 k^4 r^2 \right]$ occurs with probability $\left[\dfrac{sN \cdot dk}{k} \right]$. Another way of looking at this is that a wavefunction ψ_k that is generated by a vector potential squared term $\left[\dfrac{\alpha}{3\pi sN} \hbar^2 k^4 r^2 \right]$ can occur with $\left[\dfrac{sN \cdot dk}{k} \right]$ probability.

This is similar reasoning to that used in the semi-classical Lamb shift explanation of section 2.1.1. In the first bracketed term of Eq. (2.1.4), α is the electromagnetic coupling constant, but the same logic applies for the eight gluon and gravitational zero point vector fields where we will sum appropriate amplitudes of these and square this total as our effective coupling constant in Eq. (2.1.4). But first we need to look at groups of spin zero preons that could build these wavefunctions. What mixtures of colours and electrical charges end up with the appropriate final colour and electrical charge for each of the fundamental particles or at least the ones we know of?

2.2   Spin Zero Virtual Preons from a Higgs Type Scalar Field

2.2.1   Groups of eight preons that form superpositions

In this paper preons have zero spin and can have no weak charge. The only fields they can interact with (via *primary interactions* that build superpositions as in section 1.2.3) are colour, electromagnetic and gravity. In the simplest world there would be just one type of preon that comes in three colours, always positively charged say, with their three anti colours all negatively charged. We will indeed find that this seems to work. Looking at Table **2.2.1** we see that a minimum of 6 preons is required to get the correct charge ratios of 3:2:1 between electrons, and up and down quarks. To get vector potential squared values that make all our equations work however, we need to couple to all eight gluon fields requiring a total of eight preons. Table **2.2.1** has all the basic properties required to build infinite superpositions for the fundamental particles. We need to remember when looking at this table that from section 1.2.3 the effective secondary charge is much less than the primary charge and we have no idea yet of the effective value of the primary preon electric charge. Particles only are addressed in the groups of preons in Table 2.2.1. The first point to notice, however, is that both the electron and the W^- are predominantly antipreons, yet they are both defined as particles. Have we got something wrong? When we look at relativistic masses in section 3.2.1 we get the usual plus and minus solutions and Feynman showed us how to interpret the negative solutions as antiparticles.

Table 2.2.1 Groups of eight virtual preons forming the fundamental particles. The electric charges we measure in the real world are one sixth of the group electric charges in this table. The Higgs boson is discussed in section 8.2.4, if it is a superposition it would be in the neutral group at the top.

Fundamental Particles	Preon colour	Preon electric charge	Group colour	Group electric charge
Spin ½ Neutrino family Spin 1 photons, Z_0 Neutral gluons Spins 1 & 2 gravitons Possibly Higgs boson	Any colour + its Anticolour Red Antired Green Antigreen Blue Antiblue	1 -1 1 -1 1 -1 1 -1	Colourless	0
Spin ½ Electron family Spin 1 W^-	Any colour + its Anticolour Antired Antired Antigreen Antigreen Antiblue Antiblue	1 -1 -1 -1 -1 -1 -1 -1	Colourless	-6
Spin ½ Blue up quark Family	Red Antired Green Antigreen Green Blue Blue Red	1 -1 1 -1 1 1 1 1	Blue	+4
Spin ½ Red down Quark family	Green Antigreen Red Antired Green Antigreen Antiblue Antigreen	1 -1 1 -1 1 -1 -1 -1	Red	-2
Spin 1 Red to Green Gluons	Red Antigreen Red Antired Green Antigreen Blue Antiblue	1 -1 1 -1 1 -1 1 -1	Red plus Antigreen	0

If this also applies in anti preons then because they are zero spin, and the weak force discriminates between particles and antiparticles by their helicity, this discrimination can apply only in secondary interactions. The preon antiproton content of the groups in Table 2.2.1 does not necessarily tell us whether they produce particles or antiparticles. We will discuss this further in section 3.2.1; also, as of now, there is still no good understanding of the predominance of matter over antimatter in our universe. In Table 2.2.1 only one example of colour is given for quarks and gluons. Different colours can be obtained by simply changing appropriate preon colours. Various combinations of eight preons in this table are borrowed from a scalar field for time $\Delta T \leq \hbar / 2\Delta E$, this process continually repeating in time. Conservation of charge normally allows only opposite sign pairs of electric charges to appear out of the vacuum. Let us imagine that these virtual preons are building an electron, for example, whose electric charge exists continually unless it meets a positron and is annihilated. This charged electron is thus due to a continuous appearance out of and back into the vacuum of virtual charged preons in a steady state process existing for the life of the superposition, and not conflicting with conservation of charge. If the electron itself does not conflict, then neither do the borrowed preons that build it.

2.2.2   **Primary coupling constants behave differently and are constant**

QED informs us that the bare (electric) charge of an electron, for example, increases logarithmically inversely with radius from its centre. Polarizations of the vacuum (of virtual charged pairs) progressively shield the bare charge from a radius of approximately one Compton radius λ_C inwards towards the centre. When an electron (for example) is created in some interaction the full bare charge is exposed for an infinitesimal time.

Instantaneously after its creation, shielding due to polarization of the vacuum builds progressively outward from the centre of its creation at the velocity of light. For radii $\geq \lambda_C$ we measure the usual fundamental charge e. There are similar but more complicated processes that occur to the colour charge. Camouflage is the dominant one where the colour charge grows with radius as the emitted gluons themselves have colour charge. At the instant of their birth the preons are bare and at this time, $t = 0$ say, all the zero point vector fields can act on these bare colour and electric charges as there is simply no time for shielding and other effects to build. The primary coupling constants that we use must consequently be the same for all values of k, in complete contrast to those for secondary interactions. We don't know what this primary electromagnetic coupling constant is, so we will just call it α_{EMP}. Also, we will find that to get any sense out of our equations the primary colour coupling has to be very close to 1. A coupling of one is a natural number and simply reflects certainty of coupling. Provided the secondary colour coupling can be in line with the SM, and there does not seem to be any other good reason to pick a number less than 1, we will make the (apparently arbitrary) assumption that the bare primary colour coupling is exactly 1. (In section 4.1.1 we will find that this seems to be consistent with the SM.)

2.2.3 Primary interactions also behave differently

Let us define a frame in which the central origin of the wavefunctions ψ_k of our infinite superposition is at rest. The laboratory or rest frame we will refer to as the LF. The preons that build each ψ_k are born from a Higg's type scalar field with zero momentum in this frame. This has very relevant consequences as their wavelength is infinite in this rest frame at time $t = 0$, and after they become wavefunction ψ_k their wavelength is of the order $1/k$ for times $0 < t < \hbar/2E$. This implies that there could possibly be significant differences in the way amplitudes are handled between primary and secondary interactions.

Let us consider secondary interactions first with an electron and positron, for example, located approximately distance r apart. For photon wavelengths $<< r$ both the electron and the positron each emit virtual photons with probabilities proportional to α, but for wavelengths $>> r$ their amplitudes cancel. Returning to primary interactions, zero momentum preons must always have an infinite wavelength which is greater than the wavelengths (or $1/k$ values) of the zero point quanta they interact with, for all $k \neq 0$. This implies that we cannot simply add or subtract amplitudes algebraically as the charged preons can be always further apart than the wavelength of the interacting quanta (except when $k = 0$, but we will see there is always a minimum k value, i.e. $k_{min} > 0$ in sections 5 & 6). In fact, if algebraic addition of amplitudes did apply in primary interactions, infinite superpositions for colourless and electrically neutral neutrinos would be impossible. So how can infinitely far apart preons of differing charge generate wavefunctions of all dimensions down to Planck scale? This can happen only if the amplitudes of all eight preons are somehow linked over infinite space, all at the same time $t = 0$ contributing to generating the wavefunction ψ_k. This non-local behaviour is not new. All experiments confirm that what Einstein struggled to come to terms with is, in fact, true; he called it "spooky action at a distance". While these experiments are currently limited in the distance over which they demonstrate entanglement, there is now wide acceptance that it can reach across the universe. In the same manner wavefunctions covering all space can instantly collapse. We want to suggest that this same non-locality applies in primary interactions; our eight virtual preons all unite instantaneously at time $t = 0$ across infinite space in generating each ψ_k. Also, the vector potential squared equations that they generate must always be the same for all the preon combinations in Table **2.2.1**. This can happen only if the amplitudes of all eight are added, regardless of charge sign for primary interactions. This applies to both colour and electric charge.

The opposite is true for the secondary interactions. At time $t = 0$ all eight preons instantaneously collapse into some sort of virtual composite particle that for times $0 < t < \hbar/2E$ obeys wavefunction ψ_k. The dimensions of ψ_k are of the same order as the wavelength of the interacting quanta, and the usual algebraic total electric charge and nett colour charge must now apply as in the group charges in Table **2.2.1**. All of this may seem contrary to current thinking which has gradually been built up over several centuries of secondary interaction experiments; however, it may not be so out of place when viewed in the context of the counter intuitive results of entanglement experiments. The key point to bear in mind is that the predictions of this paper must agree or at least be able to fit the SM, or

secondary interaction experiments; as we may never be able to look into virtual primary interactions, but only observe their effects.

Amplitudes to interact are complex numbers which we can draw as a vector. This applies to both colour and electric coupling, where these two vectors can be at the same complex angle or at different angles. The simplest case is if they are in line and we will assume this is true for both colour and electromagnetic primary interactions which are both spin 1. This seems to work and when we later include gravity, a spin 2 interaction, we find that the spin 2 vector only works if it is at right angles to the two in line spin 1 vectors. Let us start in a zero gravity world by simply adding the eight preon colour vectors of amplitude one and the eight primary electromagnetic vectors of amplitude $\sqrt{\alpha_{EMP}}$ together, as all this only works if they are all in line.

The total colour plus electromagnetic primary amplitude is $8 + 8\sqrt{\alpha_{EMP}}$ (2.2.1)

This equation is always true regardless of signs as in section 2.2.3

The colour plus electromagnetic primary coupling constant is $\left(8 + 8\sqrt{\alpha_{EMP}}\right)^2$ (2.2.2)

Inserting this into Eq. (2.1.4) we get

(2.2.3)

$$Q^2 A^2 = \left[\frac{\left[8 + 8\sqrt{\alpha_{EMP}}\right]^2}{3\pi sN} \hbar^2 k^4 r^2\right] \cdot \left[\frac{sN \cdot dk}{k}\right]$$

Again we interpret this just as we did in section 2.1.2 and Eq. (2.1.4) as a vector potential squared term

(2.2.4)

$$Q^2 A^2 = \frac{\left[8 + 8\sqrt{\alpha_{EMP}}\right]^2}{3\pi sN} \hbar^2 k^4 r^2 \text{ occurring with probability } = \frac{sN \cdot dk}{k}$$

Where Q is a symbol representing the entire eight colour and eight electric amplitudes combined, with s the spin and $N = 1$ for massive superpositions, but $N = 2$ for infinitesimal mass superpositions. (Table 4.3.1, section 6 and its subsections cover this more fully.)

2.3 Virtual Wavefunctions that form Infinite Superpositions

2.3.1 Infinite families of similar virtual wavefunctions

Consider the family of wave functions where ignoring time:

$$\psi_{nk} = U(nrk)Y(\theta\varphi)$$
$$U(nrk) = C_{nk}r^l \exp(-n^2k^2r^2/18) \qquad (2.3.1)$$

$U\left(nrk\right)$ is the radial part of ψ_{nk}, $Y\left(\theta\phi\right)$ the angular part, C_{nk} a normalizing constant, and we will find that l is the usual angular momentum quantum number. There is an infinite family of ψ_{nk}, one for each value k where $0 < k < \infty$ in a zero gravity world.

$$\text{Now put } R(nrk) = rU(nrk) = C_{nk}r^{l+1}\exp(-n^2k^2r^2/18) \qquad (2.3.2)$$

As we are dealing with zero spin preons we use Klein-Gordon equations [22]. The Klein-Gordon equation is based on the relativistic equation $\mathbf{p}^2 = E^2/c^2 - m_0^2c^2$ and in a spherically symmetric squared vector potential the time independent Klein Gordon Equation is

$$\hat{P}^2\psi = -\hbar^2\nabla^2\psi + Q^2A^2\psi = \left[\frac{E^2}{c^2} - m_0^2c^2\right]\psi \qquad (2.3.3)$$

Using $\qquad \dfrac{\nabla^2\psi}{\psi} = \dfrac{1}{R}\dfrac{\partial^2 R}{\partial r^2} - \dfrac{l(l+1)}{r^2} \qquad$ we get the time independent

radial Klein Gordon equation $\quad \dfrac{\hbar^2}{R}\dfrac{\partial^2 R}{\partial r^2} = \dfrac{l(l+1)\hbar^2}{r^2} + Q^2A^2 - \left[\dfrac{E^2}{c^2} - m_0^2c^2\right] \qquad (2.3.4)$

For each ψ_{nk} the energy is E_{nk} a function of $n\,\&\,k$, and we will label the rest mass as m_{0snk} a function of spin s, $n\,\&\,k$, but also a function of the particle rest mass m_0. Using different colours to more clearly compare the next two equations this becomes

$$\frac{\hbar^2}{R}\frac{\partial^2 R}{\partial r^2} = \frac{l(l+1)\hbar^2}{r^2} + Q^2A^2 - \left[\frac{E_{nk}^2}{c^2} - m_{0snk}^2c^4\right] \qquad (2.3.5)$$

Differentiating $R(nrk) = rU(nrk) = C_{nk}r^{l+1}\exp(\dfrac{-n^2k^2r^2}{18})$ twice with respect to r, multiplying by $\hbar^2$ and dividing by R

$$\frac{\hbar^2}{R}\frac{\partial^2 R}{\partial r^2} = \frac{l(l+1)\hbar^2}{r^2} + \frac{n^4\hbar^2k^4r^2}{81} - \frac{(2l+3)n^2\hbar^2k^2}{9} \qquad (2.3.6)$$

Comparing Eqs. (2.3.5) & (2.3.6) we see that l is the usual angular momentum quantum number and the vector potential squared required to generate these wavefunctions is

$$Q^2 A^2 = \frac{n^4 \hbar^2 k^4 r^2}{81} = \left[\frac{n}{3}\right]^4 \hbar^2 k^4 r^2 \qquad (2.3.7)$$

The momentum squared is $\mathbf{p}_{nk}^2 = \dfrac{E_{nk}^2}{c^2} - m_{0snk}^2 c^2 = \dfrac{(2l+3)n^2\hbar^2 k^2}{9}$ (2.3.8)

For $l = 3$ wavefunctions this becomes $\mathbf{p}_{nk}^2 = n^2\hbar^2 k^2$ & $\left|\mathbf{p}_{nk}\right| = n\hbar k$ (2.3.9)

2.3.2 Eigenvalues of these virtual wavefunctions and parallel momentum vectors

From Eqs. (2.3.8) & (2.3.9) as $k \to \infty$, the energy squared $E_{nk}^2 \to \mathbf{p}_{nk}^2 c^2 = n^2\hbar^2\omega^2$ and thus if $l = 3$ when $k \to \infty$ energy $E_{nk} \to n\hbar\omega$ (considering only the positive solution). (2.3.10)

This suggests that n must be integral. If it is integral when $k \to \infty$, we will conjecture that it must be integral for all values of k. This is a virtual or "off shell" process, where energy can depart from $E^2 = m_0^2 c^4 + \mathbf{p}^2 c^2$ for time $\Delta T \approx \hbar / 2\Delta E$. We can also perhaps think of Eq. (2.3.9) as integral n parallel momentum vector $\left|\mathbf{p}\right| = \hbar k$ quanta, transferring total momentum $\left|\mathbf{p}_{nk}\right| = n\hbar k$ and energy $E \le n\hbar\omega$ from the zero point fields to generate the virtual wavefunction ψ_{nk}. Using different colours for both operator and wavefunction, we can say that provided $Q^2 A^2 = (n/3)^4 \hbar^2 k^4 r^2$ as in Eq. (2.3.7) the operator $\hat{P}^2 = (-\hbar^2\nabla^2 + Q^2 A^2)$ applied to the virtual wavefunction $\psi_{nk} = C_{nk} r^3 \exp(-n^2 k^2 r^2 / 18) Y(\theta\varphi)$ produces $\hat{P}^2 |\psi_{nk}\rangle = (-\hbar^2\nabla^2 + Q^2 A^2) |\psi_{nk}\rangle = n^2\hbar^2 k^2 |\psi_{nk}\rangle$, where n is integral, but k is continuous as for free particles. Thus, we conjecture that:

$\psi_{nk} = C_{nk} r^3 \exp(-n^2 k^2 r^2 / 18) Y(\theta\varphi)$ are eigenfunctions with (2.3.11)

eigenvalues $\mathbf{p}_{nk}^2 = n^2\hbar^2 k^2$ with continuous k but integral n.

Also, there are no scalar potentials involved, only squared vector potentials, so this is a magnetic or vector type interaction. Particles in classical magnetic fields have a constant magnitude of linear momentum which is consistent with the squared momentum eigenvalues of Eq. (2.3.11). This also implies that each ψ_{nk} is formed from quanta of wave number k only and that secondary interactions with ψ_{nk} emit or absorb $\left|\hbar k\right|$ virtual quanta if n changes by ± 1. The wavefunction ψ_{nk} is virtual and in this sense both the energy E_{nk} and rest mass m_{0snk} in Eq. (2.3.8) are also virtual quantities borrowed from zero point vector fields and its time component or a scalar Higgs type field. We use these virtual quantities to calculate the amplitude that the wavefunction ψ_{nk} is in an m state of angular momentum in section 3.1, and in section 3.2 to calculate the total angular momentum and rest mass. As in section 2.3.2 above, we can think of $\left|\mathbf{p}_{nk}\right| = n\hbar k$ as n parallel momentum vectors $\left|\mathbf{p}\right| = \hbar k$. As spin 3 (or $l = 3$) needs at least three spin 1 quanta to build it, n must be at least 3. When $n = 3$ we can think of this as three of the eight preons each absorbing quanta $\left|\hbar k\right|$ at time $t = 0$. We will find that a spin ½ state has a dominant $n = 6$ eigenfunction where six of the eight preons each

absorb quanta $|\hbar k|$. It needs at least two smaller side eigenfunctions $n=5$ & $n=7$ with either five or seven respectively, of the eight preons each absorbing quanta $|\hbar k|$ respectively at $t=0$. (Figure 3.1.4 illustrates the three n modes of a positron superposition.)

From Eq. (2.3.7) $Q^2A^2 = \left[\dfrac{n}{3}\right]^4 \hbar^2 k^4 r^2 = 16\hbar^2 k^4 r^2$ for this dominant $n=6$ mode.

Thus using Eq. (2.2.4) $Q^2A^2 = \dfrac{\left[8+8\sqrt{\alpha_{EMP}}\right]^2}{3\pi s N} \hbar^2 k^4 r^2 = 16\hbar^2 k^4 r^2$ for an $n=6$ mode.

Now $s=1/2$ & $N=1$ for spin ½ fermions and $\dfrac{2\left[8+8\sqrt{\alpha_{EMP}}\right]^2}{3\pi} = 16$ if we have only an $n=6$

mode. Thus $8+8\sqrt{\alpha_{EMP}} = \sqrt{24\pi}$ and $\alpha_{EMP}^{-1} \approx 137.1$, but this is true for an $n=6$ eigenfunction only, and we have a superposition where the amplitudes of the smaller side eigenfunctions $n=5$ & $n=7$ determine the ratio between the primary to secondary (colour and electromagnetic) coupling amplitudes or the value of α_3^{-1} @ k_{cutoff} (Section 3.3). The Q^2A^2 required to produce this superposition with amplitudes c_n is, using Eq. (2.3.7)

$$Q^2A^2 = \sum_{n=5,6,7} c_n * c_n \frac{n^4 \hbar^2 k^4 r^2}{81} \tag{2.3.12}$$

Repeating the same procedure as above for three member superpositions using Eq. (2.3.12) we find the strength of α_{EMP} required increases considerably (see section 4.1 & Table 4.1.1 As the secondary electromagnetic coupling α_{EMS}^{-1} @ k_{cutoff} must be constant for all spin ½ leptons and quarks, the amplitudes of the smaller side eigenfunctions $n=5$ & $n=7$ that determine this must also be constant for all the fermions, implying that Eq. (2.3.12) must be the same for all fermions. The same arguments apply to the other groups of fundamental particles but we return to this in sections 3.3 where we see that the same also applies with graviton emission.

3   Properties of Infinite Superpositions

3.1   The Amplitude that Wavefunction ψ_{nk} is Spherically Symmetric

3.1.1   Four vector transformations

The rules of quantum mechanics tell us that if we carry out any measurement on a real spherically symmetric $l=3$ wavefunction it will immediately fall into one of the seven possible states $l=3, m=0,\pm1,\pm2,\pm3$ [23]. But ψ_{nk} is a virtual $l=3$ wave function so we cannot measure its angular momentum. During its brief existence it must always remain in some virtual superposition of the above seven possible states and we can describe only the

amplitudes of these. So, is there any way to calculate these amplitudes, as they must relate to the amplitudes of the angular momentum states of the spin 1 quanta it absorbs from the zero point vector fields?

First consider the 4 vector wavefunction of a spin 1 particle and start with a time polarized state which has equal probability of polarization directions. It is thus spherically symmetric, which we will label as ss. Using 4 vector (t, x, y, z) notation

In frame A, a time polarized or ss spin 1 state is (1,0,0,0).
Let frame B move along the z axis at velocity $\beta = v/c$ in the z direction.
In frame B the polarization state transforms to $(\gamma, 0, 0, \gamma\beta)$.

But this is γ^2 time polarized $|ss\rangle$ states minus $\gamma^2\beta^2 \times z$ polarized or $|m=0\rangle$ states

In frame B the probabilities are $\gamma^2 |ss\rangle - \gamma^2\beta^2 |m=0\rangle$ states.

Now $\gamma^2 - \gamma^2\beta^2 = \gamma^2(1-\beta^2) = 1$ is an invariant probability in all frames and in removing $\gamma^2\beta^2 \times m=0$ states from $\gamma^2 \times ss$ states, the new ratio of spherical symmetry is $(\gamma^2 - \gamma^2\beta^2)/\gamma^2 = 1-\beta^2$. Thus, a spherically symmetric state is transformed from probability 1 in frame A, to $1-\beta^2$ in frame B. Also removing $m=0$ states from spherically symmetric states leaves a surplus of $m=\pm1$ states, as spherically symmetric states are equal superpositions of $|m=-1\rangle$, $|m=0\rangle$, & $|m=+1\rangle$ states.

Thus in Frame B the probabilities are $(1-\beta^2)|ss\rangle + \beta^2 |m=\pm1\rangle$ states. (3.1.1)

We can describe this as a virtual superposition of $\frac{1}{\gamma}|ss\rangle + \beta|m=\pm1\rangle$ states. (3.1.2)

As $\beta^2 \to 1$ we have transverse polarized states, the same as real photons. Now transverse polarized spin 1 states can be either left ($m=-1$), or right ($m=+1$) circular polarization, or equal superpositions of $(1/\sqrt{2})|L\rangle + (1/\sqrt{2})|R\rangle$ as in x & y polarization. If we think of individual spin zero preons absorbing these spin 1 quanta at $t=0$ they must also have this same β^2 probability of transversely polarized spin 1 states. If they then merge into some composite $l=3$ particle (as in Figure 3.1.4) for time $0 < t < \hbar/2E$, the probability of it being in some particular state $(l=3, m=0)$, $(l=3, m=\pm1)$, $(l=3, m=\pm2)$ or $(l=3, m=\pm3)$, must be the same β^2. We initially write the amplitudes in these three equations in terms of β_{nk} & γ_{nk} as this is the most convenient way to express them. Velocity operators are momentum operators over relativistic masses. Our eigenvalues are $\mathbf{p}_{nk}^2 = n^2\hbar^2k^2$ for each n & k, and this allows the velocity operators to give constant β_{nk}^2. Later in Eqs. (3.1.11) and (3.1.12) we write β_{nk} & γ_{nk} in momentum terms. Even though the mass in these operators is virtual, we can still use it to calculate $|\beta_{nk}|$. For each k and integral n there will be a constant $|\beta_{nk}|$ and $\gamma_{nk} = (1-\beta_{nk}^2)^{-1/2}$. As we will see, β_{nk} can be thought of as the magnitude of the velocity of an imaginary centre of momentum frame in which these interactions take place. We will also draw our Feynman diagrams of these interactions in terms of β_{nk} & γ_{nk} for convenience, even though this is unconventional. To proceed from here we define two frames as follows:

1) The Laboratory Frame (LF) or Fixed Frame as in section 2.2.3

The infinite superposition has rest mass m_0 and zero nett momentum in this frame. Each ψ_{nk} is centred here with magnitude of momentum $\left|\mathbf{p}_{nk}\right| = n\hbar k$. Even though we have no idea of the direction of this momentum vector we will define it as the z direction. The eight preons are born in this frame with zero momentum and can thus be considered here as being at rest or with zero velocity and infinite wavelength at their birth. The Feynman diagram of the interaction in this frame that builds ψ_{nk} is illustrated in Figure 3.1.3.

2) The Centre of Momentum Frame (CMF)

This (imaginary) frame is the centre of momentum of the interaction that builds ψ_{nk}. The CMF moves at velocity β_{nk} relative to the laboratory frame in the z direction or parallel to the unknown momentum vector direction $\mathbf{p}_{nk}$. In this CMF the momenta and velocities of the preons at birth and after the interaction are equal and opposite. This is illustrated in Figure 3.1.2 again in terms of $m_0, \beta_{nk}, \& \gamma_{nk}$. In the LF the velocity of the preons at birth is zero, in the CMF this is $-\beta_{nk}$ and after the interaction $+\beta_{nk}$, where both $-\beta_{nk}$ and $+\beta_{nk}$ are in the unknown z direction. In the LF the particle velocity $\beta_{nk}(\text{particle}) = \beta_{nkp}$ is the simple relativistic addition of the two equal velocities β_{nk} as in Figure 3.1.1.
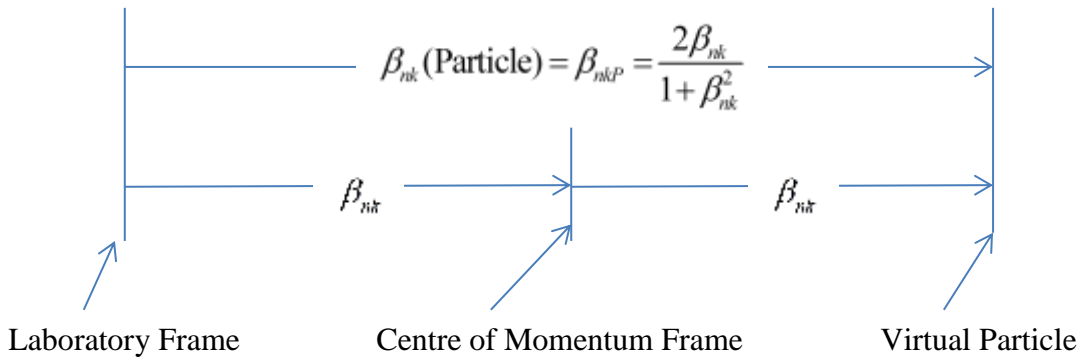
Figure 3.1.1 Velocities in unknown but the same directions in different frames.

3.1.2 Feynman diagrams of primary interactions

Let us start with

$$\beta_{nk}(\text{Particle}) = \beta_{nkP} = \frac{2\beta_{nk}}{1+\beta_{nk}^2} \quad \text{and} \quad \gamma_{nkP} = (1-\beta_{nkp}^2)^{-1/2} = \gamma_{nk}^2(1+\beta_{nk}^2) \tag{3.1.3}$$

If the particle rest mass is m_0 let each preon have a virtual rest mass $m_0 / (8\gamma_{nk}\sqrt{2s})$.

The eight preons are effectively a virtual particle of rest mass $m_{0snk} = \dfrac{m_0}{\gamma_{nk}\sqrt{2s}}$ \hfill (3.1.4)

The particle momentum in the LF is zero at birth. After the interaction using these equations

26

$$\left| \mathbf{p}_{nk} \right| = n\hbar k = m_{0snk}\beta_{nkP}\gamma_{nkP}c = \left[\frac{m_0}{\gamma_{nk}\sqrt{2s}} \right]\left[\frac{2\beta_{nk}}{1+\beta_{nk}^2} \right]\left[\gamma_{nk}^2(1+\beta_{nk}^2) \right]c$$

The particle momentum after the interaction in the LF $\left| \mathbf{p}_{nk} \right| = n\hbar k = \dfrac{2m_0\beta_{nk}\gamma_{nk}c}{\sqrt{2s}}$ (3.1.5)

Using Eq. (3.1.4), in the LF the particle energy at birth is

$$m_{0snk}c^2 = \frac{m_0 c^2}{\gamma_{nk}\sqrt{2s}}$$ (3.1.6)

In the LF the particle energy after the interaction is by using Eq. (3.1.3)

$$m_{0snk}\gamma_{pnk}c^2 = \frac{m_0}{\gamma_{nk}\sqrt{2s}}\gamma_{nk}^2(1+\beta_{nk}^2)c^2 = \frac{m_0\gamma_{nk}}{\sqrt{2s}}(1+\beta_{nk}^2)c^2$$ (3.1. 7)

In the CMF the momentum at birth is using Eq. (3.1.4)

$$-m_{0snk}\gamma_{nk}\beta_{nk} = \frac{-m_0\beta_{nk}}{\sqrt{2s}}$$ (3.1.8)

In the CMF the momentum after the interaction is equal but in the opposite direction

$$= \frac{+m_0\beta_{nk}}{\sqrt{2s}}$$ (3.1.9)

In the CMF the energy at birth, and after the interaction is

$$m_{0snk}\gamma_{nk}c^2 = \frac{m_0 c^2}{\sqrt{2s}}$$ (3.1.10)

These values are all summarized in Figure 3.1.2 and Figure 3.1.3 but with $c=1$.

From Eq. (3.1.5) $\left| \mathbf{p}_{nk} \right| = n\hbar k = \dfrac{2m_0\beta_{nk}\gamma_{nk}c}{\sqrt{2s}}$ and $\beta_{nk}\gamma_{nk} = \dfrac{n\hbar k\sqrt{2s}}{2m_0 c} = \dfrac{\lambdabar_c nk\sqrt{2s}}{2}$

(where $\lambdabar_C = \dfrac{\hbar}{m_0 c}$ is the Compton wavelength). We can now express β_{nk} & γ_{nk} in momentum

terms:

Let $K_{nk} = \beta_{nk}\gamma_{nk} = \dfrac{n\hbar k\sqrt{2s}}{2m_0 c} = \dfrac{\lambdabar_c nk\sqrt{2s}}{2}$ (3.1.11)

In terms of K_{nk}: $\beta_{nk}^2 = \dfrac{K_{nk}^2}{1+K_{nk}^2}$ and $\gamma_{nk}^2 = 1+K_{nk}^2$ (3.1.12)

Each infinite superposition has fixed $\lambdabar_C$. Each wavefunction ψ_{nk} of this infinite
superposition has fixed n & s, thus $K_{nk} \propto k$.

For example, we can put $\dfrac{dK_{nk}}{K_{nk}} = \dfrac{dk}{k}$ (3.1.13)

27

These simple expressions and what follows are not possible if $m_{0snk} \neq m_0 / \gamma_{nk} \sqrt{2s}$, and when we include gravity we find $m_{0snk} = m_0 / (\gamma_{nk} \sqrt{2s})$ is essential (section 4.2).

After merging: $(\dfrac{m_0}{\sqrt{2s}}, 0, 0, \dfrac{+m_0}{\sqrt{2s}} \beta_{nk})$

$q^{\mu} = (0, 0, 0, 2\dfrac{m_0}{\sqrt{2s}} \beta_{nk})$

Eight preons at birth: $(\dfrac{m_0}{\sqrt{2s}}, 0, 0, \dfrac{-m_0}{\sqrt{2s}} \beta_{nk})$
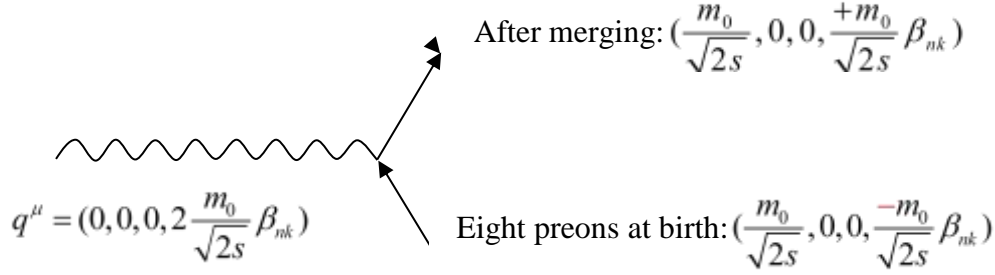
Figure 3.1.2 Feynman diagram in an imaginary centre of momentum frame.

After merging: $(\dfrac{m_0}{\sqrt{2s}} \gamma_{nk}(1 + \beta_{nk}^2), 0, 0, +2\dfrac{m_0}{\sqrt{2s}} \gamma_{nk} \beta_{nk})$

$q^{\mu\prime} = (2\dfrac{m_0}{\sqrt{2s}} \gamma_{nk} \beta_{nk}^2, 0, 0, 2\dfrac{m_0}{\sqrt{2s}} \gamma_{nk} \beta_{nk})$

Eight preons at birth: $(\dfrac{m_0}{\gamma_{nk}\sqrt{2s}}, 0, 0, 0)$
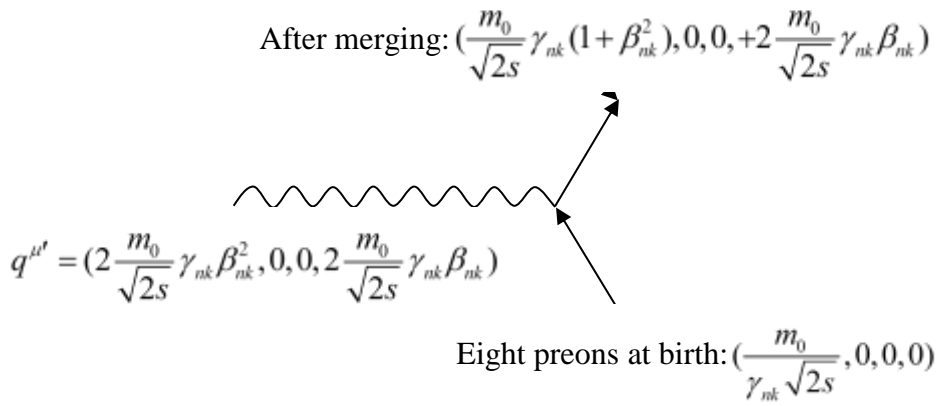
Figure 3.1.3 Feynman diagram in the laboratory frame.

The interaction in the Feynman diagrams above is with spin 1 quanta. The Feynman transition amplitude of this interaction shows that the polarization states of these exchanged quanta is determined by the sum of the components of the initial, plus final 4 momentum $(p_i + p_f)^{\mu}$. Ignoring all other common factors this says that the space polarized component is the sum of the momentum terms $(\mathbf{p}_i + \mathbf{p}_f)$ and the time polarized component is the sum of the energy terms $(p_i + p_f)^0$. We have defined our momentum as in an unknown z direction:

The ratio of z polarization to time polarization amplitudes is $\dfrac{(p_i + p_f)^z}{(p_i + p_f)^0}$ (3.1.14)

In the CMF $(p_i + p_f)^z = 0$, thus an interaction in the CMF exchanges only time polarized, or spherically symmetric $l = 1$ states. In the LF the ratio of z (or $m = 0$) polarization, to time polarization in the LF is β_{nk}^2,

where $\dfrac{(p_i + p_f)^z}{(p_i + p_f)^0} = \dfrac{2m_0\gamma_{nk}\beta_{nk}}{2m_0\gamma_{nk}} = \beta_{nk}$ (3.1.15)

From section 3.1.1 these are probabilities of $\gamma_{nk}^2 |ss\rangle - \gamma_{nk}^2 \beta_{nk}^2 |m=0\rangle$ states, or as $l=1$ here $(1-\beta_{nk}^2)|ss\rangle + \beta_{nk}^2 |m=\pm 1\rangle$ states.

In the LF this is a virtual superposition of $(\dfrac{1}{\gamma_{nk}}|ss\rangle + \beta_{nk}|m=\pm 1\rangle)$ states.

(3.1.16)

From section 3.1.1 as these quanta from the scalar and vector zero point fields build each ψ_{nk} this implies that:

(3.1.17)

In the LF ψ_{nk} has virtual superposition amplitudes $\dfrac{1}{\gamma_{nk}}|ss\rangle + \beta_{nk}|m\rangle$ states.

From section 3.1.1 appropriate $l=1, m=\pm 1$ superpositions can build any $l=3$, m state. Figure 3.1.4 is an example of such a ψ_{nk} for $n=5,6,\&7$ $|l=3, m=+2\rangle$ states.

3.1.3 Different ways to express superpositions

We have expressed all superpositions here in terms of spherically symmetric and m states for convenience and simplicity. We could have expressed them in the form:

$$\frac{1}{\gamma_{nk}\sqrt{7}}\Big[|m=-3\rangle + |m=-2\rangle + |m=-1\rangle + |m=0\rangle + |m=+1\rangle + |m=+2\rangle + |m=+3\rangle\Big] + \beta_{nk}|m=+2\rangle$$

This is equivalent to (as above we ignore complex number amplitude factors for clarity)

$$\psi_{nk} = \frac{1}{\gamma_{nk}}|ss\rangle + \beta_{nk}|m=+2\rangle \text{ where we have put m} = +2 \text{ in this example.}$$

Because all these wavefunctions are virtual they cannot be measured in the normal way that collapses them into any of these eigenstates, it is more convenient to use the method adopted here which is similar to QED virtual photon superpositions.

$n=5$

At birth $t=0$

$\mathbf{p}=0$ → ◯ Any colour &

$\mathbf{p}=0$ → ◯ anticolour

$0<t<\hbar/2E$ after effectively merging.

$\mathbf{p}=0$ → ●

$\mathbf{p}=\hbar\mathbf{k}$ → ● $m=+1$

$\mathbf{p}=\hbar\mathbf{k}$ → ● $m=+1$

$\mathbf{P}_{5k}=5\hbar\mathbf{k}$

$\mathbf{p}=\hbar\mathbf{k}$ → ● $m=+1$ $l=3,\ m=+2$

$\mathbf{p}=\hbar\mathbf{k}$ → ● $m=-1$

$\mathbf{p}=\hbar\mathbf{k}$ → ● $(m=-1)/\sqrt{2}$ & $(m=+1)/\sqrt{2}$

$n=6$

$\mathbf{p}=0$ → ◯ Any colour &

$\mathbf{p}=0$ → ◯ anticolour

$\mathbf{p}=\hbar\mathbf{k}$ → ● $m=+1$

$\mathbf{p}=\hbar\mathbf{k}$ → ● $m=+1$

$\mathbf{p}=\hbar\mathbf{k}$ → ● $m=+1$ $\mathbf{P}_{6k}=6\hbar\mathbf{k}$

$\mathbf{p}=\hbar\mathbf{k}$ → ● $m=+1$ $l=3,\ m=+2$

$\mathbf{p}=\hbar\mathbf{k}$ → ● $m=-1$

$\mathbf{p}=\hbar\mathbf{k}$ → ● $m=-1$

$n=7$

$\mathbf{p}=0$ → ◯ Any colour &

$\mathbf{p}=\hbar\mathbf{k}$ → ◯ $m=+1$ anticolour

$\mathbf{p}=\hbar\mathbf{k}$ → ● $m=+1$

$\mathbf{p}=\hbar\mathbf{k}$ → ● $m=+1$

$\mathbf{p}=\hbar\mathbf{k}$ → ● $m=+1$ $\mathbf{P}_{7k}=7\hbar\mathbf{k}$

$\mathbf{p}=\hbar\mathbf{k}$ → ● $m=-1$ $l=3,\ m=+2$

$\mathbf{p}=\hbar\mathbf{k}$ → ● $m=-1$

$\mathbf{p}=\hbar\mathbf{k}$ → ● $(m=-1)/\sqrt{2}$ & $(m=+1)/\sqrt{2}$

Figure 3.1.4 Eight preons forming $m=+2$ states as part of a positron superposition. If a zero spin and zero momentum preon absorbs a quantum its momentum becomes $\mathbf{p}=\hbar\mathbf{k}$ and its angular momentum becomes either $m=\pm1$, or an $m=0$ equal superposition of $m=\pm1$, states. When it does not absorb a quantum it remains at both spin zero and momentum $\mathbf{p}=0$. There is no significance in which preons have absorbed quanta.

3.2 Mass and Total Angular Momentum of Infinite Superpositions

3.2.1 Total mass of massive infinite superpositions

We will consider first the total mass of an infinite superposition, and to help illustrate, consider only one integral n eigenfunction ψ_{nk} at a time; temporarily assuming that the amplitude c_n of each ψ_{nk} has magnitude $|c_n| = 1$. Each time ψ_{nk} is born it borrows mass from a scalar Higgs field (or a zero point field time component) and momentum from a zero point field spatial component. The mass that it borrows is exactly cancelled by an equal debt in the Higgs scalar field (or the zero point field time component) so this sums to zero for all k. (This is a different way of looking at what generates mass; however, the end result is identical.) But what about the momenta borrowed from the spatial component of zero point fields, do these momenta also leave momentum debts in the vacuum? At any fixed value of k the momentum is a constant of the motion in a squared vector potential A^2. We can think of this as in any particular direction there is some probability of momentum $\mathbf{p}_{nk} = n\hbar\mathbf{k}$ due to this A^2 field. When interacting with the magnetic or the spatial component of any electromagnetic field the velocity squared factor β_{nk}^2 determines the rate of quanta absorbed.

Our wavefunctions ψ_{nk} are generated from a vector potential squared term A^2 derived in section 2.1.2 which in turn came from a B^2 type term as in section 2.1.1. As discussed in section 2.3.2 the eigenvalues $\mathbf{p}_{nk}^2 = n^2\hbar^2 k^2$ confirm the constant momentum squared feature of magnetic, or space mode interactions. Also in section 2.1.1 the scalar virtual photon emission probability is directly related to the force squared term $F^2 = \varepsilon^2 E^2$. Magnetic type coupling probabilities are related to a magnetic type force squared term $F^2 = \beta^2\varepsilon^2 B^2 / c^2 = \beta^2\varepsilon^2 E^2$, where from section 3.1.2 and Eqs. (3.1.14) & (3.1.15) the ratio of this scalar to magnetic coupling is β_{nk}^2. Thus when $k < \infty$ and the exchanged energy $E_X \neq \hbar\omega$, $\beta_{nk}^2 n$ quanta $|\hbar k|$ are absorbed from the vacuum and

$$\text{we can expect a momentum debt of } \mathbf{p}_{nk}(debt) = -\beta_{nk}^2 n\hbar\mathbf{k} \tag{3.2.1}$$

We could sum $\sum \mathbf{p}_{nk}^2$ & $\sum \mathbf{p}_{nk}^2(debt)$ but both vectors $\mathbf{p}_{nk}$ and $\mathbf{p}_{nk}(debt)$ are antiparallel in the same unknown direction. We can pair them together giving a nett momentum per pair of:

$$\mathbf{p}_{nk}(nett) = \mathbf{p}_{nk} + \mathbf{p}_{nk}(debt) = (1 - \beta_{nk}^2)n\hbar\mathbf{k} = \frac{n\hbar\mathbf{k}}{\gamma_{nk}^2} = \frac{\mathbf{p}_{nk}}{\gamma_{nk}^2} \text{ at wavenumber } k. \tag{3.2.2}$$

We have said above that the mass of each virtual particle is cancelled by an equal and opposite debt in the Higgs scalar field so we can now use the relativistic energy expression

$$E_n^2 = \sum_{k=0}^{k=\infty} \mathbf{p}_{nk}(nett)^2 c^2 \text{ times the probability of each pair at each wavenumber } k.$$

We will initially look at only $N = 1$ massive infinite superpositions in Eq. (2.2.4).

Thus, using probability $sN \cdot dk / k = s \cdot dk / k$, also Eqs. (3.1.11), (3.1.12), (3.1.13), & (3.2.2)

$$E_n^2 = c^2 \int_{k=0}^{k=\infty} \mathbf{p}_{nk}(nett)^2 \frac{s \cdot dk}{k} = c^2 \int_0^\infty \frac{n^2 \hbar^2 k^2}{\gamma_{nk}^4} \frac{s \cdot dk}{k} = 4m_0^2 c^4 \int_0^\infty \frac{K_{nk}^2}{(1+K_{nk}^2)^2} \frac{dK_{nk}}{2K_{nk}}$$

$$E_n^2 = m_0^2 c^4 \left[\frac{-1}{1+K_{nk}^2} \right]_0^\infty = m_0^2 c^4 \ \text{ or } \ E_n = \pm m_0 c^2 \tag{3.2.3}$$

This energy is due to summing momenta squared and it must be real, with a mass $\pm m_0$ for infinite superpositions of Eigenfunctions ψ_{nk}. These superpositions can form all the non-infinitesimal mass fundamental particles. The equations do not work if the mass m_0 is zero. (We will look at infinitesimal masses in section 6.2.) Negative mass solutions in Eq. (3.2.3) must be handled in the usual Feynman manner, and treated as antiparticles with positive energy going backwards in time. If they are spin ½ this also determines how they interact with the weak force.

3.2.2 Angular momentum of massive infinite superpositions

We will use the same procedure for the total angular momentum of $N=1$ type infinite superpositions with non-infinitesimal mass in Eq. (2.2.4).

Wavefunctions $\psi_{nk} = C_{nk} r^3 \exp(-n^2 k^2 r^2 / 18) Y(\theta, \varphi)$ have angular momentum squared eigenvalues $\mathbf{L}^2 = 12\hbar^2$ and the various m states have angular momentum eigenvalues $\mathbf{L}_z = m\hbar$. We will treat both angular momentum and angular momentum debts as real just as we did for linear momentum. Even though m state wavefunctions are part of superpositions they still have probabilities, just as the linear momenta squared above, and it seemed to work. Using exactly the same arguments as in section 3.2.1, if ψ_{nk} is in a state of angular momentum $\mathbf{L}_{zk} = m\hbar$, then it must leave an angular momentum debt in the vacuum of $\mathbf{L}_{zk}(debt) = -\beta_{nk}^2 m\hbar$ (or as in section 3.2.1) $\mathbf{L}_{zk}(nett) = \mathbf{L}_{zk} - \mathbf{L}_{zk}(debt)$.

$$\mathbf{L}_{zk}(nett) = (1 - \beta_{nk}^2) m\hbar = (1 - \beta_{nk}^2)\mathbf{L}_{zk} = \frac{\mathbf{L}_{zk}}{\gamma_{nk}^2} \quad (\text{if } \mathbf{L}_{zk} \text{ is in state } m\hbar) \tag{3.2.4}$$

But from Eq. (3.1.17) the probability that $\mathbf{L}_{zk}$ is in an m state is also β_{nk}^2 so that

$$\tag{3.2.5}$$

including this extra β_{nk}^2 probability term: $\mathbf{L}_{zk}(nett) = m\hbar \dfrac{\beta_{nk}^2}{\gamma_{nk}^2}$ at wavenumber k.

For an $N=1$ type infinite superposition $\mathbf{L}_z(Total) = \displaystyle\int_{k=0}^{k=\infty} \mathbf{L}_{zk}(nett) \frac{s \cdot dk}{k}. \ = sm\hbar \int_0^\infty \frac{\beta_{nk}^2}{\gamma_{nk}^2} \frac{dk}{2k}$

Using Eqs. (3.1.11) to (3.1.13) $\mathbf{L}_z(Total) = sm\hbar \displaystyle\int_0^\infty \frac{K_{nk}^2}{(1+K_{nk}^2)^2} \frac{dK_{nk}}{K_{nk}} \ = \frac{sm\hbar}{2}\left[\frac{-1}{1+K_{nk}^2} \right]_0^\infty$

$$\mathbf{L}_z(Total) = m'\hbar = \frac{sm\hbar}{2} \quad \text{ or } \quad m' = \frac{s}{2} m \tag{3.2.6}$$

Where m' is the angular momentum state of the infinite superposition and m the state of ψ_{nk}. Thus for spin ½ particles with $s = $ ½ in Eq. (3.2.6) $m' = m/4$ but m' can be only $\pm$ ½, implying the m state of ψ_{nk} that generates spin ½ must be $m = \pm 2$. An $N = 1$ massive spin 1 particle has $s = 1$ with $m' = m/2$. ($N = 2$ is covered in section 6.2.) This is summarized in the following three member infinite superpositions ignoring complex number factors.

$$\text{Massive } (N=1) \text{ Spin } \tfrac{1}{2}, \; \left|\psi_{\infty,1/2,\pm 1/2}\right\rangle = \sum_{n=5,6,7} c_n \int_{k=0}^{k=\infty} \left[\frac{\left|\psi_{nk,ss}\right\rangle}{\gamma_{nk}} + \beta_{nk} \left|\psi_{nk,\pm 2}\right\rangle \right] \sqrt{\frac{1}{2k}} dk \qquad (3.2.7)$$

$$\text{Massive } (N=1) \text{ Spin } 1, \; \left|\psi_{\infty,1,m}\right\rangle = \sum_{n=4,5,6} c_n \int_{k=0}^{k=\infty} \left[\frac{\left|\psi_{nk,ss}\right\rangle}{\gamma_{nk}} + \beta_{nk} \left|\psi_{nk,2m}\right\rangle \right] \sqrt{\frac{1}{k}} dk \qquad (3.2.8)$$

The spin vectors of each ψ_{nk} with $|\mathbf{L}| = 2\sqrt{3}\hbar$, and their spin vector debts in the zero point vector fields, have to be aligned such that the sum in each case is the correct value: $|\mathbf{L}| = \sqrt{3}\hbar/2$, $|\mathbf{L}| = \sqrt{2}\hbar$ or $|\mathbf{L}| = \sqrt{6}\hbar$ for spins ½, 1 & 2 respectively.

Spherically symmetric massive $N = 1$ spin 1 states are a superposition of three states $\frac{1}{\sqrt{3}}\left[\left|m'=-1\right\rangle + \left|m'=0\right\rangle + \left|m'=+1\right\rangle\right]$, and using Eq. (3.2.8) can be formed as follows

$$\text{Massive spin 1} \begin{bmatrix} \dfrac{1}{\sqrt{3}}\left|\psi_{\infty,1,m'=-1}\right\rangle = \dfrac{1}{\sqrt{3}} \sum_{n=4,5,6} c_n \int_{k=0}^{k=\infty} \left[\dfrac{\left|\psi_{nk,ss}\right\rangle}{\gamma_{nk}} + \beta_{nk} \left|\psi_{nk,m=-2}\right\rangle \right] \sqrt{\dfrac{1}{k}} dk \\[2em] + \dfrac{1}{\sqrt{3}}\left|\psi_{\infty,1,m'=0}\right\rangle = \dfrac{1}{\sqrt{3}} \sum_{n=4,5,6} c_n \int_{k=0}^{k=\infty} \left[\dfrac{\left|\psi_{nk,ss}\right\rangle}{\gamma_{nk}} + \beta_{nk} \left|\psi_{nk,m=0}\right\rangle \right] \sqrt{\dfrac{1}{k}} dk \\[2em] + \dfrac{1}{\sqrt{3}}\left|\psi_{\infty,1,m'=+1}\right\rangle = \dfrac{1}{\sqrt{3}} \sum_{n=4,5,6} c_n \int_{k=0}^{k=\infty} \left[\dfrac{\left|\psi_{nk,ss}\right\rangle}{\gamma_{nk}} + \beta_{nk} \left|\psi_{nk,m=+2}\right\rangle \right] \sqrt{\dfrac{1}{k}} dk \end{bmatrix} \qquad (3.2.9)$$

3.2.3   Mass and angular momentum of multiple integer n superpositions

In sections 3.2.1 & 3.2.2 for simplicity we looked at single integer n superpositions ψ_{nk}. For superpositions $\psi_k = \sum_n c_n \psi_{nk}$, we replace K_{nk}^2 with $\left\langle K_k \right\rangle^2$. Equation (2.3.9) appears to suggest $\left|\mathbf{p}_k\right|^2 = \sum_n c_n * c_n n^2 \hbar^2 k^2 = \left\langle n^2 \right\rangle \hbar^2 k^2$ and $\left\langle \left|\mathbf{p}_k\right| \right\rangle = \hbar k \sqrt{\left\langle n^2 \right\rangle}$. In section (3.5.1) we discuss why $\left\langle \left|\mathbf{p}_k\right| \right\rangle \neq \hbar k \sqrt{\left\langle n^2 \right\rangle}$ but $\left\langle \left|\mathbf{p}_k\right| \right\rangle = \hbar k \sum_n c_n * c_n \cdot n = \hbar k \left\langle n \right\rangle$. Thus using Eq. (3.1.11)

$$\left\langle K_k \right\rangle = \frac{\lambdabar_C k \sqrt{2s}}{2} \left\langle n \right\rangle \; \& \; \left\langle K_k \right\rangle^2 = \frac{\lambdabar_C^2 k^2 s}{2} \left\langle n \right\rangle^2 \text{ but } \left\langle K_k \right\rangle^2 \neq \frac{\lambdabar_C^2 k^2 s}{2} \left\langle n^2 \right\rangle \qquad (3.2.10)$$

Replacing K_{nk}^2 with $\left\langle K_k \right\rangle^2 = \lambdabar_C^2 k^2 s \left\langle n \right\rangle^2 / 2$ in the key equations (3.2.3) & (3.2.6) does not change the final results. The laws of quantum mechanics tell us the total angular momentum is

precisely integral $\hbar$ or half integral $\hbar/2$. Looking at the above integrals used to derive total angular momentum we see that N must be 1 (we discuss $N=2$ in section 6.2) and s must be exactly ½ or one for spin ½ & spin 1 massive particles respectively in our probability formula Eq. (2.2.4). Also, these integrals are infinite sums of positive and negative integral $\hbar$ that are virtual and cannot be observed. If an infinite superposition for an electron is in a spin up state and flips to spin down in a magnetic field, a real $m=\pm1$ photon is emitted carrying away the change in angular momentum. This is the only real effect observed from this infinity of $(l=3, m=+2)$ virtual wavefunctions all flipping to $(l=3, m=-2)$ states, plus an infinite flipping of the virtual zero point vector debts. Also, Eqs. (3.2.3) and (3.2.6) are true only if our high energy cutoff is at infinity and the low frequency cutoff is at zero. We look at high energy Planck scale cutoffs in section 4.2 and in section 6 low energy cutoffs near the radius of the causally connected horizon.

3.3   Ratios between Primary and Secondary Coupling

3.3.1   Initial simplifying assumptions

This section is based on a special case thought experiment that tries to illustrate, hopefully in a simple way, how superpositions interact with one another; in the same way as virtual photons, for example, interact with electrons. It is unfortunately long and not very rigorous, but it illustrates how, in all interactions between fundamental particles represented as infinite superpositions, the actual interaction is between only the same k single wavenumber superpositions of each particle. We will later conjecture that an interacting virtual particle is a single wavenumber k superposition only, and not a full infinite superposition. Only real particles whose properties we can measure are full infinite superpositions. The full properties do not exist until measurement, just as in so many other examples in quantum mechanics. This will be clearer as we proceed. It is also important to remember here, that because primary coupling constants are to bare charges (section 2.2.2), and thus fixed for all k, while secondary coupling constants run with k, the coupling ratios can be defined only at the cutoff value of k applying to the bare charge (sections 4.1.1 & 4.2.2). From Table **2.2.1** there are six fundamental primary charges for electrons and positrons. But electrons and positrons are defined as fundamental charges. In other words, what we define as a fundamental electric charge is in reality six primary charges. Of course, we can never in reality measure six as their effect is reduced by the ratio between primary and secondary coupling. Because electromagnetic and colour coupling are both via spin one bosons their coupling ratios are fundamentally the same, but because of the above they are related as $6^2 = 36:1$.

$$\frac{1}{\chi_{Colour}} = \frac{36}{\chi_{EM}} \qquad (3.3.1)$$

We define the colour and electromagnetic ratios as follows (leaving gravity till section 6.2.6)

$$\frac{1}{\chi_{Colour}} = \frac{\alpha_{Colour\,(Secondary)}}{\alpha_{Colour\,(Primary)}} = \frac{\alpha_{3S}}{\alpha_{3P}} \qquad \text{and} \qquad \frac{1}{\chi_{EM}} = \frac{\alpha_{EM\,(Secondary)}}{\alpha_{EM\,(Primary)}} = \frac{\alpha_{EMS}}{\alpha_{EMP}} \qquad (3.3.2)$$

The secondary coupling constants α_{EMS} & α_{3S} are the bare charge values, both at the fermion interaction cutoff near the Planck length Eq. (4.2.10). Also we assumed in section 2.2.2 that $\alpha_{3P} = 1$; thus from Eq. (3.3.2)
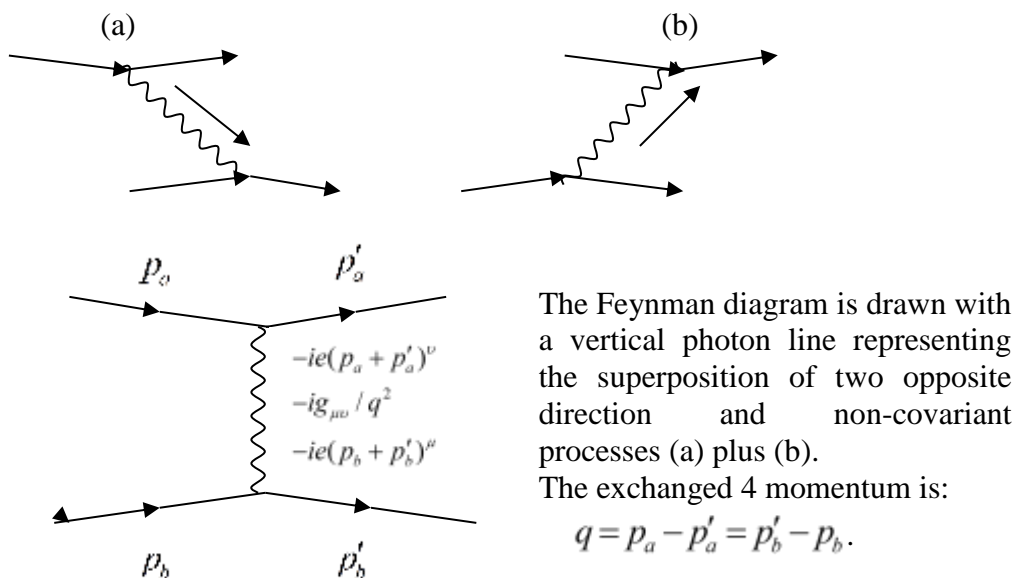
$$\chi_C = \alpha_{3S}^{-1} = \alpha_3^{-1} @ k_{cutoff} \approx 2.029 \times 10^{18} GeV \qquad (3.3.3)$$

In other words, provided $\alpha_{3P} = 1$, the ratio χ_C (or χ_{Colour}) is also the inverse of the colour coupling constant α_3 at the high energy interaction cutoff near the Planck length. In this respect χ_C or χ_{Colour} is the fundamental ratio we will use mainly from here on. From the above paragraphs, to find the coupling ratios we need secondary interactions that are between bare charges. But this implies extremely close spacing where the effects of spin dominate. If the spacing is sufficiently large the effects of spin can be ignored but then we are not looking at bare charges. However, we can ignore the effects of shielding due to virtual charged pairs by imagining, as a simple thought experiment, an interaction between bare charges even at such large spacing. We can also simplify things further by considering only scalar or coulomb type elastic interactions at this large spacing. We are also going to temporarily ignore Eq. (3.3.2) and imagine that we have only one primary electric and or one colour charge. Consider two superpositions and (due to the above simplifying assumptions) imagine them as spin zero charges. QED considers the interaction between them as a single covariant combination of two separate and opposite direction non-covariant interactions (a) plus (b) as in the Feynman diagram of Figure 3.3.1 below. The Feynman transition amplitude is invariant in all frames [22], so let us consider a special simple case in a CM frame where we have identical particles on a head-on (elastic) collision path with spatial momenta:

$$\mathbf{p}_a = -\mathbf{p}'_a = -\mathbf{p}_b = +\mathbf{p}'_b \qquad (3.3.4)$$

From Eq. (3.3.4) the initial and final spatial momenta are reversed with mirror images of each other at each vertex. Of course, when we know momenta accurately we have no idea where the particles are when this takes place, so in reality there is no head-on collision. We are also going to assume in what follows that the vertices of this interaction are on opposite sides of the interacting boson superposition. While we have no idea where this boson superposition is centred, what we do know in this simple special scalar case is that the transferred four momentum squared is simply the transferred three momentum squared, and ignoring the minus sign for q^2 (due to i^2) in what we are doing here for simplicity we can say :

$$q^2 = (p_a - p'_a)^2 = (p_b - p'_b)^2 = 4\mathbf{p}_a^2 = 4\mathbf{p}_b^2. \qquad (3.3.5)$$

(a)　　　　　　　　　　(b)

p_a　　　　　p_a'

$-ie(p_a + p_a')^\nu$

$-ig_{\mu\nu}/q^2$

$-ie(p_b + p_b')^\mu$

p_b　　　　　p_b'

The Feynman diagram is drawn with a vertical photon line representing the superposition of two opposite direction and non-covariant processes (a) plus (b).
The exchanged 4 momentum is:

$$q = p_a - p_a' = p_b' - p_b.$$

Figure 3.3.1 Feynman diagram of virtual photon exchange between two spin zero particles of charge e.

$\frac{4\pi}{k} R*R$

$\psi_{7k}(n=7)$

$\psi_{6k}(n=6)$　　Spin ½ Fermion superpositions

$\psi_{5k}(n=5)$　　Massive spin 1 Boson superpositions

$\psi_{4k}(n=4)$

$\psi_{3k}(n=3)$　　Infinitesimal mass spins 1 & 2 Boson superpositions

$\rightarrow kr$
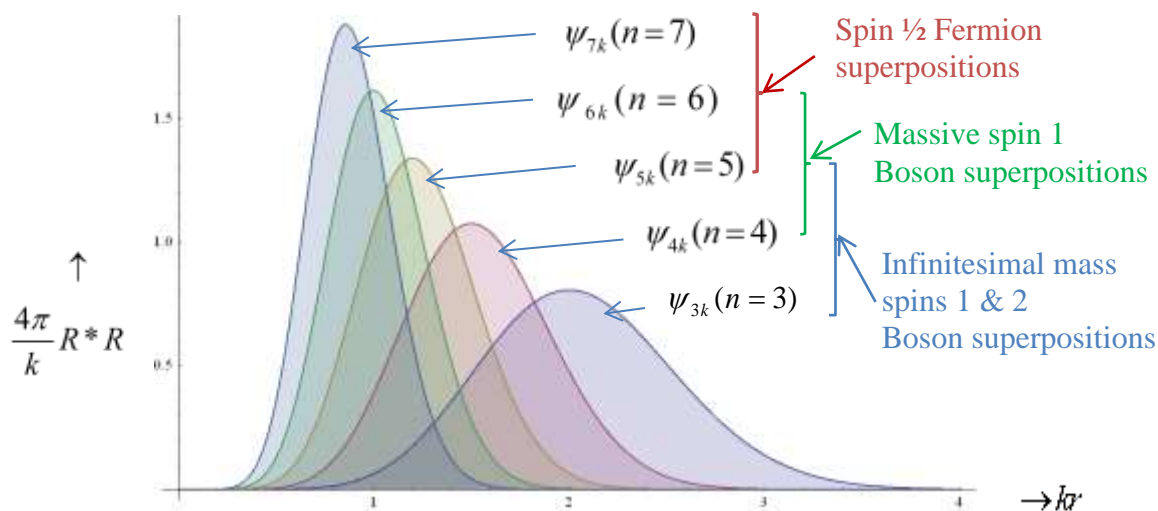
Figure 3.3.2 All eigenfunctions ψ_{nk} in the groups of three overlap at a fixed wavenumber k.

If we look at Figure 3.3.2 we see that at any fixed value of k, all modes ψ_{nk} in the groups of three overlapping superpositions for the various spins ½, 1 & 2 occupy similar sized regions of space. The directions of their linear momenta are unknown but let us imagine some particular vector $\hbar\mathbf{k}$ that is parallel to the above vectors $\mathbf{p}_a = \mathbf{p}_b$. As we are considering only scalar interactions, all these modes must be spherically symmetric or time polarized. Equation (3.1.16) says spherical symmetry is $\propto 1/\gamma_{nk}$ and Eqs. (3.1.11) and (3.1.12) tell us $\gamma_{nk} \to 1$ as $\beta_{nk} \to 0$. But we are considering bare charges at large spacings where the exchanged virtual photons have small momenta and are time polarized as in Eq. (3.1.15). At a fixed value of k they thus have momenta $\pm n\hbar\mathbf{k}$. Also, as they overlap each other, we can imagine units of $\pm\hbar\mathbf{k}$ quanta somehow transferring between these superpositions so that the values of n in each mode can change temporarily by ± 1 for times $\Delta T \approx \hbar/\Delta E$. The directions of these

momentum transfers causing either repulsion or attraction depending on the charge signs of the superpositions at each vertex, whether the same or opposite.

3.3.2 Restrictions on possible eigenvalue changes

Before we look at changing these eigenvalues by $n = \pm 1$ we need to consider what restrictions there are on these changes.

From Eq. (2.3.12) superposition ψ_k requires $Q^2 A^2 = \sum_n c_n * c_n \frac{n^4 \hbar^2 k^4 r^2}{81}$ and Eq. (2.2.4) informs

us the available $Q^2 A^2 = \frac{\left[8 + 8\sqrt{\alpha_{EMP}}\right]^2}{3\pi sN} \hbar^2 k^4 r^2$ occurs with probability $= \frac{sN \cdot dk}{k}$.

For very brief periods the required value of $Q^2 A^2$ can fluctuate, such as during these changes of momentum, but if its average value changes over the entire process then Eq. (2.2.4) says that the probability $sN \cdot dk / k$ changes also, and we have shown in section 3.2.1 that this is disallowed. For example, in a spin ½ superposition $\psi_{5k}, \psi_{6k}, \psi_{7k}$, (see Table 4.3.1) the average values of $|c_5|, |c_6| \& |c_7|$ must each remain constant. This can only happen if n remains within its pre-existing boundaries of $(5 \leq n \leq 7)$. For example, if ψ_7 adds $+\hbar\mathbf{k}$ (we will ignore the subscript k in ψ_{nk} from here assuming that it will be understood) it can create ψ_8, but $|c_8|$ must average zero, which it can do only if it fluctuates either side of zero, and $|c_n|$ cannot be negative. Similarly $|c_4|$ must average zero, thus $\psi_4 \& \psi_8$ are forbidden fermion superposition states. Keeping the average values of $|c_n|$ constant is also equivalent to a constant internal average particle energy (we have shown in section 3.2.1 that rest mass is a function of $\sum c_n * c_n . \mathbf{p}_{nk}^2$). By changing these eigenvalues by $n = \pm 1$ there are only four possibilities: $\psi_6 \& \psi_7$ can both reduce by $-\hbar\mathbf{k}$ quanta; $\psi_6 \& \psi_5$ can both increase by $+\hbar\mathbf{k}$ quanta. If ψ_6 becomes ψ_7, $|c_7|$ also increases and $|c_6|$ decreases, but then ψ_7 has to drop back becoming ψ_6, with $|c_7|$ decreasing back down and $|c_6|$ increasing back up in exact balance. If we view this as one overall process the average values of both $|c_6|$ and $|c_7|$ remain constant but fluctuate continuously. We can use exactly the same argument if ψ_5 increases which has to be followed by ψ_6 dropping, where if we view this as one process again, the average values of both $|c_5|$ and $|c_6|$ remain constant. This is similar to a particle not being able to absorb a photon in a covariant manner, it has to re-emit within time $\Delta T \approx \hbar / E$. Just as transversely polarized photons are the equal left and right superposition of circular polarizations $|L\rangle / \sqrt{2} + |R\rangle / \sqrt{2}$, we can perhaps express Eq. (2.3.9) $\mathbf{p}_{nk}^2 = n^2 \hbar^2 k^2$ as equivalent to:

$$\mathbf{p} = \pm n\hbar\mathbf{k} \text{ is the equal superposition } \mathbf{p} = |+n\hbar\mathbf{k}\rangle / \sqrt{2} + |-n\hbar\mathbf{k}\rangle / \sqrt{2}. \qquad (3.3.6)$$

This superposition is in opposite directions of the vector $\mathbf{k}$, implying equal 50% probabilities of momentum vectors for any pair of opposite directions. (It is a virtual superposition so neither of these two components can be observed.) Thus if n changes by +1 say, there are equal 50% probabilities of the momentum transfers $\mathbf{p} = +\hbar\mathbf{k}$ and $\mathbf{p} = -\hbar\mathbf{k}$. And the same is true if n changes by -1. Spin 1 bosons transfer momentum $\Delta\mathbf{p} = \pm\hbar\mathbf{k}$, which means that two 50% probability transfers are required, such as $\psi_{5k} \rightarrow \psi_{6k}$ combined with a $\psi_{6k} \rightarrow \psi_{5k}$ provided the momentum directions add appropriately as in the Figure 3.3.3 top diagram But if

$\psi_{5k} \rightarrow \psi_{6k}$ and $\psi_{6k} \rightarrow \psi_{5k}$, with $\mathbf{p} = \pm n\hbar\mathbf{k}$ keeping the same sign during this process, there is no nett 3 momentum transfer as in the lower half of Figure 3.3.3. The probability of these two processes is identical, and we will use this same probability for spin 2 graviton probability densities when looking at gravity which Einstein showed is not a force, as particles simply follow geodesics in the warped spacetime surrounding any mass. For all the two way transitions at both vertices, similar to those discussed above, the following is true:

Probability of all transitions similar to $\psi_5 \rightleftarrows \psi_6$ is equal in either direction. (3.3.7)

As we are looking at virtual interactions between fermions and bosons we will use subscripts *a* for spin ½ and *b* for spins 1 and 2 superpositions in what follows.
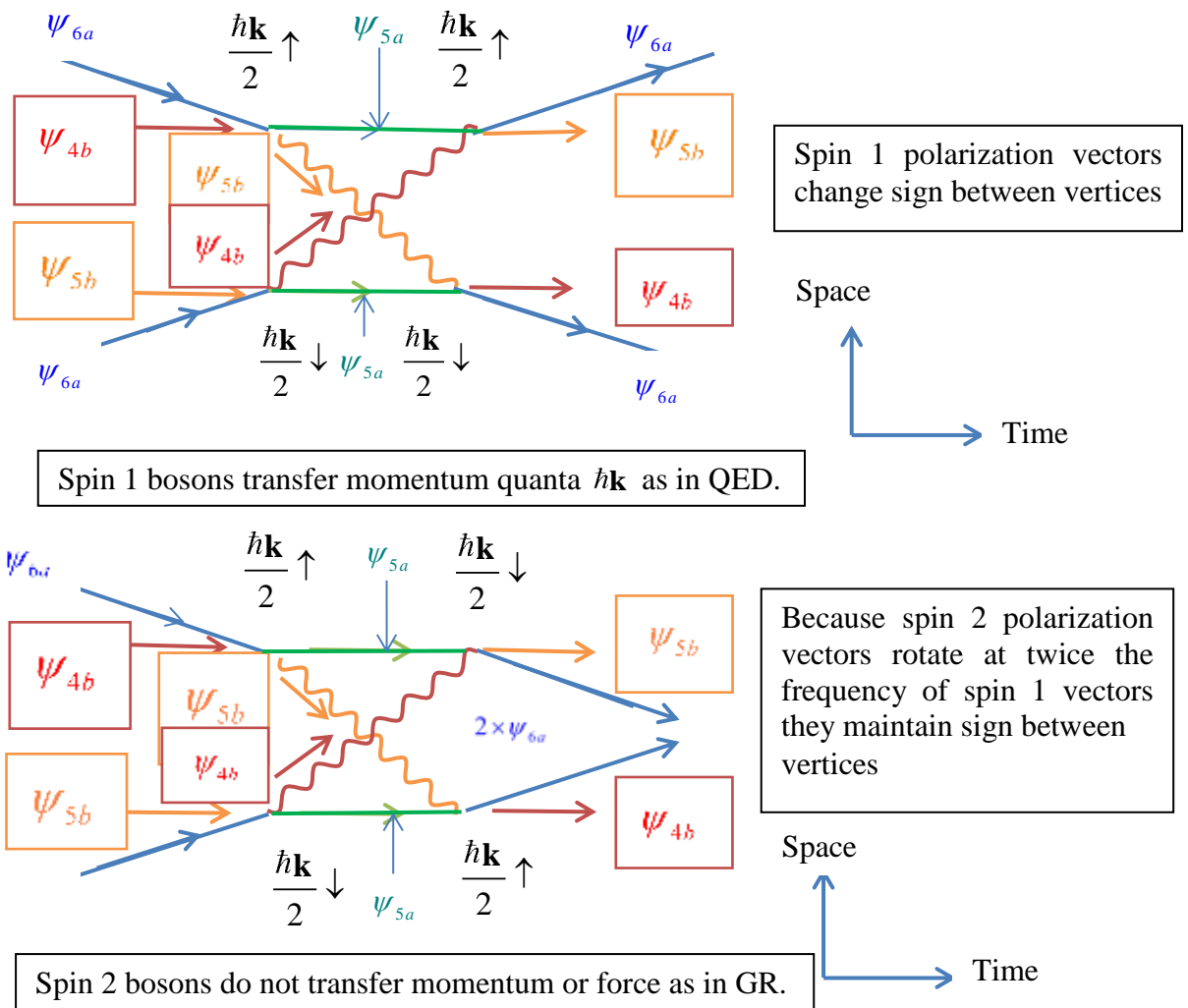
Figure 3.3.3 Covariant interaction (as in Eq. (3.3.4) and Figure 3.3.1) between fermion (subscript a) and boson (subscript *b* and in boxes) eigenfunctions, with spin 1 photons in the top diagram, and spin 2 gravitons in the bottom diagram. Orange and magenta are used for bosons, blue and green for spin 1/2 to help identify the transitions at each of the four spacetime corners. This is one process, but a superposition of two diagonal components splitting the 3 momentum $\hbar\mathbf{k}$ equally. Momentum is transferred in the spin 1 case only, but real spin 2 gravitons however, as in gravitational waves from rotating binary pairs for example, do carry energy and momentum,

We can think of the interactions in both the top and bottom of Figure 3.3.3 as a spacetime rectangle. Starting with the top left corner, the key factors are the superposition component/member amplitudes c_{6a} & c_{4b}, then proceeding clockwise (the order is irrelevant) c_{5a} & c_{4b}, c_{5a} & c_{5b}, and finally c_{6a} & c_{5b}. As this is part of one process, we can rearrange all terms and multiply them to get $(c_{4b} * c_{4b})(c_{5b} * c_{5b})(c_{6a} * c_{6a})(c_{5a} * c_{5a})$.
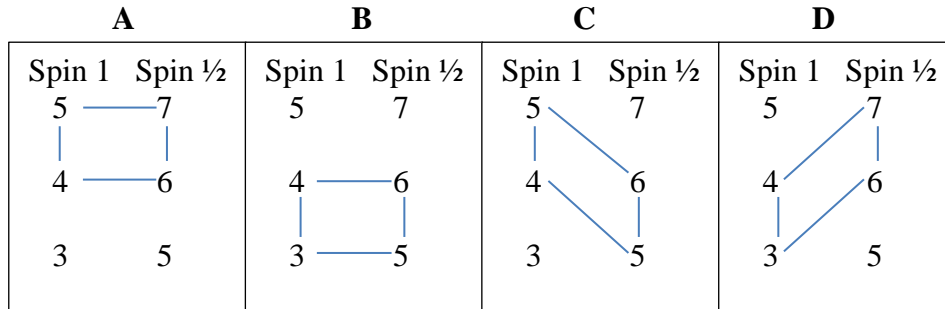
Putting $P_{4b} = c_{4b} * c_{4b}$, $P_{5a} = c_{5a} * c_{5a}$etc.

$$(c_{4b} * c_{4b})(c_{5b} * c_{5b})(c_{6a} * c_{6a})(c_{5a} * c_{5a}) \equiv P_{4b} P_{5b} P_{6a} P_{5a} \tag{3.3.8}$$

However, our superposition members (ψ_{nk} shortened to ψ_n) are all Eigenfunctions with Eigenvalues $\mathbf{p}_{nk}^2 = n^2 \hbar^2 k^2$ having equal probabilities of momentum vectors $\mathbf{k}$ pointing in opposite directions, as in Eq.(**3.3.7**) and the following paragraph. Thus, we can interchange the red and orange boson ψ_{4b} & ψ_{5b} and also the blue and green fermion ψ_{5a} & ψ_{6a} in Figure 3.3.3 with no change in exchanged momentum. These four possibilities increase the amplitude factor for this group by four, so that (if all other factors are one) Eq. (**3.3.8**) becomes:

$$2^2 (c_{4b} * c_{4b})(c_{5b} * c_{5b})(c_{6a} * c_{6a})(c_{5a} * c_{5a}) \equiv 4 P_{4b} P_{5b} P_{6a} P_{5a} \tag{3.3.9}$$

But there are four different groups of four Eigenfunctions **A, B, C & D** as in Figure 3.3.4 below, and we have only been considering group **C** above.

A		B		C		D	
Spin 1	Spin ½	Spin 1	Spin ½	Spin 1	Spin ½	Spin 1	Spin ½
5	7	5	7	5	7	5	7
4	6	4	6	4	6	4	6
3	5	3	5	3	5	3	5

Figure 3.3.4 Interaction between the four Eigenfunction groups A, B, C and D

Using Eq. (**3.3.9**), if all other factors are one the amplitudes for the groups in Figure 3.3.4 are:

$$A = 4(c_{4b} * c_{4b})(c_{5b} * c_{5b})(c_{6a} * c_{6a})(c_{7a} * c_{7a}) = 4 P_{4b} P_{5b} P_{6a} P_{7a} \tag{3.3.10}$$
$$B = 4(c_{3b} * c_{3b})(c_{4b} * c_{4b})(c_{6a} * c_{6a})(c_{5a} * c_{5a}) = 4 P_{3b} P_{4b} P_{6a} P_{5a}$$
$$C = 4(c_{4b} * c_{4b})(c_{5b} * c_{5b})(c_{6a} * c_{6a})(c_{5a} * c_{5a}) = 4 P_{4b} P_{5b} P_{6a} P_{5a}$$
$$D = 4(c_{3b} * c_{3b})(c_{4b} * c_{4b})(c_{6a} * c_{6a})(c_{7a} * c_{7a}) = 4 P_{4b} P_{5b} P_{6a} P_{7a}$$

These amplitudes are all numbers as $P_{4b} = c_{4b} * c_{4b}$, $P_{5a} = c_{5a} * c_{5a}$etc. are just probabilities. But we can perhaps imagine these numbers as in the complex plane. From section 2.2.2 and Figure 3.1.4, however, the three eigenfunctions forming each of the interacting particles are born simultaneously. It would thus seem reasonable to assume that the amplitudes of each group of three eigenfunctions have the same complex phase angle. So whether they are in the complex plane or not, provided they are all at the same angle we can get the overall

probability of this virtual exchange by simply adding the four amplitudes *A,B,C&D* from Eq. (**3.3.10**) and squaring the total to get:

Overall interaction probability if all other factors are one $= (A+B+C+D)^2$

$$= 16\left[P_{4b}P_{5b}P_{6a}P_{7a} + P_{3b}P_{4b}P_{6a}P_{5a} + P_{4b}P_{5b}P_{6a}P_{5a} + P_{3b}P_{4b}P_{6a}P_{7a} \right]^2 \quad (3.3.11)$$

$$= 16\left[P_{4b}(P_{3b} + P_{5b}) \right]^2 \left[P_{6a}(P_{5a} + P_{7a}) \right]^2$$

Using different colours again for common terms in each of the equations following and then using $c_{3b}*c_{3b} + c_{4b}*c_{4b} + c_{5b}*c_{5b} = c_{5a}*c_{5a} + c_{6a}*c_{6a} + c_{6a}*c_{6a} = 1$ the interaction probability is

$$(A+B+C+D)^2 = 2^4\left[c_{4b}*c_{4b}(1 - c_{4b}*c_{4b}) \right]^2 \left[c_{6a}*c_{6a}(1 - c_{6a}*c_{6a}) \right]^2 \quad (3.3.12)$$

We have assumed to here that all other amplitude factors are one. However at each vertex there are both fermion and boson superposition probabilities from Eq. (2.2.4). *Writing the superposition probability at each vertex $sN \cdot dk/k$ as $s_{1/2}N_1 dk/k$, $s_1 N_2 dk/k$ for clarity* where spin $1 = s_1$, $N = 1$ is N_1 etc. Including these factors (if all other factors are one) in Eq. (3.3.12) our overall probability at wavenumber k is

$$\left[\frac{2s_{1/2}N_1 c_{6a}*c_{6a}(1 - c_{6a}*c_{6a})}{k} \right]^2 \left[\frac{2s_1 N_2 c_{4b}*c_{4b}(1 - c_{4b}*c_{4b})}{k} \right]^2$$

$$= \frac{\left[2s_{1/2}N_1 c_{6a}*c_{6a}(1 - c_{6a}*c_{6a}) \right]^2 \left[2s_1 N_2 c_{4b}*c_{4b}(1 - c_{4b}*c_{4b}) \right]^2}{(k)^4}.$$

The momentum per transfer is a total of $\pm\hbar\mathbf{k}$ and using Eqs. (3.3.5), (3.3.6) & $(\pm\hbar\mathbf{k})^4 = q^4$ then putting $\hbar = 1$ the interaction probability is

$$\frac{\left[2s_{1/2}N_1 c_{6a}*c_{6a}(1 - c_{6a}*c_{6a}) \right]^2 \left[2s_1 N_2 c_{4b}*c_{4b}(1 - c_{4b}*c_{4b}) \right]^2}{q^4} \quad (3.3.13)$$

This is the scalar interaction probability between two spin ½ fermions exchanging infinitesimal rest mass spin 1 bosons at very large spacings, where the fermions are effectively spin zero, imagining them as bare charges and all other factors being one. When exchanging spin 2 infinitesimal rest mass time polarized gravitons (as in the bottom half of Figure 3.3.3 with no 3 momentum) we can simply keep using wavenumber k in the denominator for the interaction probability between fermions and gravitons. If all other amplitude factors are one this interaction probability becomes (using subscript c for spin 2 and $N = 2 = N_2$ for clarity):

$$\frac{\left[2s_{1/2}N_1 c_{6a}*c_{6a}(1 - c_{6a}*c_{6a}) \right]^2 \left[2s_2 N_2 c_{4c}*c_{4c}(1 - c_{4c}*c_{4c}) \right]^2}{k^4} \text{ gravitons \& fermions.} \quad (3.3.14)$$

And if, for example, two spin 1 photons exchange spin 2 gravitons (all infinitesimal rest mass with $N = 2 = N_2$) the interaction probability if all other amplitude factors are one becomes

$$\frac{\left[2s_1 N_2 c_{4b} * c_{4b}(1 - c_{4b} * c_{4b})\right]^2 \left[2s_2 N_2 c_{4c} * c_{4c}(1 - c_{4c} * c_{4c})\right]^2}{k^4} \text{ for } N = 2 \text{ photons.}$$ (3.3.15)

If two massive $N = 1$ photons (as in Figure 3.3.2) exchange spin 2 gravitons the interaction probability if all other factors are one becomes

$$\frac{\left[2s_1 N_1 c_{5b} * c_{5b}(1 - c_{5b} * c_{5b})\right]^2 \left[2s_2 N_2 c_{4c} * c_{4c}(1 - c_{4c} * c_{4c})\right]^2}{k^4} \text{ for } N = 1 \text{ photons.}$$ (3.3.16)

According to GR (section 1.2.2) the emission of gravitons is identical for both mass and energy. Keeping all other factors (such as mass/energy) in Eqs. (3.3.14), (3.3.15) and (3.3.16) constant, the graviton interaction probabilities must be the same in each. We can thus put them equal to each other and cancel out all the common red terms on the RH sides above:

$$2s_1 N_2 c_{4b} * c_{4b}(1 - c_{4b} * c_{4b}) = 2s_1 N_1 c_{5b} * c_{5b}(1 - c_{5b} * c_{5b}) = 2s_{1/2} N_1 c_{6a} * c_{6a}(1 - c_{6a} * c_{6a})$$

or (3.3.17)

$$4c_{4b} * c_{4b}(1 - c_{4b} * c_{4b}) = 2c_{5b} * c_{5b}(1 - c_{5b} * c_{5b}) = c_{6a} * c_{6a}(1 - c_{6a} * c_{6a})$$
$$N = 2 \text{ Spin 1} \qquad\qquad N = 1 \text{ Spin 1} \qquad\qquad N = 1 \text{ Spin 1/2}$$

In this special case as in Eq. (**3.3.4**) we have shown that the time polarized interaction probabilities are the same whether 3 momentum is exchanged or not, and this equation for the above ratios is identical for both virtual spin 2 graviton and virtual spin 1 photon exchanges. Ignoring complex numbers for simplicity, we can use either 4 momentum q or wavenumber k interchangeably. Now assume that all other factors (other than coupling constants) are one, and remember that we are simplifying with a thought experiment by looking at spin ½ superpositions sufficiently far apart so we can treat them as approximately spherically symmetric or effectively spin zero, even if they are supposed to be bare charges with spin. Under these same scalar exchange conditions QED says that with electrons, for example:

The probability of scalar spin one photon exchange in Eq. (3.3.13) $= \dfrac{4\alpha^2}{q^4}$. (3.3.18)

(This probability is for one momentum k direction only, but the mode density of these is
$k^2 dk / \pi^2$. *We can perhaps think of* $\dfrac{4\alpha^2}{k^4} \cdot \dfrac{k^2 dk}{\pi^2} = \left(\dfrac{2\alpha}{\pi k}\right)^2 dk$ *as an imaginary emission*
probability $\dfrac{2\alpha}{\pi}\dfrac{dk}{k}$, *multiplied by an imaginary absorption probability* $\dfrac{2\alpha}{\pi}\dfrac{dk}{k}$ *in all possible*
directions.

The rest of this paper is mainly about virtual particles which cannot be experimentally detected. However, as we will see, imaginary probability densities can have real world consequences. This is similar to our postulated infinite virtual superpositions being undetectable, but the particles they generate can certainly be experimented on in the real world.

This paper uses these imaginary probabilities throughout, as it allows a very simple approximate way to look at gravity using only very long wavelength time polarized gravitons. We demonstrate how it works in the next section on electromagnetic energy between charges. Let us now temporarily ignore the fact that gluons have limited range and imagine our thought experiment applying to colour charges exchanging gluons. The α of Eq. (3.3.18) becomes the usual colour coupling α_3. To get the fundamental coupling ratio labelled as $\chi_C = \alpha_3^{-1}$ @ k_{cutoff} we substitute the α of Eq. (3.3.18) with $\alpha = \chi_C^{-1}$ as we assumed $\alpha_3(Primary) = 1$. Substituting $2s_{1/2} = 1$, $2s_1 = 2$, $N_1 = 1$ & $N_2 = 2$ and equating Eqs. (3.3.13) & (3.3.18)

$$\frac{\left[c_{6a}*c_{6a}(1-c_{6a}*c_{6a})\right]^2 \left[4c_{4b}*c_{4b}(1-c_{4b}*c_{4b})\right]^2}{q^4} = \frac{4(\chi_C^{-1})^2}{q^4}$$

$$\left[c_{6a}*c_{6a}(1-c_{6a}*c_{6a})\right]\left[4c_{4b}*c_{4b}(1-c_{4b}*c_{4b})\right] = 2\chi_C^{-1} \qquad (3.3.19)$$

But from Eq. (3.3.17) the blue and green terms are equal (also the magenta terms) and we can solve for the fundamental coupling ratio by combining Eqs. (3.3.17) & (3.3.19).

$$N = 2 \ \text{Spin 1} \qquad N = 1 \ \text{Spin 1} \qquad N = 1 \ \text{Spin 1/2} \qquad (3.3.20)$$

Photons or Gluons   Massive Photons   Fermions

$$4c_{4b}*c_{4b}(1-c_{4b}*c_{4b}) = 2c_{5b}*c_{5b}(1-c_{5b}*c_{5b}) = c_{6a}*c_{6a}(1-c_{6a}*c_{6a}) = \sqrt{2/\chi_C}$$

The coupling ratio is fundamentally the same for colour and electromagnetism apart from the six primary electric charges of Eq. (3.3.1) because of the way electric charge is defined. Equations (3.3.17), (3.3.19) & (3.3.20) tell us that for any interactions between two superpositions, the inverse coupling ratio always involves the product of the central superposition member probability by the probability of the other two members combined $\times N \times spin$ of the first superposition, times the equivalent product for the other superposition. In section 4 we introduce gravity and solve these ratios. Despite all the simplifications and lack of rigour, the above equations are surprisingly consistent with the SM, provided there are only three families of fermions. Even though we used gravity to derive Eq. (3.3.17) we leave discussing the gravity coupling ratio till section 6.2.6.

3.4   Electrostatic Energy between two Infinite Superpositions

3.4.1   Using an approximate but simple quantum mechanical approach

In section 3.3 we showed that fermion superpositions can exchange boson superpositions in the same way as electrons can exchange virtual photons for example. Providing the superposition amplitudes are appropriate, the coupling constants can be just as in QED, though we will look further at this in section 4.1.1. So, it might seem that evaluating electrostatic energy between superpositions is unnecessary. However, when we look at

gravity, we find that the spacetime warping around mass concentrations could possibly be related to cosmic wavelength virtual graviton probability densities. Virtual particle exchange probabilities, in QED/QCD etc, use perturbation theory to calculate particle scattering cross-sections, and electron g factor corrections with incredible precision. Both space and time polarizations are involved. However, as we later focus on virtual cosmic wavelength graviton probability densities at large spacings, we will use a simple but only approximate (but true at large spacings) quantum mechanical method based on only time polarized photon probability densities to find the scalar potentials between two charges (or infinite superpositions). This same method also allows a simple solution to the magnetic energy between superpositions (again at large spacings) in section 3.5, where we modify relevant equations in a simple manner. In section 5 we will use some of these same equations when looking at why borrowing energy and mass from zero point fields requires the universe to expand after the Big Bang and distort spacetime around mass concentrations. We assume spherically symmetric $l = 3$ superpositions emit virtual scalar (time polarized) photons in this section and $l = 3, m = \pm 2$ superpositions emit virtual $m = \pm 1$ photons in section 3.5. As section 3.3 has shown that we can achieve the same electromagnetic coupling constant α we can use the scalar photon emission probability $(2\alpha / \pi)(dk / k)$ covered in section 2.1.1 and the section in italics after Eq.(**3.3.18**). From section 3.3 we can also see that the effective average emission point has to be the centre of superpositions. For a virtual photon $\Delta E \cdot \Delta T \leq \hbar / 2$, and the range over which it can be found is roughly $r \approx \Delta T \approx 1/2\Delta E \approx 1/2k$ when $\hbar = c = 1$. The radial probability of finding the centre of the spin 1 superposition representing the interacting virtual photon decays exponentially with radius as e^{-2kr}. The normalized wavefunction ψ for such a virtual scalar photon of wave number k emitted at $r = 0$ is:

$$\psi = \sqrt{\frac{2k}{4\pi}} \, \frac{e^{-kr}e^{+i(kr-\omega t)}}{r} = \sqrt{\frac{2k}{4\pi}} \, \frac{e^{-kr}e^{+ikr}}{r} \quad @ \text{ time } t = 0.$$
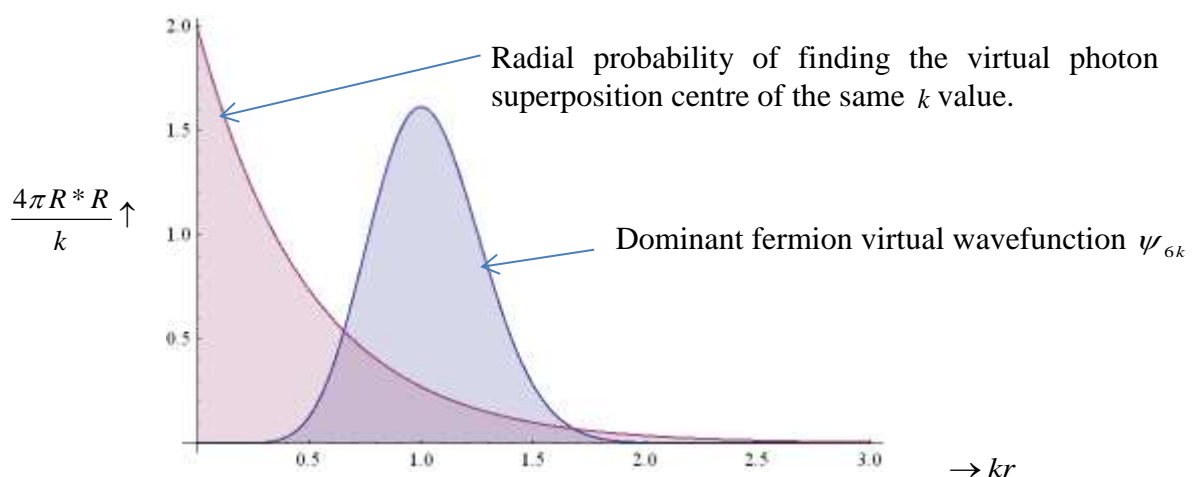
Figure 3.4.1 Radial probabilities of ψ_{6k} and the exponential decay with radius of a virtual photon of the same k value $R^*R \propto 2ke^{-2kr}$. These curves look the same for all k, applying equally to virtual photons, gravitons and to large k value gluons etc.

Wavefunction ψ is spherically symmetric as scalar photons are time polarized. Figure 3.4.1 plots the radial probabilities of the exponentially decaying virtual photon and the dominant $n = 6$ mode of its relating superposition Ψ_k. The effective range of a wavenumber k virtual photon is of a similar order to the radial probability dimensions of ψ_{6k}. For simplicity, in what follows we locate two superpositions (which we refer to as sources) in cavities that are small in relation to the distance between them. The accuracy of our results depends on how far apart they are in relation to the cavity size. Consider two spherically symmetric sources distance $2C$ apart emitting virtual scalar photons as in Figure 3.4.2 where point P is r_1 from source one, and r_2 from source 2. Let ψ_1 be the amplitude from source one, and ψ_2 be the amplitude from source two and for simplicity and clarity let $t = 0$.

$$\text{Thus} \qquad \psi_1 = \sqrt{\frac{2k}{4\pi}} \frac{e^{-kr_1 + ikr_1}}{r_1} \quad \& \quad \psi_2 = \sqrt{\frac{2k}{4\pi}} \frac{e^{-kr_2 + ikr_2}}{r_2} \qquad (3.4.1)$$

Consider $\quad (\psi_1 + \psi_2) * (\psi_1 + \psi_2) \quad = \psi_1 * \psi_1 + \psi_1 * \psi_2 + \psi_2 * \psi_1 + \psi_2 * \psi_2$

Now $\psi_1 * \psi_1 \quad \& \quad \psi_2 * \psi_2$ are just the normal probability densities around sources one and two as though they are infinitely far apart but the work done per pair of superpositions k on bringing two sources closer together is in the interaction term: $\psi_1 * \psi_2 + \psi_2 * \psi_1$.

$$\psi_1 * \psi_2 = \frac{2k}{4\pi r_1 r_2} e^{-kr_1} e^{-kr_2} e^{-ikr_1} e^{+ikr_2} = \frac{2k}{4\pi r_1 r_2} e^{-k(r_1+r_2)} e^{-ik(r_1-r_2)}$$

$$\psi_2 * \psi_1 = \frac{2k}{4\pi r_1 r_2} e^{-kr_2} e^{-kr_1} e^{-ikr_2} e^{+ikr_1} = \frac{2k}{4\pi r_1 r_2} e^{-k(r_1+r_2)} e^{+ik(r_1-r_2)}$$

$$\psi_1 * \psi_2 + \psi_2 * \psi_1 = \frac{2k}{4\pi r_1 r_2} e^{-k(r_1+r_2)} \left[e^{+ik(r_1-r_2)} + e^{-ik(r_1-r_2)} \right]$$

$$= \frac{4k}{4\pi r_1 r_2} e^{-k(r_1+r_2)} \cos k(r_1 - r_2)$$

$$\text{Now put } (A = r_1 + r_2, B = r_1 - r_2) \quad \& \quad \psi_1 * \psi_2 + \psi_2 * \psi_1 = \frac{4k}{4\pi r_1 r_2} e^{-Ak} \cos(kB) \qquad (3.4.2)$$

Real work is done when bringing superpositions together and we can treat these interacting virtual photons as having real energy $\hbar\omega = \hbar k c$. Using virtual photon emission probability $(2\alpha/\pi)(dk/k)$ from section 2.1.1

$$\text{Energy per virtual photon} \times \text{Probability} = \hbar k c \times \left[\text{Probability} \frac{2\alpha}{\pi} \frac{dk}{k} \right] = \frac{2\alpha\hbar c}{\pi} dk \qquad (3.4.3)$$

Including Eq. (3.4.3) the interaction energy @ k is thus $(\psi_1 * \psi_2 + \psi_2 * \psi_1) \left[\frac{2\alpha\hbar c}{\pi} dk \right]$ and

using Eq. (**3.4.2**) the interaction energy @ k is $\left[\frac{2\alpha\hbar c}{\pi} dk \right] \frac{4k}{4\pi r_1 r_2} e^{-Ak} \cos(kB)$.

The total interaction energy density due to $\psi_1 * \psi_2 + \psi_2 * \psi_1$ for all k is

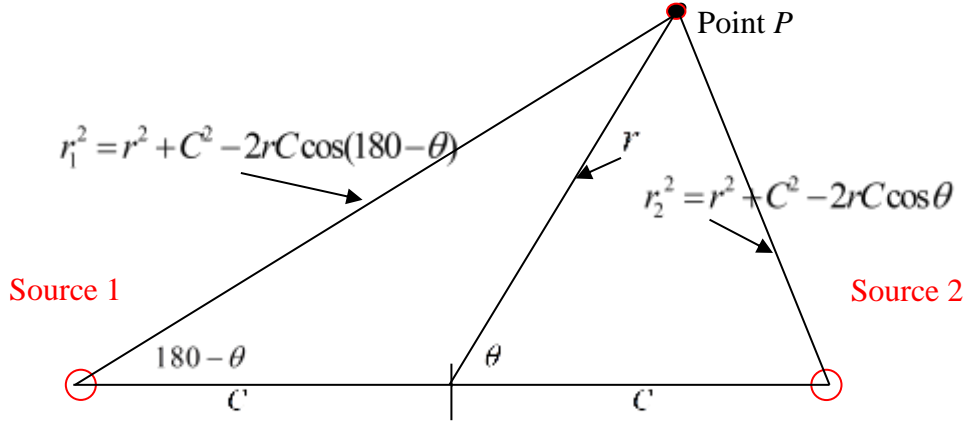$$\frac{2\alpha\hbar c}{\pi}\frac{4}{4\pi r_1 r_2}\int_0^\infty ke^{-Ak}\cos(Bk)dk$$

$$\int_0^\infty ke^{-Ak}\cos(Bk)dk = \frac{A^2 - B^2}{(A^2 + B^2)^2} \tag{3.4.5}$$

Where $\qquad A^2 = (r_1 + r_2)^2 = r_1^2 + 2r_1 r_2 + r_2^2 \quad \& \quad B^2 = (r_1 - r_2)^2 = r_1^2 - 2r_1 r_2 + r_2^2$

Thus $\quad A^2 = (r_1 + r_2)^2 = r_1^2 + 2r_1 r_2 + r_2^2 \quad \& \quad A^2 + B^2 = 2(r_1^2 + r_2^2)$ $\qquad$ (3.4.6)

$$= 2(r^2 + C^2) \quad \text{as} \quad \cos(180 - \theta) = -\cos\theta$$

and $\quad A^2 + B^2 = 4(r^2 + C^2)$ $\qquad\qquad$ (3.4.7)

Figure 3.4.2 Distances to a point from two sources as a function of angle θ and radius r.

Putting Eqs. (3.4.4), (3.4.5), (3.4.6) & (3.4.7) together $\dfrac{A^2 - B^2}{(A^2 + B^2)^2} = \dfrac{4r_1 r_2}{16(r^2 + C^2)^2}$

$$\int_0^\infty ke^{-Ak}\cos(Bk)dk = \frac{r_1 r_2}{4(r^2 + C^2)^2}$$

$$\frac{2\alpha\hbar c}{\pi}\frac{4}{4\pi r_1 r_2}\int_0^\infty ke^{-Ak}\cos(Bk)dk = \frac{2\alpha\hbar c}{\pi}\frac{4}{4\pi r_1 r_2}\frac{r_1 r_2}{4(r^2 + C^2)^2}$$

$$\frac{2\alpha\hbar c}{\pi}\frac{4}{4\pi r_1 r_2}\int_0^\infty ke^{-Ak}\cos(Bk)dk = \frac{2\alpha\hbar c}{\pi}\frac{1}{4\pi}\frac{1}{(r^2 + C^2)^2} \tag{3.4.8}$$

This is the total interaction energy density of time polarized virtual photons at point P due to $\psi_1{}^*\psi_2 + \psi_2{}^*\psi_1$ for all k and there are no directional vectors to take into account. We will use similar equations for the vector potential ($m = \pm 1$) photons for magnetic energies but will then need directional vectors. Equation (3.4.8) is the energy due to the interaction of

amplitudes at any radius r from the centre of the pair. It is independent of θ, and to get the total energy of interaction we multiply by $4\pi r^2 dr$ for layer dr and integrate from $r = 0 \rightarrow \infty$.

The total interaction energy is
$$\frac{2\alpha\hbar c}{\pi} \int_0^\infty \int_0^\infty (\psi_1 * \psi_2 + \psi_2 * \psi_1) dk \; 4\pi r^2 dr$$

Using Eq. (3.4.8)
$$= \frac{2\alpha\hbar c}{\pi} \frac{1}{4\pi} \int_0^\infty \frac{4\pi r^2 dr}{(r^2 + C^2)^2}$$

Thus
$$\frac{2\alpha\hbar c}{\pi} \int_0^\infty \int_0^\infty (\psi_1 * \psi_2 + \psi_2 * \psi_1) dk dv = \frac{2\alpha\hbar c}{\pi} \int_0^\infty \frac{r^2 dr}{(r^2 + C^2)^2}$$

$$\int_0^\infty \frac{r^2 dr}{(r^2 + C^2)^2} = \frac{1}{2C} \frac{\pi}{2}$$

The interaction or potential energy is $\quad \dfrac{\alpha\hbar c}{2C} = \dfrac{\alpha\hbar c}{R}$ $\qquad$ (3.4.9)

If $R = 2C$ is the distance between the centres of our assemblies, this is the classical potential. The procedure used here, with small changes, simplifies the derivation of the magnetic moment; we reuse some equations, but in a slightly modified form taking polarization vectors into account. We also reuse some of these simple but approximate derivations when looking at gravity in Section 5.

3.5 Magnetic Energy between two Spin Aligned Infinite Superpositions

In this section we are going to consider two infinite superpositions that form Dirac spin ½ states. We will look at the magnetic energy between them when they are both in a spin up state, say along some z axis as in Figure 3.5. 1. We are not looking at the magnetic energy here when they are both coupled in a spin 0 or spin 1 state. That is, both Dirac spin ½ states have their $\sqrt{3}\hbar/2$ spin vectors randomly oriented around the z axis with $\hbar/2$ components aligned along this z axis. Also, in this section we will be dealing with transversely polarized virtual photons and must take account of polarization vectors. In section 3.2.2 and Eq. (3.2.7) spin ½ states are generated only from $l = 3, m = 2$ states and as transversely polarized photons are superpositions of $m = \pm 1$ photons they can only be emitted from these $l = 3, m = 2$ states; the remaining states are spherically symmetric and cannot emit transversely polarized photons. We don't yet know the value of amplitudes $|c_n|$ so we will derive the magnetic energy in terms of these. We will then equate this energy to the Dirac values assuming a value of $g = 2$ before QED corrections; this allows us to evaluate in section 4.3 the amplitudes $|c_n|$ in terms of the ratio χ_{EM} between primary and secondary electromagnetic coupling. We can then evaluate in section 4.1 the primary electromagnetic coupling constant α_{EMP} in terms of the ratio χ_{EM}. (Section 3.5 uses the same format as Chapter 18, "The Feynman Lectures on Physics" Volume 3, Quantum Mechanics[24] .
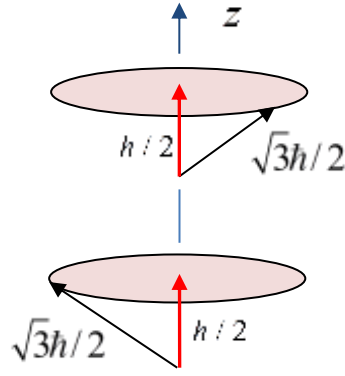
Figure 3.5. 1 Two spin aligned superpositions.

An $l = 3, m = 2$ state can emit a right hand circularly (R.H.C.) polarized $(m = +1)$ photon in the $+z$ direction. Let the amplitude for this be temporarily $|R\rangle$.

An $l = 3, m = -2$ state can emit a left hand circularly (L.H.C.) polarized $(m = -1)$ photon in the $+z$ direction. Let the amplitude for this also be temporarily $|L\rangle$.

First rotate the z axis about the y axis by angle θ (call this operation $S|R\rangle$) then use $\langle x'| = (1/\sqrt{2})[\langle R'| + \langle L'|]$ and multiply on the right by operation $S|R\rangle$.

The amplitude to emit a transversely polarized photon in the x' direction is thus

$$\langle x'|S|R\rangle = \frac{1}{\sqrt{2}}[\langle R'|S|R\rangle + \langle L'|S|R\rangle]$$

Where $\langle R'|S|R\rangle = \langle 3,+2'|S|3,+2\rangle = (1/4)\left[2 + 2\cos\theta - 4\sin^2\theta + 3\sin^2\theta\cos\theta\right]$ is the amplitude an $l = 3, m = 2$ state remains in an $l = 3, m = 2$ state after rotation by angle θ.

Also $\langle L'|S|R\rangle = -\langle 3,-2'|S|3,+2\rangle = (1/4)\left[2 - 2\cos\theta - 4\sin^2\theta - 3\sin^2\theta\cos\theta\right]$ is minus the amplitude that an $l = 3, m = 2$ state is in an $l = 3, m = -2$ state after rotation by θ.

Putting this together $\qquad \langle x'|S|R\rangle = \dfrac{1 - 2\sin^2\theta}{\sqrt{2}} = \dfrac{\cos 2\theta}{\sqrt{2}}$ $\qquad (3.5.1)$

An $l = 3, m = 2$ state can also emit an $(m = +1)$ photon in the $-z$ direction but it will now be left hand circularly polarized. Let this amplitude be temporarily: $|L\rangle$.

Similarly an $l = 3, m = -2$ state can emit an $(m = -1)$ photon in the $-z$ direction which is right hand circularly polarized. Let this amplitude be temporarily: $|R\rangle$.

We can go through the same procedure as above to get $\langle x'|S|L\rangle = \dfrac{\cos 2\theta}{\sqrt{2}}$ $\qquad (3.5.2)$

This amplitude Eq. (3.5.2) is for a photon emitted in the opposite direction to amplitude Eq. (3.5.1) but $\cos 2\theta = \cos 2(180 + \theta)$ and we can simply add these two amplitudes. Let us assume, however, that an $l = 3, m = 2$ state has equal amplitudes to emit in the $+z$ & $-z$ directions of $|R\rangle/\sqrt{2}$ and $|L\rangle/\sqrt{2}$.

With these amplitudes; $\dfrac{1}{\sqrt{2}}\left[\langle x'|S|R\rangle+\langle x'|S|L\rangle\right]=\dfrac{\cos 2\theta}{2}+\dfrac{\cos 2\theta}{2}=\cos 2\theta$ (3.5.3)

Equation (3.5.3) is the angular component of the amplitude for a transverse x' polarization in the new z' direction where $x \to x'$ & $z \to z' = \theta$. When $\theta = 0$ or 180 the on-axis amplitude for transverse polarization is one as expected ignoring other factors. Using the same normalization factors (we check the validity of this in section 3.5.2) we can still use the amplitudes and phasing of our original time mode photons Eqs. (3.4.1) but instead of including polarization vectors we will for simplicity just use the cosine of the angle $(\gamma - \delta)$ between them (as in Figure 3.5. 2) as a multiplying factor. Including the angular factor Eq. (3.5.3) in our earlier scalar amplitudes Eqs. (3.4.1) we have for our new wavefunctions:

$$\psi_1 = \cos 2\delta \sqrt{\frac{2k}{4\pi}}\frac{e^{-kr_1+ikr_1}}{r_1} \quad \& \quad \psi_2 = \cos 2\gamma \sqrt{\frac{2k}{4\pi}}\frac{e^{-kr_2+ikr_2}}{r_2} \qquad (3.5.4)$$
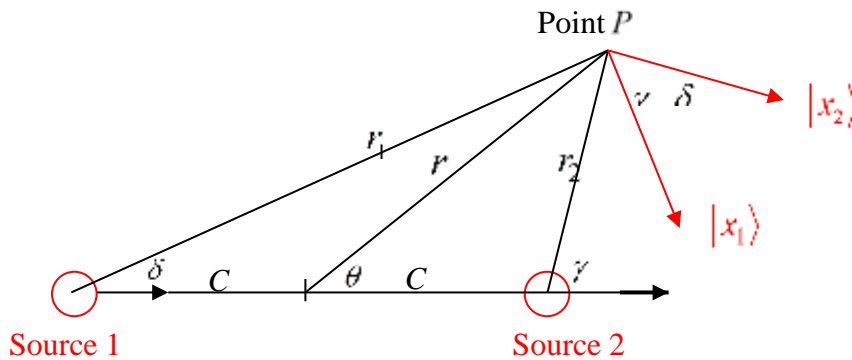
The transverse polarized photons from sources (1) & (2) have polarization vectors $|x_1\rangle$ and $|x_2\rangle$ at angle to each other $(\gamma - \delta)$, (Figure 3.5. 2) and the complex product becomes:

$$(\psi_1 + \psi_2)*(\psi_1 + \psi_2) = \psi_1{}^*\psi_1 + (\psi_1{}^*\psi_2 + \psi_2{}^*\psi_1)(\cos(\gamma - \delta) + \psi_2{}^*\psi_2$$

Where the interaction term is now: $(\psi_1{}^*\psi_2 + \psi_2{}^*\psi_1)\cos(\gamma - \delta)$ and as in the scalar case (section 3.4.1) but now using Eqs. (3.5.4)

$$\psi_1{}^*\psi_2 \cos(\gamma - \delta) = \cos 2\delta \cos 2\gamma \frac{2k}{4\pi r_1 r_2}e^{-k(r_1+r_2)}e^{-ik(r_1-r_2)}\cos(\gamma - \delta)$$

$$\psi_2{}^*\psi_1 \cos(\gamma - \delta) = \cos 2\delta \cos 2\gamma \frac{2k}{4\pi r_1 r_2}e^{-k(r_1+r_2)}e^{+ik(r_1-r_2)}\cos(\gamma - \delta)$$

$$(\psi_1{}^*\psi_2 + \psi_2{}^*\psi_1)\cos(\gamma - \delta) = \cos 2\delta \cos 2\gamma \frac{4k}{4\pi r_1 r_2}e^{-Ak}\cos(kB)\cos(\gamma - \delta) \qquad (3.5.5)$$
(Where as in section 3.4.1, Eq. (**3.4.2**) $A = r_1^2 + r_2$ & $B = r_1 - r_2$.)

Figure 3.5. 2 Two sources $2C$ apart, both with $\beta_{nk}^2 \times (m = +2)$ states along the joining line, δ & γ are the respective angles to P, r_1 & θ are the respective distances to point P.

3.5.1 Amplitudes of transversely polarized virtual emitted photons

In the laboratory frame ψ_{nk} has amplitude β_{nk} to be in an $m = +2$ state (section 3.1). For a multiple integer n superposition $\psi_k = \sum c_n \psi_{nk}$. At each fixed wavenumber k, we cannot distinguish which integer n a virtual photon comes from, so we must add amplitudes from each individual integer n superposition. To keep integrals simple we will assume that $\beta_{nk} <<<< 1$ or that spacing $2C$ is very large, and our interacting k values are very small. (We can make a comparison with the Dirac values at any large spacing, so accuracy need not be affected.) Thus if $\beta_{nk} <<< 1$ and $\gamma_{nk} \approx 1$, we can approximate Eq. (3.1.11) as

$$K_{nk} = \beta_{nk}\gamma_{nk} \approx \beta_{nk} \approx \frac{n\hbar k\sqrt{2s}}{2m_0 c} \approx \frac{|\mathbf{p}_{nk}|\sqrt{2s}}{2m_0 c} \approx \frac{\lambda_c nk\sqrt{2s}}{2} \approx \frac{\lambda_c nk}{2} \quad \text{for spin ½ fermions.}$$

Adding amplitudes for multiple integer n superpositions $\langle \beta_k \rangle \approx \frac{\lambda_c \langle n \rangle k}{2}$ (3.5.6)

(When deriving Eq. (3.2.10) we said $\langle |\mathbf{p}_k| \rangle = \hbar k \langle n \rangle$ and not $\langle |\mathbf{p}_k| \rangle = \hbar k \sqrt{\langle n^2 \rangle}$. How do we justify this? When $\beta_{nk} << 1$ as above $\beta_{nk} \propto n\hbar k = |\mathbf{p}_{nk}|$ So adding amplitudes β_{nk} to get $\langle \beta_k \rangle$ is equivalent to adding $\mathbf{p}_{nk}$ to get $\langle \mathbf{p}_k \rangle$ and not adding $\mathbf{p}_{nk}^2 = n^2\hbar^2 k^2$ to get $\langle |\mathbf{p}_k| \rangle = \hbar k \sqrt{\langle n^2 \rangle}$. If this is true when $\beta_{nk} << 1$ it must be true for $0 \le \beta_{nk} \le 1$.)

3.5.2 Checking our normalization factors

Let us pause and check the reasonableness of all this and our normalization factors. From Eqs. (3.4.1) for scalar photons $\left[\psi * \psi = \frac{2k}{4\pi} \frac{e^{-2kr}}{r^2} \right]$ × (emission probability $\frac{2\alpha}{\pi} \frac{dk}{k}$) gives a

Scalar ψ_k emission probability density $\psi * \psi \left[\frac{2\alpha}{\pi} \frac{dk}{k} \right] = \frac{2k}{4\pi} \frac{e^{-2kr}}{r^2} \left[\frac{2\alpha}{\pi} \frac{dk}{k} \right]$.

The transversely polarized probability density, using Eqs. (3.5.4) & (3.5.7) plus $\langle \beta_k \rangle^2$ is

$$\langle \beta_{nk} \rangle^2 \psi' * \psi' \frac{2\alpha}{\pi} \frac{dk}{k} = \langle \beta_k \rangle^2 \left[\cos^2 2\delta \frac{2k}{4\pi} \frac{e^{-2kr}}{r^2} \right] \frac{2\alpha}{\pi} \frac{dk}{k}$$

(Where $2\delta = 2\gamma$ & $r_1 = r_2$.) If we now consider the on-axis $\delta = 0$ case the transverse polarized on axis emission probability density at k is:

$$\langle \beta_k \rangle^2 \left[\frac{2k}{4\pi} \frac{e^{-2kr}}{r^2} \right] \frac{2\alpha}{\pi} \frac{dk}{k} = \langle \beta_k \rangle^2 \ \psi * \psi \frac{2\alpha}{\pi} \frac{dk}{k}$$

Just as in QED the factor $\langle\beta_k\rangle^2$ is the factor we need for this on-axis emission probability density ratio between transverse and scalar polarization. This justifies using the same normalization constant $(2k/4\pi)^{1/2}$ for both the scalar and magnetic wavefunctions. Using the same virtual photon emission probability and energy $\hbar kc$ as in Eq. (3.4.3) for both the scalar and transverse polarization cases:

$$\text{Energy per transverse photon} \times \text{Probability} = \hbar kc \times \left[\text{Probability} \; \frac{2\alpha}{\pi}\frac{dk}{k}\right] = \frac{2\alpha\hbar c}{\pi}dk \qquad (3.5.7)$$

Multiplying Eq. (3.5.5) by Eq. (3.5.6) squared, and Eq. (3.5.7) we get the transverse interaction energy at wavenumber ψ_{6k}:

$$\langle\beta_k\rangle^2 (\psi_1 * \psi_2 + \psi_2 * \psi_1)\cos(\gamma-\delta)\left[\frac{2\alpha\hbar c}{\pi}dk\right]$$

$$= \left[\frac{\lambda_C^2 \langle n\rangle^2 k^2}{4}\right]\cos 2\delta \cos 2\gamma \frac{4k}{4\pi r_1 r_2}e^{-Ak}\cos(kB)\left[\frac{2\alpha\hbar c}{\pi}dk\right]$$

Rearranging this: $\quad\langle\beta_k\rangle^2 (\psi_1 * \psi_2 + \psi_2 * \psi_1)\cos(\gamma-\delta)\left[\frac{2\alpha\hbar c}{\pi}dk\right]$

$$= \frac{2\langle n\rangle^2 \lambda_C^2 \alpha\hbar c}{\pi}\frac{\cos 2\delta \cos 2\gamma \cos(\gamma-\delta)}{4\pi r_1 r_2}\left[k^3 e^{-Ak}\cos(kB)dk\right] \qquad (3.5.8)$$

As in the scalar case we integrate over k first but now with a k^3 term due to the inclusion of the $\langle\beta_k\rangle^2$ factor which is approximately proportional to k^2 from Eq. (3.5.6).

Using $\quad A = r_1 + r_2 \quad \& \quad B = r_1 - r_2 \quad$ and $\quad$ Eqs. (3.4.6) & (3.5.6)

$$\int_0^\infty \left[k^3 e^{-Ak}\cos(kB)dk\right] = \frac{3}{8}\left[\frac{2r_1^2 r_2^2 - (r^2 + C^2)^2}{(r^2 + C^2)^4}\right]$$

And thus: $\quad\int_0^\infty \langle\beta_k\rangle^2 (\psi_1 * \psi_2 + \psi_2 * \psi_1)\cos(\gamma-\delta)\frac{2\alpha\hbar c}{\pi}dk$

$$= \frac{2\langle n\rangle^2 \lambda_C^2 \alpha\hbar c}{\pi}\frac{\cos 2\delta \cos 2\gamma \cos(\gamma-\delta)}{4\pi r_1 r_2} \times \frac{3}{8}\left[\frac{2r_1^2 r_2^2 - (r^2 + C^2)^2}{(r^2 + C^2)^4}\right] \qquad (3.5.9)$$

Equation (3.5.9) is the magnetic interaction energy density at point P for all wave numbers k. Figure 3.5. 2 is a plane of symmetry that can be rotated through angle 2π around the axis of symmetry (the joining line along the axis of the two spin aligned sources). To evaluate the total magnetic energy density over all space we multiply by $4\pi r^2 \sin\theta d\theta dr$.

We thus integrate Eq. (3.5.9) $\times$ $4\pi r^2 \sin\theta d\theta dr$ to get

$$\frac{3\langle n\rangle^2 \lambdabar_C^2 \alpha\hbar c}{4\pi}\int_0^\infty\int_0^{\pi/2}\frac{\cos 2\delta\cos 2\gamma\cos(\gamma-\delta)}{r_1 r_2}\left[\frac{2r_1^2 r_2^2-(r^2+C^2)^2}{(r^2+C^2)^4}\right]r^2\sin\theta\,d\theta\,dr \qquad (3.5.10)$$

Now $\displaystyle\int_0^\infty\int_0^{\frac{\pi}{2}}\frac{\cos 2\delta\cos 2\gamma\cos(\gamma-\delta)}{r_1 r_2}\left[\frac{2r_1^2 r_2^2-(r^2+C^2)^2}{(r^2+C^2)^4}\right]r^2\sin\theta\,d\theta\,dr$ can be reduced to the

single integral: $\displaystyle\frac{1}{8C^3}\int_0^1\sqrt{1-x^2}\left[\frac{(7-5x^2)}{x^3}\ln\frac{1+x}{1-x}-\frac{14}{x^2}+\frac{16}{3}\right]dx$ which can be expressed as an

infinite series in p (to not confuse with superposition value n):

$$\frac{1}{8C^3}\sum_{p=1}^{p=\infty}\left[\frac{14}{2p+3}-\frac{10}{2p+1}\right]\frac{(2p-1)!}{(p-1)!(p+1)!4^p}\cdot\frac{\pi}{2}\quad=\frac{1}{8C^3}\frac{(160-51\pi)}{6}\cdot\frac{\pi}{2}$$

$$\text{(Putting } R=2C\text{)}\quad=\frac{1}{R^3}\frac{(160-51\pi)}{6}\cdot\frac{\pi}{2}\qquad(3.5.11)$$

This infinite series is approximately $\quad\approx-\frac{1}{R^3}\frac{\pi}{54(1.0045062....)}\qquad(3.5.12)$

Putting Eq. (3.5.12) into Eq. (3.5.9) the total magnetic interaction energy over all frequencies and all space for two spin aligned infinite superpositions is:

$$U'\approx\frac{3\langle n\rangle^2\lambdabar_C^2\alpha\hbar c}{4\pi}\left[-\frac{1}{R^3}\frac{\pi}{54(1.0045062....)}\right]$$

We will call this $\quad U\left(\text{superpositions}\right)\approx-\left[\frac{\langle n\rangle^2\lambdabar_C^2\alpha\hbar c}{72R^3(1.0045062....)}\right]\qquad(3.5.13)$

We can equate this magnetic energy to the classical value assuming the Dirac value of $g=2$ for spin ½ (No QED corrections have been applied so it must be $g=2$). For the arrangement of spins as in Figure 3.5. 1 the Dirac magnetic energy between two spin ½ states is

$$U\left(\text{Dirac}\right)=-\left[\frac{2\mu^2}{4\pi\varepsilon_o c^2 R^3}\right]\qquad(3.5.14)$$

Using the Dirac magnetic moment $\mu=\frac{e\hbar}{2m_0}=\frac{e\hbar c}{2m_0 c}=\frac{ec\lambdabar_C}{2}$ the Dirac magnetic energy is

$$U(\text{Dirac})=-\left[\frac{\lambdabar_C^2\alpha\hbar c}{2R^3}\right]$$

The approximation used in deriving Eq. (3.5.6) $\gamma^2\beta^2\approx\beta^2$ for $\beta^2<<<1$ is true only when $R>>>\lambdabar_C$. This error in β^2 is of the order of $\lambdabar_C^2/R^2$ and rapidly tends to zero with

increasing R. There is no upper limit on the value of distance R we can choose. Thus, comparing our estimate of the magnetic energy with Dirac's value when $R >>> \hbar_C$.

$$U(\text{Dirac}) = U(\text{Superpositions}) \text{ or } -\left[\frac{\hbar_C^2 \alpha \hbar c}{2R^3}\right] \approx -\left[\frac{\langle n \rangle^2 \hbar_C^2 \alpha \hbar c}{72R^3(1.0045062....)}\right] \qquad (43.5.15)$$

All symbols cancel except $\langle n \rangle$ leaving: $\qquad \langle n \rangle^2 \approx 36(1.0045062.....)$

The expectation value $\langle n \rangle$ in our superposition is slightly more than $n = 6$ our dominant mode. This is why we have used a three member superposition centred on this dominant $n = 6$ mode. The two side modes $n = 5$ and $n = 7$ are smaller so that:

$$\langle n \rangle = \sum_{n=5,6,7.} (c_n * c_n)n \approx \sqrt{36(1.0045062...)} \approx 6.01350345 \qquad (3.5.16)$$

This is for Dirac spin ½ particles. This mean value of n creates a $g = 2$ fermion which QED corrections (which are secondary interactions) increase slightly to the experimental value. In section 4.1 we solve the primary electromagnetic coupling constant in terms of ratio χ_{EM} using Eq. (3.5.16). It is important to remember this magnetic energy derivation applies to two infinite assemblies (or particles) localized in small cavities in relation to their distance R apart. They must be both on the z axis with spins aligned (or anti aligned) along this z axis as in Figure 3.5. 1 & Figure 3.5. 2. Also, the agreement with Dirac and in what follows is possible if superposition ψ_k interacts *only with virtual photons of the same wavenumber k*.

4   High Energy Superposition Cutoffs

4.1   Electromagnetic Coupling to Spin ½ Infinite Superpositions

Equation (3.5.16) is the key requirement for spin ½ superpositions to behave as Dirac fermions, allowing us to solve α_{EMP}^{-1} as a function of coupling ratio χ using Eq. (3.5.16).

$$\langle n \rangle = \sum_{n=5,6,7.} (c_n * c_n)n \approx \sqrt{36(1.0045062...)} \approx 6.01350345$$

Thus $5c_5 * c_5 + 6c_6 * c_6 + 7c_7 * c_7 = 6.01350345$ but $6c_5 * c_5 + 6c_6 * c_6 + 6c_7 * c_7 = 6$

and $\qquad\qquad c_7 * c_7 - c_5 * c_5 = 0.01350345$

As $c_7 * c_7 + c_5 * c_5 = 1 - c_6 * c_6$ we can now solve for $c_7 * c_7$ & $c_5 * c_5$ in terms of $c_6 * c_6$

$$c_7 * c_7 \approx 0.50675172 - \frac{c_6 * c_6}{2} \quad \& \quad c_5 * c_5 \approx 0.49324827 - \frac{c_6 * c_6}{2} \qquad (4.1.1)$$

From Eq. (2.3.12) the Q^2A^2 required to produce this superposition with amplitudes c_n is

$$Q^2A^2 = \sum_{n=5,6,7} c_n * c_n \frac{n^4 \hbar^2 k^4 r^2}{81} \text{ and using Eq.(4.1.1)}$$

$$\sum_{n=5,6,7} c_n * c_n \, n^4 = 625c_5 * c_5 + 1296c_6 * c_6 + 2401c_7 * c_7 \approx 1524.991 - 217c_6 * c_6$$

Thus $Q^2A^2 = \sum_{n=5,6,7} c_n * c_n \frac{n^4 \hbar^2 k^4 r^2}{81} \approx [18.82705 - 2.67901c_6 * c_6]\hbar^2 k^4 r^2$ is the *required* vector

potential squared to produce this spin ½ superposition. From Eq. (2.2.4) with $s = $ ½ & $N = 1$

for massive fermions $Q^2A^2 = \dfrac{2[8 + 8\sqrt{\alpha_{EMP}})]^2}{3\pi} \hbar^2 k^4 r^2$ is the *available* Q^2A^2.

Equating *required and available*: $2[8 + 8\sqrt{\alpha_{EMP}})]^2 \approx 3\pi[18.82705 - 2.67901c_6 * c_6]$

$$[1 + \sqrt{\alpha_{EMP}})]^2 \approx [1.386256 - 0.197258c_6 * c_6]$$

$$\alpha_{EMP} \approx \left[\sqrt{1.386256 - 0.197258c_6 * c_6} - 1\right]^2 \qquad (4.1.2)$$

From Eqs. (3.3.1) & (3.3.20), $c_6 * c_6(1 - c_6 * c_6) = \sqrt{2/\chi_C} = 6\sqrt{2/\chi_{EM}}$ and we can solve for α_{EMP} as a function of either χ_{EM} or χ_C. We then use Eq. (3.3.20) again to get $\alpha_{EMS}^{=1}$ @ k_{cutoff}. Now both χ_{EM} and χ_C are fundamentally the same ratio differing only by 36:1, because electron superpositions have six primary charges whereas we define them as one fundamental charge (section 3.3.1) and quarks have only one colour charge (Table **2.2.1**) Because $\chi_C = \alpha_3^{-1}$ at the cutoff near L_p it is more convenient to work with. From Eq. (3.3.20)

$$c_6 * c_6 = \frac{1}{2} \pm \frac{1}{2}\sqrt{1 - 4\sqrt{\frac{2}{\chi_C}}} \quad \text{and there are two solutions for each } \chi_C.$$

One has $c_6 * c_6$ dominant with two smaller $c_5 * c_5$ & $c_7 * c_7$ side modes, the other is the reverse with $c_6 * c_6$ the minor player and two larger $c_5 * c_5$ & $c_7 * c_7$ side modes. As the values for α_{EMP} with $c_6 * c_6$ dominant fit the SM very closely, we include only these. (This only applies to spin ½ fermions, and the spins 1 & 2 boson superpositions in Table 4.3.1 are the opposite, with minor centre modes.) Table 4.1.1 shows possible coupling ratios χ_C in the range $\chi_C = 50 \rightarrow 51$. The yellow row corresponds to the cutoff energy in Eq. (4.2.10) and Figure

4.1.2. Table 4.1.1 shows these dominant $c_6 * c_6$ mode results for $\chi_C = \alpha_3^{-1}$ at various possible cutoffs in the range $\chi_C = 50 \rightarrow 51$, as this range fits the SM.

Coupling Ratio χ_C	$c_6 * c_6$	$\alpha_{EM\text{Primary}}^{-1}$	$\alpha_{EM\text{Secondary}}^{-1}@k_{cutoff}$
50.00	≈ 0.723607	≈ 75.4414	≈ 104.7798
50.20	≈ 0.724497	≈ 75.5447	≈ 105.3429
50.40	≈ 0.725378	≈ 75.6472	≈ 105.9060
50.4053	≈ 0.725401	≈ 75.6499	≈ 105.9210
50.60	≈ 0.726250	≈ 75.7488	≈ 106.4692
50.80	≈ 0.727115	≈ 75.8497	≈ 107.0324
51.00	≈ 0.727970	≈ 75.9499	≈ 107.5956

Table 4.1.1. Possible coupling ratios χ_C versus α^{-1} (EM Secondary) in the range $\chi_C = 50 \rightarrow 51$. The yellow row corresponds to the interaction cutoff energy in Figure 4.1.2 & Eq. (4.2.10) as there can be only one solution for this cutoff.

4.1.1 Comparing this with the standard model

In the real world of SM secondary interactions the electromagnetic force splits into two components $\alpha_1 \& \alpha_2$ at energies greater than the mass/energy of the Z_0 boson or $\approx 91.1876\ GeV$. [25]. However we want to compare these SM couplings with the values derived in Table 4.1.1 at the ≈ 2.0288 Gev. cutoff of Eq. (4.2.10). Assuming three families of fermions and one Higgs field the SM [26] predicts

$$\alpha_1^{-1} \approx 58.98 \pm 0.08 - \frac{4.1}{2\pi} \log_e \frac{Q}{91.1876}$$

$$\alpha_2^{-1} \approx 29.60 \pm 0.04 + \frac{19}{6 \times 2\pi} \log_e \frac{Q}{91.1876} \qquad (4.1.3)$$

$$\alpha_3^{-1} \approx 8.47 \pm 0.22 + \frac{7}{2\pi} \log_e \frac{Q}{91.1876}$$

The weak force split obeys $\qquad \alpha_{EM}^{-1} = \frac{5}{3}\alpha_1^{-1} + \alpha_2^{-1}$

$$(4.1\ 4)$$

Also $\alpha_1^{-1} = \frac{3}{5}\alpha_{EM}^{-1} Cos^2\theta_W$ & $\alpha_2^{-1} = \alpha_{EM}^{-1} Sin^2\theta_W$ where θ_W is the Weinberg angle.

Combining these equations $\alpha_{EM}^{-1} = \frac{5}{3}\alpha_1^{-1} + \alpha_2^{-1} \approx 127.90 \pm 0.173 - \frac{11}{3 \times 2\pi}\log_e \frac{Q}{91.1876}$ $\qquad (4.1.5)$

Figure 4.1.1 plots these four inverse coupling constants. Figure 4.1.2 plots the intersection of $\alpha_{EM\text{Secondary}}^{-1}$ predicted in Table 4.1.1 and the SM prediction for α_{EM}^{-1} in Eq. (4.1.5). It would initially seem in Figure 4.1.2 that there is an unusually large error band in the predicted results. However $\Delta\alpha_{EM\text{Secondary}}^{-1} / \Delta\chi^{-1} \approx 2.8$ is approximately constant in this table and the error band in the SM colour coupling α_3^{-1} of ± 0.22 in Eqs (4.1.3) translates into the larger error band for $\alpha_{EM\text{Secondary}}^{-1}$ of $\pm 0.22 \times 2.8 \approx \pm 0.62$ in Figure 4.1.2.
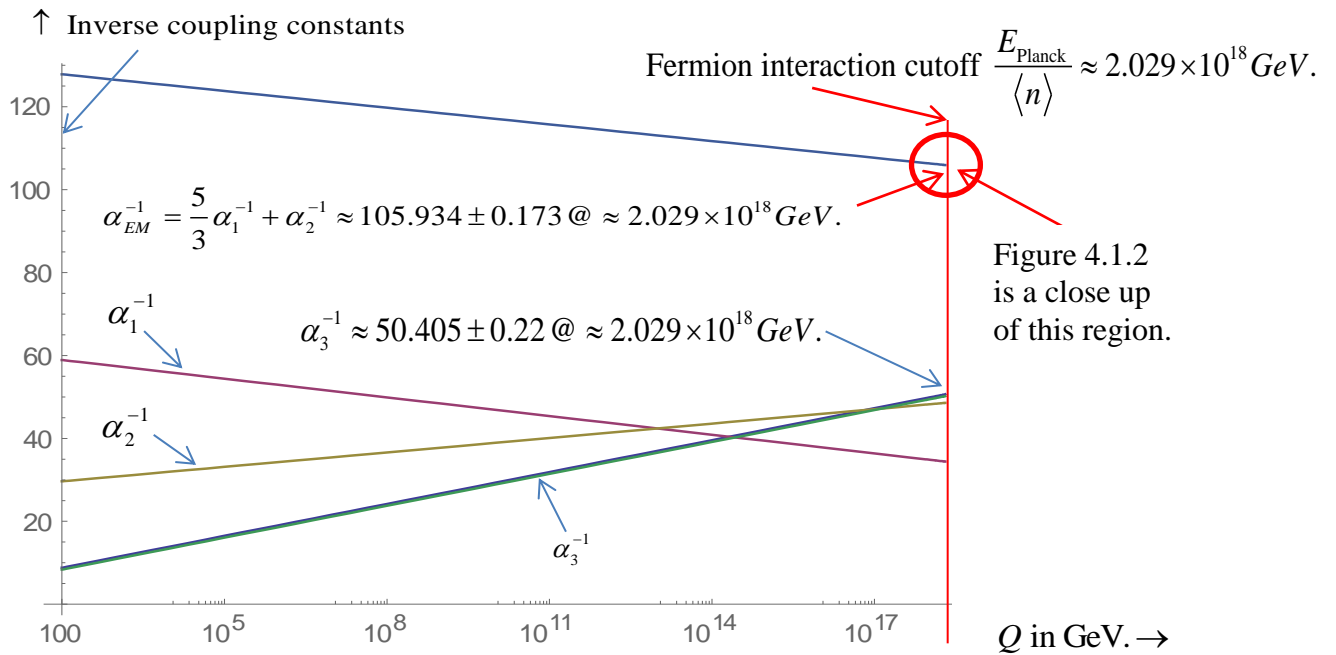
Figure 4.1.1 Standard Model based on three families of fermions and one Higgs field.

Within the figure:

↑ Inverse coupling constants

Fermion interaction cutoff $\dfrac{E_{\text{Planck}}}{\langle n \rangle} \approx 2.029 \times 10^{18}\,GeV.$

$\alpha_{EM}^{-1} = \dfrac{5}{3}\alpha_1^{-1} + \alpha_2^{-1} \approx 105.934 \pm 0.173 \, @ \approx 2.029 \times 10^{18}\,GeV.$

$\alpha_3^{-1} \approx 50.405 \pm 0.22 \, @ \approx 2.029 \times 10^{18}\,GeV.$

α_1^{-1}

α_2^{-1}

α_3^{-1}

Figure 4.1.2 is a close up of this region.

Q in GeV. →

Within the figure:

Planck Energy $\dfrac{}{\langle n \rangle}$

Possible values for α_{EMS}^{-1} (Secondary) from Table 4.1.1. There can of course, only be one solution here.

Standard Model $\dfrac{5}{3}\alpha_1^{-1} + \alpha_2^{-1} = \alpha_{EM}^{-1}$

Figure 4.1.1 expanded

Q in $GeV.$ →

Figure 4.1.2 A close up of the intersecting region of the SM that Eq. (4.1.5) and Table 4.1.1 predicts. This fermion interaction cutoff is perhaps more consistent with the SM than we might expect; as we have assumed, for simplicity, a square superposition cutoff at k_{Cutoff}. An exponential cutoff of some type is much more likely, but it may have only small effect.

4.2 Introducing Gravity into our Equations

4.2.1 Simple square superposition cutoffs

In section 3.2 we looked at single integer n superpositions of ψ_{nk} initially for clarity, and later found multiple integer n superpositions gave the same results; we will do the same here. We also found in Eqs. (3.2.3) & (3.2.6) that the integrals for both angular momentum and rest masses are of similar form. They both ended up including the term

$$\left[\frac{-1}{1+K_{nk}^2}\right]_0^\infty \text{ which if } K_{nk}\text{cutoff} < \infty \text{ becomes } \left[\frac{-1}{1+K_{nk}^2}\right]_0^{K_{nk}\text{cutoff}} \text{ and this is equal to}$$

$$1 - \frac{1}{1+K_{nk}^2\text{cutoff}} = \frac{K_{nk}^2\text{cutoff}}{1+K_{nk}^2\text{cutoff}} = \frac{1}{1+1/K_{nk}^2(\text{cutoff})} = \frac{1}{1+\varepsilon} \tag{4.2.1}$$

where using Eq. (3.1.11) the infinitesimal $\varepsilon = \dfrac{1}{K_{nk}^2\text{cutoff}} = \dfrac{2m_0^2c^2}{n^2\hbar^2(\text{k}_{\text{cutoff}})^2 s}$ (4.2.2)

For integral or half integral $\hbar$ angular momentum precision is required but Eq. (3.2.6) now gives us $\mathbf{L}_z(Total) = \dfrac{sm\hbar}{2}\left[\dfrac{-1}{1+K_{nk}^2}\right]_0^{K_{nk}\text{cutoff}} = \dfrac{sm\hbar}{2}\dfrac{1}{1+\varepsilon}$. So, can the effect of gravity increase

our probabilities from $sN \cdot \dfrac{dk}{k}$ to $sN \cdot (1+\varepsilon)\dfrac{dk}{k}$?

We will initially address only massive infinite superpositions where $N = 1$ in Eq. (2.2.4).

The first question we need to address is what is the effective preon mass to be used when coupling to gravity? In Eq. (3.1.4) we said the preon rest mass is $m_0/(8\gamma_{nk}\sqrt{2s})$ for each of the eight preons that build a spin ½ particle of rest mass m_0 . Now gravitons couple to the total mass including the kinetic energy. At the start of the interaction each preon mass is $m_0/(8\gamma_{nk}\sqrt{2s})$ and after the interaction (Figure 3.1.3) it is $m_0\gamma_{nk}(1+\beta_{nk}^2)/(8\sqrt{2s})$. Let us think semi-classically again and see where it leads us. We have been using magnitudes of velocities as they are the most convenient way to express our equations, even if not the conventional language of quantum mechanics. The interaction with the zero point fields takes the momentum of each preon from zero to $2m_0\gamma_{nk}\beta_{nk}c/(8\sqrt{2s})$ (Figure 3.1.3). While this happens as a quantum step change, let us imagine it as a virtually infinite acceleration from zero velocity to $2\beta_{nk}/(1+\beta_{nk}^2)$, which is the relativistic velocity addition (see Figure 3.1.1) of two equal steps of β_{nk}. At the half way point after one step the velocity is β_{nk} (the velocity of the CMF, the preon mass has increased to $m_0/(8\sqrt{2s})$. We can imagine this as being like the central point of a quantum interaction.

We will conjecture this midway point preon mass $m_0/(8\sqrt{2s})$ is the mass value that gravitons couple to and we will see that it is indeed the only value that fits all equations. Also, it does not make sense to choose either of the end point masses. We can also get reassurance from the properties of the Feynman transition amplitude which informs us in Eq. (3.1.15) that

$$\frac{(p_i + p_f)^z}{(p_i + p_f)^0} = \frac{2m_0 \gamma_{nk} \beta_{nk}}{2m_0 \gamma_{nk}} = \beta_{nk} \quad \text{and the ratio of space to time polarization in the LF is } \beta_{nk}^2.$$

This centre of momentum velocity gives us the key properties of the interaction. We will thus assume we have eight preons in each ψ_{nk} of effective gravitational mass $m_0 / (8\sqrt{2s})$ with effective *total* gravitational mass $m_0 / \sqrt{2s}$. To put the gravitational constant in the same form as the other coupling constants we need to divide it by $\hbar c$. The gravitational coupling amplitude is thus $m_0 \sqrt{G_P / (2s\hbar c)}$ to the gravitational zero point field, where $\sqrt{G_P}$ is the primary amplitude for a Planck mass to emit or absorb a graviton. Now this gravitational amplitude can be regarded as a complex vector just as colour and electromagnetism. We assumed for simplicity, as they are both spin 1 field particles, that colour and electromagnetism are parallel. Spin 2 gravity could be at a different complex angle to the other two. In fact, the equations only have the correct properties if gravity is at right angles to colour and electromagnetism. Putting $G_{Primary} = \chi'_G \cdot G_{Secondary}$ we conjecture that the

$$\text{gravitational coupling amplitude is } im_0 \sqrt{G_P / (2s\hbar c)} = im_0 \sqrt{\chi'_G \cdot G_S / (2s\hbar c)}$$
$$= im_0 \sqrt{\chi'_G \cdot G / (2s\hbar c)}$$

(4.2.3)

We have put the secondary gravitational coupling constant to a bare Planck mass G_s in Eq. (4.2.3) equal to the measured gravitational constant G. We can only do this if $\alpha_G = 1$ between Planck masses. (See Eq.(5.1.7) and the preceding paragraph.) We will later find that α_G does not need to be one and is in fact less than one. Consequently we temporarily label the ratio between the primary and secondary gravitational constants as χ'_G, returning to it in section 6.2.6. So, modifying Eqs. (2.2.1) to (2.2.3) by adding Eq. (4.2.3)

$$Q^2 A^2 = \left[\frac{\left| 8 + 8\sqrt{\alpha_{EMP}} + im_0 \sqrt{\chi'_G \cdot G / (2s\hbar c)} \right|^2}{3\pi sN} \hbar^2 k^4 r^2 \right] \cdot \left[\frac{sN \cdot dk}{k} \right]$$

$$Q^2 A^2 = \left[\frac{\left[8 + 8\sqrt{\alpha_{EMP}} \right]^2}{3\pi sN} \hbar^2 k^4 r^2 \right] \cdot \left[\frac{sN(1 + \varepsilon')dk}{k} \right] \text{ where } \varepsilon' = \frac{m_0^2 \chi'_G \cdot G}{2s\hbar c(8 + 8\sqrt{\alpha_{EMP}})^2}$$

Our previous wavefunctions ψ_k required $Q^2 A^2 = \dfrac{\left[8 + 8\sqrt{\alpha_{EMP}} \right]^2}{3\pi sN} \hbar^2 k^4 r^2$ from Eq. (2.2.4).

Thus primary graviton interaction can increase the probability of our previous wavefunctions ψ_k by $1 + \varepsilon'$ as required to obtain precision in our integrals for $\hbar / 2 \, \& \, \hbar$ if $K_{nk} cutoff < \infty$.

Using Eq.(4.2.2) now put $\varepsilon' = \dfrac{m_0^2 \chi'_G \cdot G}{2s\hbar c(8 + 8\sqrt{\alpha_{EMP}})^2} = \varepsilon = \dfrac{1}{K_{nk}^2 cutoff} = \dfrac{2m_0^2 c^2}{sn^2 \hbar^2 (k_{cutoff})^2}$

Thus $\qquad\qquad\qquad \dfrac{\chi'_G \cdot G}{4\hbar c(8 + 8\sqrt{\alpha_{EMP}})^2} \approx \dfrac{c^2}{n^2 \hbar^2 (k_{cutoff})^2}$

$$\frac{\chi'_G}{256(1+\sqrt{\alpha_{EMP}})^2}\frac{G\hbar}{c^3} \approx \frac{1}{n^2(k_{cutoff})^2}$$

But $L_P{}^2 = \dfrac{G\hbar}{c^3}$ and $\dfrac{\chi'_G \cdot L_P{}^2}{256(1+\sqrt{\alpha_{EMP}})^2} \approx \dfrac{1}{n^2(k_{cutoff})^2}$

For $N=1$ single integer n superpositions $\quad \chi'_G \approx \dfrac{256(1+\sqrt{\alpha_{EMP}})^2}{n^2(k_{cutoff}L_P)^2}$ (4.2.4)

For $N=1$ superpositions $\psi_k = \displaystyle\sum_n c_n \psi_{nk}$, we can use the logic of section 3.5.1; replacing K_{nk}^2

with $\langle K_k \rangle^2$, and n^2 with $\langle n \rangle^2$ in Eq. (4.2.4) so that Eq. (4.2.5) becomes

for $N=1$ multiple integer n superpositions $\quad \chi'_G \approx \dfrac{256(1+\sqrt{\alpha_{EMP}})^2}{\langle n \rangle^2 (k_{cutoff}L_P)^2}$ (4.2.5)

If we now go back to Eqs. (2.3.9) & (2.3.10) as $k \to \infty$ the energy squared $E_{nk}^2 \to \mathbf{p}_{nk}^2 c^2$
$= n^2 \hbar^2 \omega^2$. Again, using the logic of section 3.5.1 for multiple integer n superpositions the
expectation value for energy squared as $k \to \infty$ is $\langle E_k \rangle^2 \to \langle |\mathbf{p}_k| \rangle^2 c^2 = \langle n \rangle^2 \hbar^2 k^2 c^2$ thus

for multiple integer n superpositions as $k \to \infty, \quad \langle E_k \rangle \to \langle |\mathbf{p}_k| \rangle c = \langle n \rangle \hbar k c$ (4.2.6)

4.2.2 All $N = 1$ superpositions cutoff at Planck energy but interactions at less

It is reasonable to assume that the cutoff superposition energy cannot exceed the Planck
energy E_{Planck} (at least for square cutoffs) and that this is true for all $N=1$ superpositions.
(Section 6.2.1 discusses N = 2 superposition E_{Planck} cutoffs.) So, for simple square cutoffs:
$N=1$ multiple integer n superpositions cutoff energy $\langle E_{k(cutoff)} \rangle = \langle n \rangle \hbar k_{cutoff} c = E_{Planck}$ (4.2. 7)

This can be written as $\quad \langle n \rangle k_{cutoff} \hbar c = E_{Planck} = \dfrac{\hbar c}{L_{Planck}}$

For $N=1$ multiple integer n superpositions $\langle n \rangle k_{cutoff} = \dfrac{1}{L_{Planck}}$ & $\langle n \rangle k_{cutoff} L_P = 1$ (4.2.8)

$N=1$ multiple integer n superposition interaction cutoff energy $\hbar c k_{cutoff} = \dfrac{E_{Planck}}{\langle n \rangle}$ (4.2.9)

Using Eq. (4.2.9) with Planck energy of $1.22 \times 10^{19} GeV$. and $\langle n \rangle \approx 6.0135$ from Eq.(3.5.16)
for simple square cutoffs (also see Figure 4.1.2).

Interactions between $N=1$ fermions cutoff @ $\approx 2.0288 \times 10^{18} GeV$.

From Table 4.3.1 we see that all other particles such as photons, gluons and gravitons etc. have $\langle n \rangle < 6$ and thus higher interaction cutoff energies than fermions i.e.. $> 2.03 \times 10^{18} GeV$., but $< E_P$. Putting $2.0288 \times 10^{18} GeV$. in the SM equations (4.1.3) and (4.1 4).

$$\alpha_1^{-1} @ \; 2.0288 \times 10^{18} GeV. \approx 34.4179 \pm 0.08 @ \; k(cutoff)$$

$$\alpha_2^{-1} \; .... \approx 48.5707 \pm 0.04....................$$

$$\alpha_3^{-1} \; .... \approx 50.4053 \pm 0.22....................$$

$$\alpha_{EM}^{-1} = \frac{5}{3}\alpha_1^{-1} + \alpha_2^{-1} .... \approx 105.934 \pm 0.173...................$$

(4.2.10)

Real world high energy secondary interactions only involve $\alpha_1, \alpha_2 \; \& \; \alpha_3$, but spin zero primary interactions do not involve the weak force. Table 4.1.1 can thus only predict $\alpha_{EM}^{-1} \approx 105.921$ at the cutoff compared to the SM combination of $(5/3)\alpha_1^{-1} + \alpha_2^{-1} = \alpha_{EM}^{-1} \approx 105.934 \pm 0.173$ of Eq. (4.2.10). (See Figure 4.1.1 & Figure 4.1.2). Also using Eqs. (3.3.3) and (4.2.10) we get the primary to secondary fundamental coupling ratio χ_C.

$$\text{Coupling Ratio } \chi_C = \alpha_3^{-1} @ \; k_{cutoff} \approx 50.405 \pm 0.22 \; (ie. @ \; 2.0288 \times 10^{18} GeV.) \qquad (4.2.11)$$

The secondary coupling constants in Eq. (4.2.10) can perhaps be thought of as those to the bare colour and electromagnetic charges.

If we now put Eq. (4.2.8) into Eq. (4.2.5) we get $\chi_G' \approx \dfrac{256(1+\sqrt{\alpha_{EMP}})^2}{\langle n \rangle^2 (k_{cutoff} L_P)^2} = 256(1+\sqrt{\alpha_{EMP}})^2$

From Eqs.(4.1.2) and Table 4.3.1 we find $(1+\sqrt{\alpha_{EMP}}) \approx 1.115$ and Eq.(4.2.5) becomes

$$\chi_G' \approx 256(1.115)^2 \approx 318.3 \qquad (4.2.12)$$

From the paragraph following Eq. (4.2.3) we see that this equation temporarily assumes $\alpha_G = 1$ If it does equal one then $\chi_G' \approx 318.3$ is the ratio between the primary graviton coupling to bare preons, and the normal measured gravitational constant G. Section 8.2.2 develops a cosmic expansion model with $\alpha_G \approx 0.004$. In section 6.2.6 we assume an approximate value of $\alpha_G \approx 1$ in Eq.(6.2.9) to get a primary to secondary graviton coupling ratio of $\chi_G' \approx 318$. When $\chi_G' \approx 318$ the contribution from gravity cancels any deficit in primary interactions providing these superpositions cutoff at Planck energy, which we argue is true for all $N = 1$ superpositions. (This section and all its equations are derived by equating the contribution due to gravity and the deficit due to the Planck energy cutoff in primary interactions.). To enable Planck energy interactions $N = 2$ infinitesimal mass bosons must also cutoff at Planck energy just as $N = 1$ superpositions do, or as in Eq. (4.2.9). Sections 6.2 & 6.2.1 discusses these $N = 2$ superposition Planck energy cutoffs.

Figure 4.2.1 plots radial probabilities for all $n = 3, 4, 5, 6 \& 7$ Planck Energy cutoff modes. They are identical as the radial probability $P_R \propto r^8 \times Exp(n^2 k^2 r^2 / 9)$, but from Eq. (4.2.6) $nk = 1$ in each Planck energy mode, so they all have radial probability $P_R \approx 8.74 \times 10^{-6} \times r^8 Exp(r^2 / 9)$.
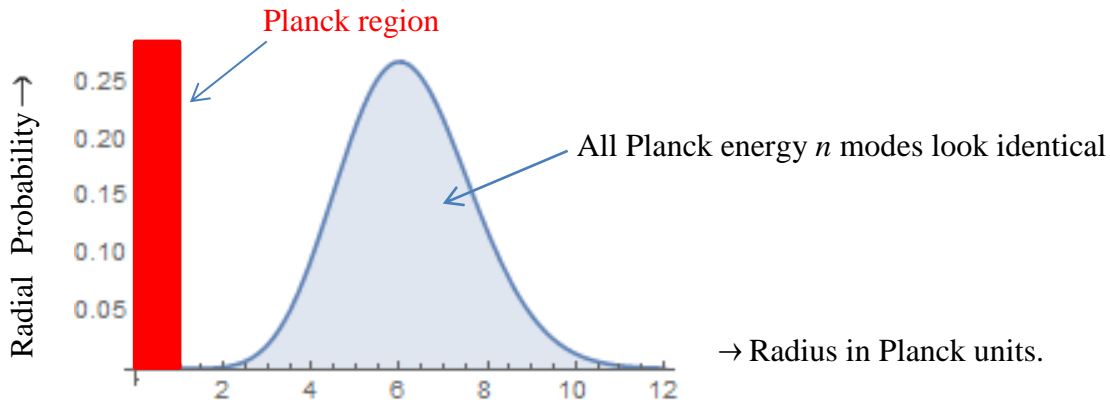
Figure 4.2.1 Plot of radial probability of all $n = 3, 4, 5, 6 \& 7$ Planck energy modes. Despite each mode having Planck energy, the probability in every case of being inside the Planck region is virtually zero at $\approx 8.9 \times 10^{-7}$.

4.3 Solving for Spin ½, Spin 1 and Spin 2 Superpositions

Superpositions with $N = 2$ are covered in section 6.2. Equation (4.2.11) and Eq. (3.3.20) can be extended by keeping $N \cdot s$ constant as in Eq. (4.4.1) allowing us to solve various combinations of spins ½, 1 or 2 and $N = 1$ or $N = 2$.

$$
\begin{array}{ccc}
(N = 2) \times (\text{Spin } 1) & (N = 1) \times (\text{Spin } 1) & (N = 1) \times (\text{Spin } \tfrac{1}{2}) \\
\text{or } (N = 1) \times (\text{Spin } 2) & \text{or } (N = 2) \times (\text{Spin } \tfrac{1}{2}) &
\end{array}
\tag{4.4.1}
$$

$$
4 c_{4b} {}^* c_{4b} (1 - c_{4b} {}^* c_{4b}) = 2 c_{5b} {}^* c_{5b} (1 - c_{5b} {}^* c_{5b}) = c_{6a} {}^* c_{6a} (1 - c_{6a} {}^* c_{6a})
$$
$$
= \sqrt{2 / \chi_C} \approx \sqrt{2 / 50.4053} \approx 0.199194
$$

Starting with spin ½ we can solve this to get $c_6 {}^* c_6 \approx 0.7254$ as the dominant value. Putting $c_6 {}^* c_6 \approx 0.7254$ into Eq.(4.1.2) or alternatively using Table 4.1.1

$$
\alpha_{EMP} \approx \left[\sqrt{1.386256 - 0.197258 c_6 {}^* c_6} - 1 \right]^2 \approx 75.6499^{-1}
\tag{4.4.2}
$$

From Eq. (2.2.4) the available $Q^2 A^2 = \dfrac{\left[8 + 8\sqrt{\alpha_{EMP}} \right)]^2}{3 \pi s N} \hbar^2 k^4 r^2$ with probability $\dfrac{s N \cdot dk}{k}$ where we ignore the infinitesimal factor of $(1 + \varepsilon)$ due to gravitons. And from Eq. (2.3.12)

$$Q^2 A^2 = \sum_n c_n * c_n \frac{n^4 \hbar^2 k^4 r^2}{81} = \frac{\left[8 + 8\sqrt{\alpha_{EMP}})\right]^2}{3\pi s N} \hbar^2 k^4 r^2$$

$$\sum_n c_n * c_n \cdot n^4 \approx 1367.58 \text{ for (spin } 1/2 \times N = 1)$$

$$\approx 683.79 \text{ for (spin } 1 \times N = 1) \text{ or (spin } 1/2 \times N = 2)$$

$$\approx 341.9 \text{ for (spin } 1 \times N = 2) \text{ or (spin } 2 \times N = 1) \quad (4.4.3)$$

$$\approx 170.95 \text{ for (spin 2, } N = 2) \text{ by extension.}$$

The same primary electromagnetic coupling α_{EMP} builds all fundamental particles, allowing Eq.(4.4.3) to be true. Using Eqs, (4.4.1), (4.4.3) & $\sum_n c_n * c_n = 1$ we get Table 4.3.1. We define the coupling ratio for gravitons in Eq.(6.2.9) section 6.2.6, where we also solve infinitesimal mass graviton superpositions. In Table 4.3.1 three member superpositions fit the SM best. In section 4.1 we solved spin ½ superpositions with a dominant centre mode $c_6 * c_6$ that fitted the SM. However when solving for spins 1 & 2 we must initially comply with Eq. (4.4.1) which defines interaction probabilities (see Eq. (3.3.20) and the following paragraph). We must also comply with Eq. (4.4.3) which determines centre or side mode dominance. In this table we have also included a massive $N = 1$, spin 2 graviton superposition as a dark matter possibility which we will look at in Section 8.2. There are other possibilities which we have not included.

Mass Type	Spin	N	$c_3 * c_3$	$c_4 * c_4$	$c_5 * c_5$	$c_6 * c_6$	$c_7 * c_7$
Infinitesimal mass gravitons	2	2	0.8342	$\approx 3 \times 10^{-5}$	0.1657		
Massive Spin 2 gravitons	2	1	0.4847	0.0526	0.4627		
Infinitesimal mass bosons	1	2	0.4847	0.0526	0.4627		
Massive bosons	1	1		0.0134	0.8878	0.0988	
Massive fermions	½	1			0.1305	0.7254	0.1441

Table 4.3.1 Approximate probabilities for known and one possible superposition.

To this point this paper has attempted to demonstrate that infinite superpositions can behave as the SM fundamental particles. The methods used may be unconventional, but it is important to remember that primary interactions are very simple and very different in comparison to secondary interactions (see sections 2.2.2 & 2.2.3).These methods are also based on simple basic quantum mechanics and SR. There is also surprising consistency with the SM. If the principles behind the outcomes of these derivations are at least on the right track, and fundamental particles can be built by borrowing energy and mass from (space and time mode) zero point fields then, as we will see in what follows, this may have some significant and profound consequences. In particular what is currently labelled Dark Matter, may possibly be a halo of virtual time polarized ($\approx 10^{-29} eV$ & $\lambda_c \approx 185,000 ly$ at this current cosmic time) massive spin 2 gravitons, with inverse radius squared density and an exponential cutoff in the region of half a million light years.

Part 2
Consequences of Infinite Superpositions

5   Exploring Possible Connections with Gravity

5.1   Zero Point Energy Densities are Limited

If the fundamental particles can be built from energy borrowed from the spatial component of zero point fields and this energy source is limited, particularly at cosmic wavelengths, there must be implications for the maximum possible densities of these particles. In section 2.2.3 we discussed how the preons that build fundamental particles are born from a Higg's type scalar field with zero momentum in the laboratory rest frame. Infinitesimal mass particles such as gravitons borrow their mass from the time component of the same zero point fields. With zero momentum in this frame they have infinite wavelength and can borrow from anywhere in the universe. This suggests there should be little effect on localized densities, but possibly on overall average densities in any universe. So, which fundamental particle is likely to be most abundant? Working in Planck, or natural units with $G=1$, assume a graviton coupling constant between Planck masses of one. The total baryonic matter in the universe according to the ΛCDM , is $\approx 4.5 \times 10^{51} Kg$ or $\approx 2 \times 10^{59}$ Planck masses. Including dark matter this is $\approx 10^{60}$ Planck masses. Their average distance apart is approximately the radius R_{OH} of this region. As a crude illustration assume one graviton of this wavelength per pair of Planck masses. Thus there should be approximately $M^2 \approx 10^{120}$ virtual gravitons with wavelengths of the order of radius R_{OH} within this same volume. (This number is in line with more accurate later calculations.) No other fundamental particle is likely to approach these values; for example, the number of virtual photons of this extreme wavelength is much smaller. (Virtual particles emerging from the vacuum are covered in section 6.2.3) If this density of virtual gravitons needs to borrow more energy from the zero point fields than what is available at these extreme wavelengths, does this somehow control the maximum possible density of a causally connected universe?

5.1.1   Virtual particles and infinite superpositions

Looking carefully at Section 3.3 we showed there that, for all interactions between fundamental particles represented as infinite superpositions, the actual interaction is only between a single wavenumber k superposition of each particle. We are going to conjecture that a virtual particle of wavenumber k, for example, is just such a single wavenumber k member. Only if we somehow interact with it do we observe the properties of the full infinite superposition representing that particle. They are virtual before this interaction, always only lasting for $\Delta T \leq \hbar / 2\Delta E$, and the full properties do not exist until observed, as in the Copenhagen interpretation of quantum mechanics. Even though they are only a single wavenumber their three superposition modes as in Table 4.3.1 partially identify them. This combination and its probability as in Eq.(2.2.4) $N \cdot s \cdot dk / k$ and the first paragraph after Eq.

(3.3.12) defines the full particle properties. We will use this conjectured virtual property when looking at the probability density of virtual gravitons of the maximum cutoff wavelength. Virtual gravitons are thus a superposition of the three modes $n = 3, 4, 5$ as in Table 4.3.1, but of a single wavenumber k only. Time polarized or spherically symmetric versions are a further equal $(1/\sqrt{5})$ superposition of $m = \pm 2, \pm 1, 0$ states of the above $n = 3, 4, 5$ mode superpositions. A spin 2 virtual graviton in an $m = +2$ state is simply a superposition of the three modes $n = 3, 4, 5$ as above, but all in an $m = +2$ state.

5.1.2   Virtual graviton density at wavenumber *k* in a causally connected universe

From this point on we will use Planck units $\hbar = c = G = 1$. (We will however, later suggest that, while $G = 1$ now that it varies with cosmic time to fit with QM.) General Relativity predicts nonlinear fields near black holes, but in the low average densities of typical universes we can assume approximate linearity. The majority of mass moves slowly relative to comoving coordinates so we can ignore momentum (i.e. $\beta << 1$), provided we limit this analyses to comoving coordinates. Spin 2 gravitons transform as the stress tensor in contrast to the 4 current Lorentz transformations of spin 1, but, at low mass velocities the only significant term is the mass density T_{00}. In comoving coordinates the vast majority of virtual gravitons will thus be time polarized or spherically symmetric which we will for simplicity call scalar. We will initially do all our calculations in these comoving coordinates where we should be able to simply apply the equations in sections 3.4 & 3.5 to spin 2 virtual graviton emissions, as they should apply equally to both spins 1 & 2 at low mass velocities. (This is not necessarily so near black holes.) We will assume spherically symmetric $l = 3$ wavefunctions emit both spin 1 & 2 scalar virtual bosons, and $l = 3, m = \pm 2$ states can emit both $m = \pm 1$ spin 1 bosons and $m = \pm 2$ spin 2 gravitons. Section 3.4 derived the electrostatic energy between infinite superpositions. In flat space we looked at the amplitude that each equivalent point charge emits a virtual photon, and then focused on the interaction terms between them. Thus we can use the same scalar wavefunctions Eq's.   (3.4.1) for virtual scalar gravitons as we did for virtual scalar photons. Using $(\psi_1 + \psi_2) * (\psi_1 + \psi_2) = \psi_1 * \psi_1 + \psi_1 * \psi_2 + \psi_2 * \psi_1 + \psi_2 * \psi_2$ we showed in section 3.4.1 that the interaction term for virtual photons is

$$\psi_1 * \psi_2 + \psi_2 * \psi_1 = \frac{4k}{4\pi r_1 r_2} e^{-k(r_1 + r_2)} \cos k(r_1 - r_2) \tag{5.1.1}$$

This equation is strictly true only in flat space but it is still approximately true if the curvature is small or when $2m/r <<<< 1$, which we will assume applies almost everywhere throughout the universe except in the infinitesimal fraction of space close to black holes. In both sections 3.4 & 3.5, for simplicity and clarity, we delayed using coupling constants and emission probabilities in the wavefunctions until necessary. We do the same here. There will also be some minimum wavenumber k which we call k_{min} where for all $k < k_{min}$ there will be insufficient zero point energy available, and Eq. (5.1.1) cuts off exponentially. We will find that this maximum wavelength is where $k_{min} \approx 1/R_{OU}$ $(= 1/R_{ObservableUniverse})$. In Section 6 we find gravitons have an infinitesimal rest mass m_0 of the same order as this minimum wavenumber k_{min}. At these extreme k values this rest mass must be included in the

wavefunction exponential term. It is normally irrelevant for infinitesimal masses. Section 6.2 looks at $N = 2$ infinitesimal rest masses finding in Eq.(**6.2.5**) that $\left\langle K_{k\min} \right\rangle^2 \approx 1$.

Using Eq. (3.1.11) and $\hbar = c = 1$

$$\left\langle K_{k\min} \right\rangle^2 = \frac{s \left\langle n \right\rangle^2 k_{\min}^2}{2m_0^2} \approx 1 \text{ so for spin 2 gravitons } \frac{\left\langle n \right\rangle^2 k_{\min}^2}{m_0^2} \approx 1 \text{ or } m_0 \approx \left\langle n \right\rangle k_{\min} \tag{5.1.2}$$

Table 4.3.1 tells us for $N = 2$ spin 2 gravitons $\left\langle n \right\rangle \approx 3.29$ so that $m_0 \approx 3.29 k_{\min}$ $\quad$ (5.1.3)

This virtual mass m_0 increases the ΔE term in $\Delta E \cdot \Delta T \leq \hbar / 2$ for a virtual graviton from $\Delta E = k$ to $\Delta E = \sqrt{k^2 + m_0^2}$ when $\hbar = c = 1$, reducing the range $r \approx \Delta T \approx \Delta E^{-1}$ over which it can be found. This range is controlled by the exponential decay term e^{-kr} in its wavefunction, becoming $e^{-\sqrt{k^2 + m_0^2}}$ near $k_{\min}$. So we can define a k' using Eq. (5.1.3)

$$k' = \sqrt{k^2 + m_0^2} \approx \sqrt{k^2 + 10.84 k_{\min}^2} \text{ and } k'_{\min} \approx \sqrt{k_{\min}^2 + 10.84 k_{\min}^2} \approx 3.44 k_{\min} \tag{5.1.4}$$

Using the normalized virtual graviton wavefunction Eq. (3.4.1) we can say that:

$$\text{A massless } \psi = \sqrt{\frac{2k}{4\pi}} \frac{e^{-kr+ikr}}{r} \text{ becomes with infinitesimal mass } \sqrt{\frac{2k'}{4\pi}} \frac{e^{-k'r+ikr}}{r} \tag{5.1.5}$$

Thus the massless interaction term in Eq. (5.1.1) becomes with this infinitesimal mass m_0

$$\psi_1 * \psi_2 + \psi_2 * \psi_1 = \frac{4k'}{4\pi r_1 r_2} e^{-k'(r_1+r_2)} \cos k (r_1 - r_2) \tag{5.1.6}$$

Let point P in Figure 5.1.1 be anywhere in the interior region of a typical universe. Let the average density (or its equivalent transformed value) be ρ_U (subscript U for universe) Planck masses/energy density per unit volume. Consider two spherical shells initially in comoving coordinates around the central point P of radii r_1 & r_2 and thicknesses dr_1 & dr_2 with masses $dm_1 = \rho_U dv_1 = 4\pi r_1^2 dr_1 \rho_U$ and $dm_2 = \rho_U dv_2 = 4\pi r_2^2 dr_2 \rho_U$
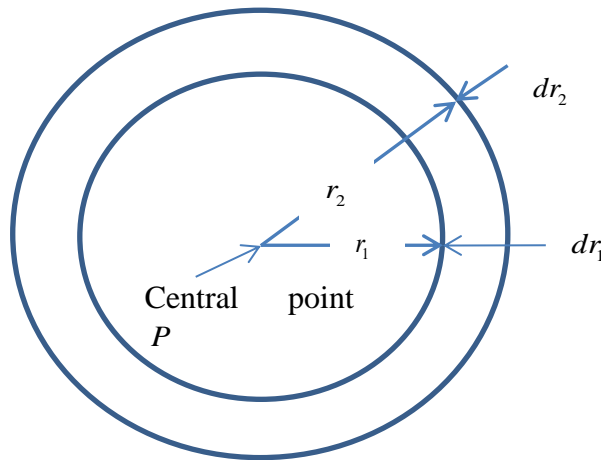
Figure 5.1.1 Two spherical shells surrounding a central point.

In Planck units we know that the gravitational constant $G = 1$ applies between Planck masses, so we might expect the graviton coupling constant is $\alpha_G = 1$ between Planck masses also, but we don't actually know this. (Its actual value has no effect on what we are going to do in section 5, but Eq.(8.2.16) finds that $\alpha_G \approx 0.004$ fits with cosmic observations.

$$\text{The secondary graviton coupling constant between Planck masses } = \alpha_G \qquad (5.1.7)$$

Section 3.4.1 in Eq. (3.4.3) used scalar emission probability $(2\alpha/\pi)(dk/k)$ for spin 1 photons. Equation (**2.1.4**) and the paragraph following tell us that this probability is proportional to $sNdk/k$. Thus Eq. (**3.3.18**) and the italics following imply that the scalar emission probability for spin 2 gravitons becomes $(4\alpha/\pi)(dk/k)$ between Planck masses, or twice that of spin 1. Equation (**6.2.8**) suggests all superpositions cutoff exponentially @ k_{min}. Looking at what we did in deriving Eq. (3.3.14) for graviton emission probability, we must include this cutoff twice i.e. $(1 - Exp[-0.65k/k_{min}])^2$, first for graviton superpositions, then for mass superpositions. (We are looking at emission probability here, not exchange probability, which requires four powers.) Now distant galaxies recede at light like and greater velocities, but all clocks in comoving coordinates tick at the same rate and quantum interactions (a bit likes Mach's principal) are instantaneous over all space. Thus, as we integrate over radii r_1 & $r_2 = 0 \rightarrow \infty$ we can still use the same equations as if the distant galaxies are not moving. (The vast majority of mass is moving relatively slowly in these comoving coordinate systems and we return to this important comoving coordinate property in section 5.3.1). Using the spin 2 coupling probability $(4\alpha_G/\pi)(dk/k)$ between Planck masses we can now integrate over both radii r_1 & r_2; but to avoid counting all pairs of masses dm_1 & dm_2 twice, we must divide the integral by two. The total probability density of virtual gravitons at any point P in the universe at wavenumber k, is using Eq.(5.1.6)

$$\rho_{Gk} = \frac{\rho_U^2}{2}\alpha_G(1 - e^{-0.65k/k_{min}})^2 \frac{4}{\pi}\frac{dk}{k}\iint_{0\rightarrow\infty} 4\pi r_1^2 dr_1 \cdot 4\pi r_2^2 dr_2 \cdot \frac{4k'}{4\pi r_1 r_2}e^{-k'(r_1+r_2)}\cos k(r_1 - r_2)$$

$$= 32\alpha_G(1 - e^{-0.65k/k_{min}})^2\rho_U^2\frac{k'}{k}dk\iint_{0\rightarrow\infty} r_1 r_2 e^{-k'(r_1+r_2)}\cos k(r_1 - r_2)\cdot dr_1 \cdot dr_2$$

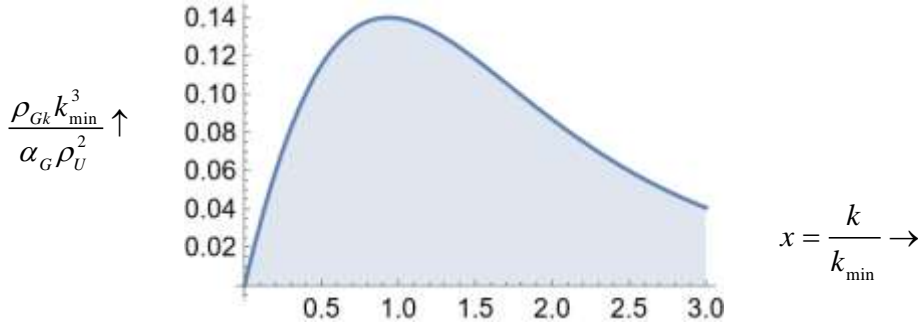Expanding $\cos k(r_1 - r_2) = \cos kr_1 \cos kr_2 + \sin kr_1 \sin kr_2$ we can then use:

$$\int_{r=0}^{r=\infty} re^{-k'r}\cos kr = \frac{k'^2 - k^2}{(k'^2 + k^2)^2} \text{ to get } \iint_{0\rightarrow\infty} e^{-k'(r_1+r_2)}\cos kr_1 \cos kr_2 dr_1 dr_2 = \frac{k'^4 - 2k'^2k^2 + k^4}{(k'^2 + k^2)^4}$$

$$\text{and } \int_{r=0}^{r=\infty} re^{-k'r}\sin kr = \frac{2k'k}{(k'^2 + k^2)^2} \text{ to get } \iint_{0\rightarrow\infty} e^{-k'(r_1+r_2)}\sin kr_1 \sin kr_2 dr_1 dr_2 = \frac{4k'^2k^2}{(k'^2 + k^2)^4}$$

Adding both together $\rho_{Gk} = 32\alpha_G(1 - e^{-0.65k/k_{min}})\rho_U^2\frac{k'}{k}dk\frac{(k'^2 + k^2)^2}{(k'^2 + k^2)^4}$

$$= 32\alpha_G(1 - e^{-0.65k/k_{min}})\rho_U^2\frac{k'}{k}dk\frac{1}{(k'^2 + k^2)^2} \qquad (5.1.8)$$

From Eq.(5.1.4) $k' = \sqrt{k^2 + m_0^2} \approx \sqrt{k^2 + 10.84k_{min}^2}$ and we can write Eq.(5.1.8) as

$$\rho_{Gk} = 32\alpha_G \rho_U^2 (1 - e^{-0.65k/k_{min}})^2 \frac{\sqrt{k^2 + 10.84k_{min}^2}}{\left(2k^2 + 10.84k_{min}^2\right)^2} \frac{dk}{k}$$

$$(5.1.9)$$

$$\rho_{Gk} \approx 32\alpha_G \frac{\rho_U^2}{k_{min}^4} \frac{(1 - e^{-0.65x})^2 \sqrt{x^2 + 10.84}}{\left(2x^2 + 10.84\right)^2} \frac{k_{min} dx}{x} \quad \text{where} \quad x = \frac{k}{k_{min}}$$

$\frac{\rho_{Gk} k_{min}^3}{\alpha_G \rho_U^2} \uparrow$

$x = \frac{k}{k_{min}} \rightarrow$

Figure 5.1.2 A plot of Eq.(5.1.9). We will show below that ρ_U / k_{min}^2 is a constant for all space time, thus this plot looks the same in all metrics, but the local measurement of k_{min} increases inversely to the local clock rate, with $k_{min} \propto g_{00}^{-1/2} = g_{rr}^{1/2}$ near mass concentrations. The wavenumber probability density of the extra gravitons emitted near mass concentrations is also identical to the above curve, but the vertical axis is proportional to Gm/r.

Converting Eq. (**5.1.9**) back to dk_{min} we can express it as follows:

Cutoff wavelength probability density $\rho_{Gk\,min} \approx \dfrac{0.154\alpha_G \rho_U^2}{k_{min}^4} dk_{min}$ when $\dfrac{k}{k_{min}} = x = 1$.

Cutoff wavelength probability density $\rho_{Gk\,min} = K_{Gk\,min} dk_{min}$ where $K_{Gk\,min} \approx \dfrac{0.154\alpha_G \rho_U^2}{k_{min}^4}$

$$(5.1.10)$$

5.2 Can we Relate all this to General Relativity?

The above assumes a homogeneous universe that is essentially flat on average. At any cosmic time T it also assumes there is always some value k_{min} where the borrowed energy density $E_{Gk\,min} = E_{ZP\,min}$, the available zero point energy density @ k_{min}. We have initially assumed comoving coordinates, but at peculiar velocities our spherical shells become ellipses and our equation $\rho_{Gk\,min} = K_{Gk\,min} dk_{min}$ should remain true at any peculiar velocity, also in all coordinates. So, what happens if we put a small mass concentration $+m_1$ at some point? The gravitons it emits must surely increase the local density of k_{min} gravitons, upsetting the balance between borrowed energy and that available. However, GR informs us that near mass concentrations the metric changes, radial rulers shrink and local observers measure larger radial lengths. This expands locally measured volumes lowering their measurement of the background $\rho_{Gk\,min}$. But clocks slowdown also, increasing the locally measured value of k_{min}. Let us look at whether we can relate these changes in rulers and clocks with the $\rho_{Gk\,min} = K_{Gk\,min} dk_{min}$ of Eq. (5.1.10).

5.2.1 Approximations with possibly important consequences

Let us refer back to Eq. (3.4.2) and the steps we took in section 3.4.1 to derive it; but now including $k' = \sqrt{k + m_0} \approx \sqrt{k^2 + 10.84 k_{min}^2}$ as in Eq.(5.1.4)

$$\psi_1 * \psi_2 + \psi_2 * \psi_1 = \frac{4 k'_{min}}{4 \pi r_1 r_2} e^{-k'_{min}(r_1 + r)} \cos[k_{min}(r_1 - r)] \tag{5.2.1}$$

Assume spacetime is approximately flat or $g_{\mu\nu} \approx \eta_{\mu\nu}$, with errors $\propto 1 - (1 - 2m/r)^{1/2} \approx m/r$. Using Figure 3.4.2, Eq. **(5.2.1)** is the probability that a virtual graviton of wavenumber k is at the point P if all other factors are one. . Let us now put mass m_1 Planck masses at the Source 1 point in Figure 3.4.2, or as in Figure 5.2.1. Also assume that the point P is reasonably close to mass m_1 (in relation to the horizon radius) at distance r_1 as in Figure 5.2.1 and the vast majority of the rest of the mass inside the causally connected or observable horizon R_{OH} is at various radii r, equal to r_2 of Eq. (5.2.1) where $r_2 = r \gg r_1$ and thus $\cos[k(r_1 - r)] \approx \cos(-kr)$ & $e^{-k'(r_1 + r_2)} \approx e^{-k'r}$. This is equivalent to localizing General Relativity to much smaller than horizon radii, but still to vast cosmic radii. Only under these conditions can we approximate Eq. (5.2.1) as

$$\psi_1 * \psi_2 + \psi_2 * \psi_1 \approx \frac{4 k'}{4 \pi r_1 r} e^{-k'r} \cos(-kr) \tag{5.2.2}$$
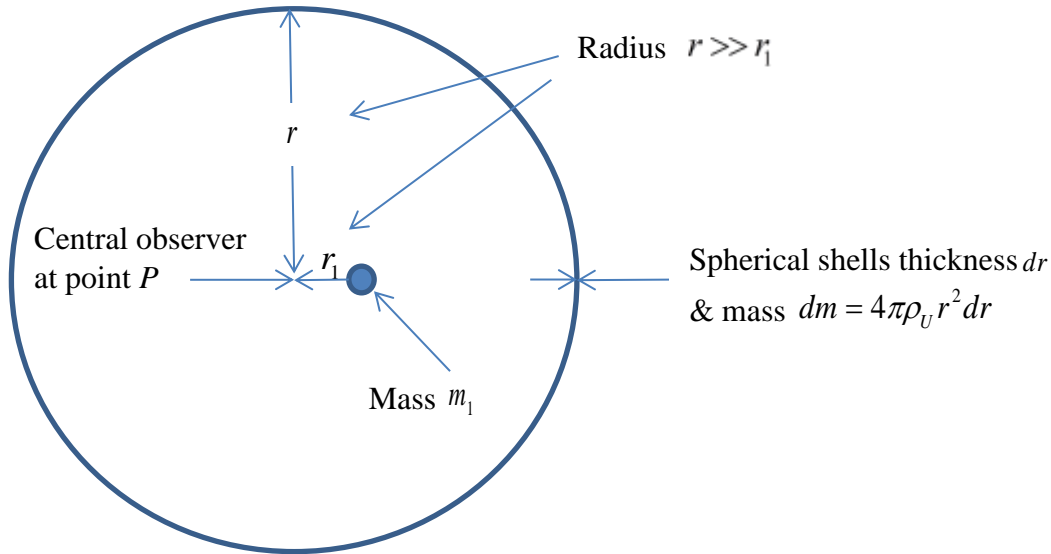
Figure 5.2.1 A central observer at a distance r_1 from a mass concentration.

We are assuming time polarized gravitons are as we are looking at the scalar potential of a central mass relative to the rest of the universe, or a time polarized/ scalar interaction with no directional effects due to spatial polarization. We can consider simple spherical shells (again initially in comoving coordinates) of thickness dr and radius r around a central observer at the point P which have mass $dm = \rho_U 4 \pi r^2 dr$. At each radius r the spin 2 gravitons coupling

factor including cutoff is $(1 - e^{-0.61k^2/k_{min}^2})^2(2\alpha_G / \pi)(dk / k)$ between Planck masses. Again assuming instantaneous quantum coupling as if space is not expanding:

$$\text{Coupling factor} = (1 - e^{-0.65k/k_{min}})^2 \frac{4\alpha_G m_1}{\pi} dm \frac{dk}{k} = (1 - e^{-0.65k/k_{min}})^2 \frac{2\alpha_G m_1}{\pi} \rho_U 4\pi r^2 dr \frac{dk}{k}$$

Including this coupling factor

$$(1 - e^{-0.65k/k_{min}})^2 (\frac{4\alpha_G m_1}{\pi} \frac{dk}{k} \rho_U 4\pi r^2 dr)(\psi_1 * \psi_2 + \psi_2 * \psi_1)$$

$$= (1 - e^{-0.65k/k_{min}})^2 \left(\frac{4\alpha_G m_1}{\pi} \frac{dk}{k} \rho_U 4\pi r^2 dr \right) \left(\frac{4k'}{4\pi r_1 r} e^{-k'r} \cos(-kr) \right) \qquad (5.2.3)$$

$$= (1 - e^{-0.65k/k_{min}})^2 \alpha_G \frac{m_1}{r_1} \frac{16\rho_U}{\pi} \frac{k'dk}{k} re^{-k'r} \cos(-kr)dr$$

This is the virtual graviton density at point P due to each spherical shell. (Ignoring the relatively small number of k_{min} gravitons emitted by mass m_1 itself $\psi_{m_1} * \psi_{m_1}$, (Section 7). Integrating over radius $r = 0 \to \infty$ the virtual graviton density at wavenumber k_{min} using Eqs.(5.1.4) and **(5.2.3)** is

$$\Delta\rho_G = (1 - e^{-0.65k/k_{min}})^2 \alpha_G \frac{m_1}{r_1} \frac{16\rho_U}{\pi} \frac{k'dk}{k} \int_0^\infty re^{-k'r} \cos(-kr)dr \qquad (5.2.4)$$

$$= (1 - e^{-0.65k/k_{min}})^2 \alpha_G \frac{m_1}{r_1} \frac{16\rho_U}{\pi} \frac{k'dk}{k} \left[\frac{(k'^2 - k^2)}{(k'^2 + k^2)^2} \right]$$

Now $k'^2 = k^2 + m_0^2 \approx k^2 + 10.82k_{min}^2$ so

$$\Delta\rho_G \approx (1 - e^{-0.65k/k_{min}})^2 \alpha_G \frac{m_1}{r_1} \frac{16\rho_U}{\pi} \frac{\sqrt{k^2 + 10.84k_{min}^2} dk}{k} \left[\frac{10.84k_{min}^2 + k^2 - k^2}{(10.84k_{min}^2 + k^2 + k^2)^2} \right]$$

$$\approx (1 - e^{-0.65k/k_{min}})^2 \alpha_G \frac{m_1}{r_1} \frac{16\rho_U}{\pi} \frac{\sqrt{k^2 + 10.84k_{min}^2} dk}{k} \left[\frac{10.84k_{min}^2}{(10.84k_{min}^2 + 2k^2)^2} \right]$$

$$\text{Putting } x = \frac{k}{k_{min}}, \ \Delta\rho_{Gk min} \approx \frac{16}{\pi} \alpha_G \frac{m_1}{r_1} \frac{\rho_U}{k_{min}^2} (1 - e^{-0.65x})^2 \frac{\sqrt{x^2 + 10.84}}{x} \left[\frac{10.84}{(2x^2 + 10.84)^2} \right] \frac{k_{min} dx}{x} \qquad (5.2.5)$$

Equation (5.1.10) hypothesizes $\rho_{Gk min} = K_{Gk min} dk_{min}$. In a metric far from masses where $g_{\mu\nu} = \eta_{\mu\nu}$, k_{min} has its lowest value. As we approach any mass k_{min} increases to k''_{min} where we use blue/green double primes when $g_{\mu\nu} \neq \eta_{\mu\nu}$ due to metric changes. This avoids confusion with the k' & k'_{min} of Eq.(5.1.4). At a radius r from mass m the Schwarzchild metric is $(1 - 2m/r)^{\pm 1/2}$ for the time and radial terms. Radial rulers shrink and clocks slow, measured volumes and frequencies both increase locally as $\approx 1 + \frac{m}{r}$. Initially ignoring any increase in frequency of k_{min} and only consider the increase in the local measured volume. We will also initially approximate with a small mass assuming the change in k_{min} is small enough

to ignore. Thus $\frac{V+\Delta V}{V} \approx 1+\frac{m}{r}$ and $\frac{\Delta V_N}{V} \approx \frac{m}{r}$ if $r >>> m$, we are also going to assume that

$\frac{\Delta \rho_{Gk}}{\rho_{Gk}} \approx \frac{\Delta V_N}{V}$ and we can say that:

$$\frac{\Delta \rho_{Gk}}{\rho_{Gk}} \approx \frac{\Delta V_N}{V} \approx \frac{m}{r} \tag{5.2.6}$$

We can now put Eqs. (**5.1.9**) and (**5.2.5**) into Eq. (**5.2.6**) and dropping the now unnecessary subscripts, the graviton coupling constant α_G and exponential cutoff $(1-e^{-0.61k^2/k_{min}^2})^2$ cancel:

$$\frac{\Delta \rho_{Gk\,min}}{\rho_{Gk\,min}} \approx \frac{\frac{16}{\pi}\alpha_G \frac{m}{r}\frac{\rho_U}{k_{min}^2}(1-e^{-0.65x})^2 \frac{\sqrt{x^2+10.84}}{x}\left[\frac{10.84}{(2x^2+10.84)^2}\right]\frac{k_{min}dx}{x}}{32\alpha_G \frac{\rho_U^2}{k_{min}^4}\frac{(1-e^{-0.65x})^2\sqrt{x^2+10.84}}{(2x^2+10.84)^2}\frac{k_{min}dx}{x}} \approx \frac{m}{r}$$

All terms in x cancel and this equation reduces to:

$$\frac{\Delta \rho_{Gk\,min}}{\rho_{Gk\,min}} \approx \frac{16 \times 10.84}{32\pi}\frac{k_{min}^2}{\rho_U}\frac{m}{r} \approx 1.725\frac{k_{min}^2}{\rho_U}\frac{m}{r} \approx \frac{m}{r} \tag{5.2.7}$$

This equation tells us that even though both ρ_U & k_{min} reduce their values with the passing of cosmic time the ratio k_{min}^2/ρ_U is always invariant, and Figure 5.1.2 is always true in any metric. To be consistent with GR; at all points inside the horizon $\frac{\rho_U}{k_{min}^2} \approx 1.765$ in Planck units at any cosmic time.

The average density of the universe $\rho_U \approx 1.725k_{min}^2 \approx 1.725\frac{\Upsilon^2}{R_{OU}^2}$

Where the parameter $\Upsilon = k_{min}R_{OH}$ is in radians. $\tag{5.2.8}$

Putting Eq, (**5.2.8**) density $\rho_U \approx 1.725k_{min}^2$ into Eq. (5.2.8gives $\rho_{Gk\,min}$ & $K_{Gk\,min}$.

$$\rho_{Gk\,min} \approx \frac{0.154\alpha_G(1.725k_{min}^2)^2}{k_{min}^4}dk \approx 0.458\alpha_G dk_{min} = K_{Gk\,min}dk_{min} \ \& \ K_{Gk\,min} \approx 0.458\alpha_G \tag{5.2.9}$$

The value of $K_{Gk\,min}$ is invariant in any metric and at any peculiar velocity, If our conjectures are true, this is the number density of maximum wavelength gravitons excluding possible effects of virtual particles emerging from the vacuum. In section 6.2.3 we argue these do not change the $K_{Gk\,min}$ of Eq. (**5.2.9**).

5.2.2 The Schwarzschild metric near large masses

At a radius r from a mass m (dropping the now unnecessary suffixes) the Schwarzschild metric is $(1-2m/r)^{\pm 1/2}$ for the time and radial terms which can be written as

$$\sqrt{g_{rr}} = \frac{1}{\sqrt{1-2m/r}} = \frac{1}{\sqrt{g_{00}}} = \frac{1}{\sqrt{1-\beta_M^2}} = \gamma_M \tag{5.2.10}$$

Velocity β_M ($c=1$) is that reached by a small mass falling from infinity and $\gamma_M^{\pm 1}$ is the metric change in clocks and rulers due to mass m. We use blue/green symbols with the subscript M for metrics $g_{\mu\nu} \neq \eta_{\mu\nu}$ as we did for $k''_{\min}$ above. The symbols $\gamma_M^{\pm 1}$ help clarity in what follows.

$$\gamma_M^2 = \frac{1}{1-2m/r} = g_{rr} = \frac{1}{g_{00}} \to \beta_M^2 = \frac{2m}{r}$$

Using these symbols $k''_{\min} = \gamma_M k_{\min}$ & $dk''_{\min} = \gamma_M dk_{\min}$ & $\rho''_{Gk\min} = \gamma_M \rho_{Gk\min}$ (5.2.11)

We can also differentiate Eq. (5.2.10) keeping the radius fixed.

$$d\frac{1}{(1-\frac{2m}{r})^{1/2}} = \frac{\frac{dm}{r}}{(1-\frac{2m}{r})^{3/2}} \text{ or } \frac{d\gamma_M}{\gamma_M} = \frac{dV}{V} = \gamma_M^2 \frac{dm}{r} \text{ which is equivalent to}$$

$$\frac{\text{The change in Frequency}}{\text{Frequency before change}} = \frac{\text{The change in Volume}}{\text{Volume before change}} = \gamma_M^2 \frac{\text{The change in Mass}}{\text{Radius of Measurement}} \quad (5.2.12)$$

Up to this point we have been working in comoving coordinates. Velocities relative to comoving coordinates are usually referred to as peculiar velocities. To distinguish them from green metric symbols we will use red symbols where $\gamma_P^2 = (1-\beta_P^2)^{-1}$. At peculiar velocity β_P the local Lorentz (or SR) transformation of universe density ρ_U is $\gamma_P^2 \rho_U$ and frequency or wavenumber $k_{\min}$ as $\gamma_P k_{\min}$. Thus $\rho_U / k_{\min}^2$ in Eq. 5.2.5 does not change at peculiar velocities, but what happens if we change the metric locally around mass concentrations? Equation 5.2.5 was derived by looking at graviton coupling between a very small central mass and the mass of the rest of the universe assuming approximately flat spacetime. In section 8 we argue that GR is highly accurate up to galactic, and galaxy cluster scales, but not cosmic scales. Even with black holes, the volume of warped spacetime in the galaxies surrounding them is infinitesimal compared to the cosmic scale wavefunction volume that is in approximately flat spacetime. Instead of complicating things with wavefunctions in curved spacetime we can perhaps try a very simple approach. Lorentz transformations or SR apply locally but not at cosmic scale, where Hubble flow galaxy velocities exceed that of light. From Table 6.2.1 the Compton wavelength of infinitesimal mass gravitons is $\lambdabar_C \approx 1.76 R_{OH}$, if we think of a large sphere of this radius or multiples of it, regardless of changes in a small localized metric, the number of atoms for example inside it, is fixed at any cosmic time. They may all have random peculiar velocities with KE relative to comoving coordinates all moving at various Hubble flow velocities due to space expansion, but the number of them inside this expanding space is constant at any cosmic time, as seen by an imaginary observer outside the cosmos. We know from GR that a mass m is the value when measured where $g_{\mu\nu} = \eta_{\mu\nu}$. In any metric, a local observer measures both mass dm, after falling to his location, and that of all the fixed number of distant atoms as having increased by γ_M. Also frequency or wavenumber $k_{\min}$ & $dk_{\min}$ increases as γ_M. Thus $\Delta\rho_{Gk\min} \propto \gamma_M^3$ in Eq(5.2.5), also $\rho_{Gk\min} \propto \gamma_M$

in Eq.(**5.1.10**), implying $\dfrac{\Delta\rho_{Gk\min}}{\rho_{Gk\min}} \propto \dfrac{\gamma_M^3 \, dm \, / \, r}{\gamma_M} \propto \gamma_M^2 \dfrac{dm}{r}$. Assuming Eq.(**5.2.7**) which used

Eq(5.2.5) is true for very small masses $\dfrac{\Delta\rho_{Gk\min}}{\rho_{Gk\min}} = \dfrac{\Delta\gamma_M}{\gamma_M} = \gamma_M^2 \dfrac{dm}{r}$ as in Eq.(**5.2.12**).

5.3 A Different Expansion to the Lambda Cold Dark Matter Model

Section 5.1.1 describes virtual gravitons as superpositions of the three modes $n = 3,4,5$ at a single wavenumber k, as in Table 4.3.1 from which we find $\langle n \rangle \approx 3.29$. Using Eqs. (3.1.11),

(3.1.12), (**3.2.10**)&(**5.1.2**); $\langle \gamma_k \rangle^2 = 1 + \langle K_k \rangle^2$, $\langle \beta_k \rangle^2 = \dfrac{\langle K_k \rangle^2}{1 + \langle K_k \rangle^2}$. For $N = 2$ spin 2 gravitons

$$\langle K_k \rangle = \frac{\langle n \rangle k}{m_0} = \frac{\langle n \rangle k}{\langle n \rangle k_{\min}} = \frac{k}{k_{\min}} \quad \text{and thus we can express these as}$$

$$\langle \gamma_k \rangle^2 = 1 + x^2 \quad \text{and} \quad \langle \beta_k \rangle^2 = \frac{x^2}{1+x^2} \quad \text{where} \quad x = \frac{k}{k_{\min}} \tag{5.3.1}$$

Using Eq. (5.1.2) $m_0 = \langle n \rangle k_{\min} \approx 3.3 k_{\min}$ and from Eq. (3.1.4), we find spin 2 gravitons borrow from time polarized quanta a mass $m_0 \, / \, (\gamma\sqrt{2s}) = m_0 \, / \, (2\gamma) = 3.3 k_{\min} \, / \, (2\sqrt{1+x^2})$. The total energy squared of a superposition mode n is the rest mass squared that is borrowed plus the momentum squared $\langle p^2 \rangle = \langle n^2 \rangle k^2 = 3.33^2 k^2$ if $\hbar = 1$. Equation (3.2.1) says $\langle \mathbf{p}_k (debt) \rangle = -\langle \beta_k \rangle^2 \langle n \rangle \hbar \mathbf{k}$ is the vacuum debt of spatially polarized quanta. But as in Eq.(**2.2.4**) even though we are considering only a single graviton emitted, its superposition occurs with probability $N \cdot s \cdot dk \, / \, k$ so we need to multiply this spatial debt by $N \cdot s = 4$ for $N = 2$ infinitesimal mass spin 2 gravitons. (See first paragraph after Eq. (3.3.12).) So putting $\hbar = 1$, multiplying by 4 and ignoring minus signs and putting $k = \dfrac{k_{\min} k}{k_{\min}} = k_{\min} x$ for gravitons:

Spatial vacuum debt per graviton at wavenumber k is $\Delta E_{kSpatial} \approx 3.3 k_{\min} \dfrac{4x^3}{1+x^2}$ $\tag{5.3.2}$

Time vacuum debt per graviton at k is $\Delta E_{kTime} \approx 4 \times \dfrac{3.3 k_{\min}}{2\sqrt{1+x^2}} \approx \dfrac{6.6 k_{\min}}{\sqrt{1+x^2}}$ $\tag{5.3.3}$

Equations (**5.1.9**) & (**5.1.10**) give the number density of gravitons at any wavenumber k and putting Eq.(**5.2.8**) $\rho_U \approx 1.722 k_{\min}^2$ into this where $32\rho_U^2 \, / \, k_{\min}^4 \approx 32 \times 1.725^2 \approx 95.22$

Graviton density at wavenumber k $\quad \rho_{Gk} \approx 95.2 k_{\min} \alpha_G dx \left[\dfrac{(1-e^{-0.65x})\sqrt{x^2+10.84}}{x(2x^2+10.84)^2} \right]$ $\tag{5.3.4}$

Multiplying Equ's. (5.3.2) & (5.3.3) by this density we get the energy densities required

$$\text{Space mode energy density required} \approx 95.2 k_{\min}^2 \alpha_G dx \left[\frac{(1\text{-}e^{-0.65x})\sqrt{x^2+10.84}}{x\left(2x^2+10.84\right)^2} \frac{3.3 \times 4x^3}{1+x^2} \right] \qquad (5.3.5)$$

$$\text{Time mode energy required} \approx 95.2 k_{\min}^2 \alpha_G dx \left[\frac{(1-e^{-0.65x})\sqrt{x^2+10.84}}{\left(2x^2+10.84\right)^2} \frac{6.6}{\sqrt{1+x^2}} \right] \qquad (5.3.6)$$

To enable numerical integration of these energies up to $k = k_{\min}$ we can use $dk = k_{\min} dx$

Integrated space mode energy density up to $k_{\min}$: $\qquad\qquad\qquad (5.3.7)$

$$k_{\min}^2 \alpha_G \int_{x=0}^{x=1} 95.2 \frac{(1\text{-}e^{-0.65x})\sqrt{x^2+10.84}}{x\left(2x^2+10.84\right)^2} \frac{3.3 \times 4x^3}{1+x^2} dx \approx 1.125 \alpha_G k_{\min}^2 .$$

Integrated time mode energy density up to $k_{\min}$: $\qquad\qquad\qquad (5.3.8)$

$$k_{\min}^2 \alpha_G \int_{x=0}^{x=1} 95.2 \frac{(1\text{-}e^{-0.65x})\sqrt{x^2+10.84}}{x\left(2x^2+10.84\right)^2} \frac{6.6}{\sqrt{1+x^2}} dx \approx 1.84 \alpha_G k_{\min}^2 .$$

But zero point energy density at @ $k_{\min}$ is $\dfrac{k_{\min}^3}{2\pi^2}$ and the integrated zero point energy available

@ $k_{\min}$ is $\dfrac{k_{\min}^4}{8\pi^2}$. Even if $\alpha_G << 1$ this is too small by about $k_{\min}^2 \approx 1/R_{OH}^2$. However, the area of

the causally connected horizon $4\pi R_{OH}^2$ suggests possible connections with holographic horizons and the AdS/CFT correspondence, but as we will find, in a very different way.

5.3.1 The Holographic Principle and Holographic Horizons

The holographic principle is a supposed property of quantum gravity and was first proposed by Gerard't Hooft. Leonard Susskind [31] described it as "The three dimensional world of ordinary experience, the universe filled with galaxies, stars, and everything we are familiar with is a hologram, an image of reality encoded on a two dimensional surface. A prime example is the AdS/CFT correspondence proposed by Malcadena [27] where anti-de Sitter or hyperbolic space with Planck modes on a 2D horizon that can perhaps be thought of as holographically generating the interior. However we are going to assume space is flat, but still use the horizon in a manner that parallels the holographic principle. We will however start with some usefull cosmology equations. Space between comoving galaxies expands with cosmic or proper time t and is called the scale factor $a(t)$. It is normally expressed as $a(t) \propto t^p$ and we will start at time $t = T_0$ with time T now.

Thus $\dot{a}(t) \propto p t^{p-1}$ and the Hubble parameter $H(t) = \dfrac{\dot{a}(t)}{a(t)} = \dfrac{p}{t}$ $\qquad\qquad (5.3.9)$

In flat space at the current time the coordinate, proper and comoving distances are all equal. Writing the present scale factor normalized so that $a(T) = 1$ implying $a(t) = t^p / T^P$, we can get the causally connected horizon radius R_{OH} and the horizon velocity V. Using Eq. (5.3.9):

$$\text{The horizon radius } R_{OH} = \int_{T_0}^{T} \frac{dt}{a(t)} = T^p \int_{T_0}^{T} \frac{dt}{t^p} = \frac{T - T_0}{1 - p} \approx \frac{T}{1 - p} \text{ if } T >> T_0 \text{ \& } p \text{ constant.} \tag{5.3.10}$$

In flat space horizon velocity $V = \dfrac{dR_{OH}}{dT} = \dfrac{d}{dT}\left[T^p \int_{T_0}^{T} \frac{dt}{t^p} \right]$, then using $d(u \cdot v) = u \cdot dv + v \cdot du$ for $(T >> T_0)$:

$\dfrac{dR_{OH}}{dT} = \dfrac{T^p}{T^p} + \dfrac{R_{OH}}{T^p}(pT^{p-1}) = 1 + \dfrac{p}{T}R_{OH}$. But $\dfrac{p}{T}$ is the Hubble parameter at time T, so

that in flat space the horizon velocity $V = 1 + H(T)R_{OH}$ regardless of how p behaves. $\qquad$ (5.3.11)

The Hubble flow velocity of a comoving galaxy on the horizon is $V' = H(T)R_{OH}$ and thus from this equation the horizon velocity is always $V = 1 + V'$. In other words, the horizon is moving at light velocity relative to comoving coordinates instantaneously on the horizon as measured by a local comoving observer. We are going to conjecture that *the space added in one unit of Planck time inside the expanding Hubble horizon creates the source of zero point quanta that we can borrow*. This extra volume is the horizon surface area $4\pi R_{OH}^2 \Delta r$ where $\Delta r = V'\Delta t$, $V' = V - 1$ is the Hubble horizon velocity, and Δt is one unit of Planck time. As preons at the centre are born with zero momentum they have infinite wavelength allowing them to borrow quanta from any point inside the causally connected horizon.

$$\text{Extra Hubble flow space volume inside horizon } 4\pi R_{OH}^2 \Delta r = 4\pi R_{OH}^2 V'\Delta t. \tag{5.3.12}$$

The density of modes available inside this extra space is:

$$\text{Mode density } = \frac{k^2}{\pi^2} dk \tag{5.3.13}$$

As zero point energies are $\hbar\omega / 2 = \hbar k / 2$ per vibration mode we need to multiply by $\hbar k / 2$. But these quanta are half time mode and half spatial. Dividing by 2 again, putting one unit of Planck time $\Delta t = 1$ then multiplying by Eq. (5.3.12):
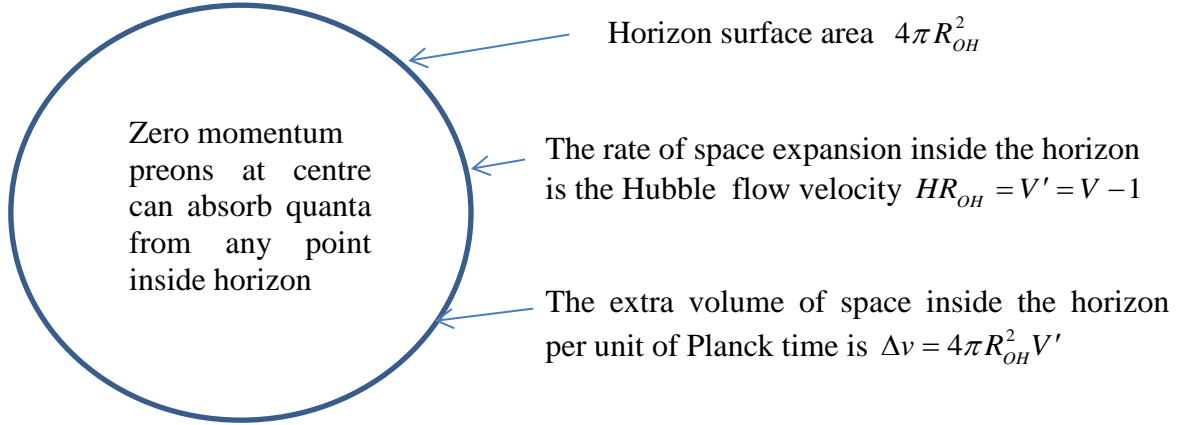
$$\text{Space and time mode energy density available} = \frac{4\pi R_{OH}^2 V'}{4} \times \frac{k^3 dk}{\pi^2} = \frac{R_{OH}^2 V' \times k^3 dk}{\pi} \tag{5.3.14}$$

Multiplying both numerator and denominator by k_{min}^2 and using Eq. $\qquad$ (5.2.8) $\Upsilon = k_{min}R_{OH}$

$$\rho_{Energy@k} \approx \frac{k_{min}^2 R_{OH}^2 V'}{\pi} dk \left[\frac{k}{k_{min}} \right]^2 \approx \frac{\Upsilon^2 V'}{\pi} \cdot k_{min}^2 x^3 dx \text{ where } x = \frac{k}{k_{min}}$$

In Eq. (**5.3.8**) we integrated the energy required by k_{min} gravitons up to k_{min}, repeating this

$$\text{Space and time mode energy density available } \rho_{Energy@k} = \frac{\Upsilon^2 V'}{4\pi} \cdot k_{min}^2 \tag{5.3.15}$$

Horizon surface area $4\pi R_{OH}^2$

The rate of space expansion inside the horizon is the Hubble flow velocity $HR_{OH} = V' = V - 1$

The extra volume of space inside the horizon per unit of Planck time is $\Delta v = 4\pi R_{OH}^2 V'$

Zero momentum preons at centre can absorb quanta from any point inside horizon

Figure 5.3.1 Preons forming a central mode k are born with zero momentum and infinite wavelength. They can borrow modes from anywhere inside the horizon. The extra volume of space available for this inside the horizon due to the scale factor expansion, can be thought of as a holographic type layer on that horizon that is the Hubble flow velocity V' thick. If $V' = 2c$ for example, this holographic layer is just two Planck lengths.

In the first half of this paper where we looked at building superpositions we assumed that mass was borrowed from a Higgs type field whereas energy was borrowed from zero point spatial modes. We will now conjecture that all *infinitesimal* mass superpositions borrow their mass from the time modes of zero point fields. This implies that we can equate Eq's. **(5.3.8)** and **(5.3.15)** at any particular cosmic time.

$$\frac{\Upsilon^2 V'}{4\pi} \cdot k_{min}^2 \approx 1.84 \alpha_G k_{min}^2$$

At all cosmic time $\quad \dfrac{\Upsilon^2 V'}{4\pi} \approx 1.84 \alpha_G$

(5.3.16)

This also implies:

At all cosmic time $\quad \Upsilon^2 \approx \dfrac{1.84 \times 4\pi \alpha_G}{V'}$

(5.3.17)

Inserting this into Eq. (5.2.8)

At all cosmic time $\quad \rho_U \approx 1.725 \dfrac{\Upsilon^2}{R_{OU}^2} \approx \dfrac{1.725 \times 1.84 \times 4\pi \alpha_G}{R_{OU}^2 V'}$

(5.3.18)

This is different to Lorentz invariant zero point densities and only works in flat expanding space with infinite wavelength preons born with zero momentum. If the above ideas are on the right track these equations may well control the expansion of space. If there is no acceleration initially as in the current ΛCDM model, we can assume a constant Hubble horizon velocity V'. Using Eq. (5.3.18) and assuming a constant mass/energy inside an expanding scale factor volume, as in current cosmology, we put the mass density $\rho \propto a^{-4}$ in the radiation dominated era and $\rho \propto a^{-3}$ in the matter dominated era. This leads to scale factors $a \propto t^{1/2}$ and $a \propto t^{2/3}$ as in current cosmology with no acceleration. Section 8.2 looks at the possibility of massive spin 2 virtual gravitons behaving as what is called dark matter, and the possibility they control space expansion acceleration in the matter dominated era. We are also going to

suggest that the time mode zero point energy in Figure 5.3.1 is also a possible source for the Higgs field.

5.3.2 A constant horizon velocity in the radiation dominated era

In the introductory notes we discussed why we can simplify things greatly in this different way of looking at gravity in flat space. We have equal coordinate, proper and comoving distances at the current time. As explained in section 8.1.2, the FLRW equation becomes a very simple $ds^2 = -c^2 dt^2 + a(t)^2 (dx^2 + dy^2 + dz^2)$ in this flat space where $a(t)$ is the scale factor at time t. Also the observable horizon radius can be very simply expressed as:

$$R_{OH} = \int V dt \text{ with } V = \frac{dR}{dt} \text{ is only true if space is flat.} \tag{5.3.19}$$

The universe density Eq. **(5.3.18)** $\rho_U \propto \dfrac{\alpha_G}{R_{OH}^2 V' G^3} \propto \dfrac{1}{a^4}$ in the radiation dominated space.

We are also going to assume a constant Hubble horizon velocity and a constant G in this era.

$$a^4 \propto R^2 \rightarrow a \propto R^{1/2} \text{ where } R = R_{OH} \tag{5.3.20}$$

The Hubble parameter $H = \dfrac{\dot{a}}{a} = \dfrac{R^{-1/2} dR/dt}{2R^{1/2}} = \dfrac{V}{2R}$ as in flat space $\dfrac{dR}{dt} = V$ the horizon velocity.

The Hubble flow velocity at $R_{OH} (= R \text{ here})$ is $V' = H \cdot R = \dfrac{V}{2}$ $\tag{5.3.21}$

As in Eq.(5.3.12) the Hubble flow velocity at the horizon is $V' = H \cdot R = V - 1$ (a comoving observer instantaneously on the horizon sees it passing him at velocity c as in local SR.)

Thus $V' = V - 1 = \dfrac{V}{2}$ or the Horizon velocity is $V = 2$ in the radiation era $\tag{5.3.22}$

A horizon velocity of $V = 2$ implies a horizon radius in flat space of $R_{OH} = \int_0^t V dt = 2t$.

From Eq.(**5.3.20**) $a \propto R^{1/2} \propto t^{1/2}$ as in current cosmology where $R = \int_0^T \dfrac{dt}{a(t)} = \int_0^T \dfrac{dt}{t^{1/2}} = 2T$.

The Stefan-Boltzmann law says $\rho_{Thermal} = \dfrac{\pi^2 k^4 T^4}{60 c^2 \hbar^3} = \dfrac{\pi^2}{60} T^4 \approx 0.1645 T^4$ in Planck units.

We can put $R_{OH} = 2t, V' = 1$ into Eq **(5.3.18)** to get the temperature in Planck units:

$\rho_{Thermal} \approx \dfrac{41.23\alpha_G}{R_{OH}^2 V'} \approx \dfrac{41.23\alpha_G}{(2t)^2} \approx 0.1645 T^4 \rightarrow T \approx 2.8 t^{-1/2} \alpha_G^{1/4}$ and converting to degrees K

Temperature $T \approx 2.8 t^{-1/2} \alpha_G^{1/4} \times 1.417 \times 10^{32} K \approx 4 \times 10^{32} t^{-1/2} \alpha_G^{1/4} K$ $\tag{5.3.23}$

Planck temperature T_{Planck} @ $t \approx \sqrt{4\alpha_G^{1/4}} \approx 2\alpha_G^{1/2}$ Planck units

Planck temperature $\approx 1.4 \times 10^{32} K$ @ $t \approx 2.2 \alpha_G^{1/2}$ Planck time.
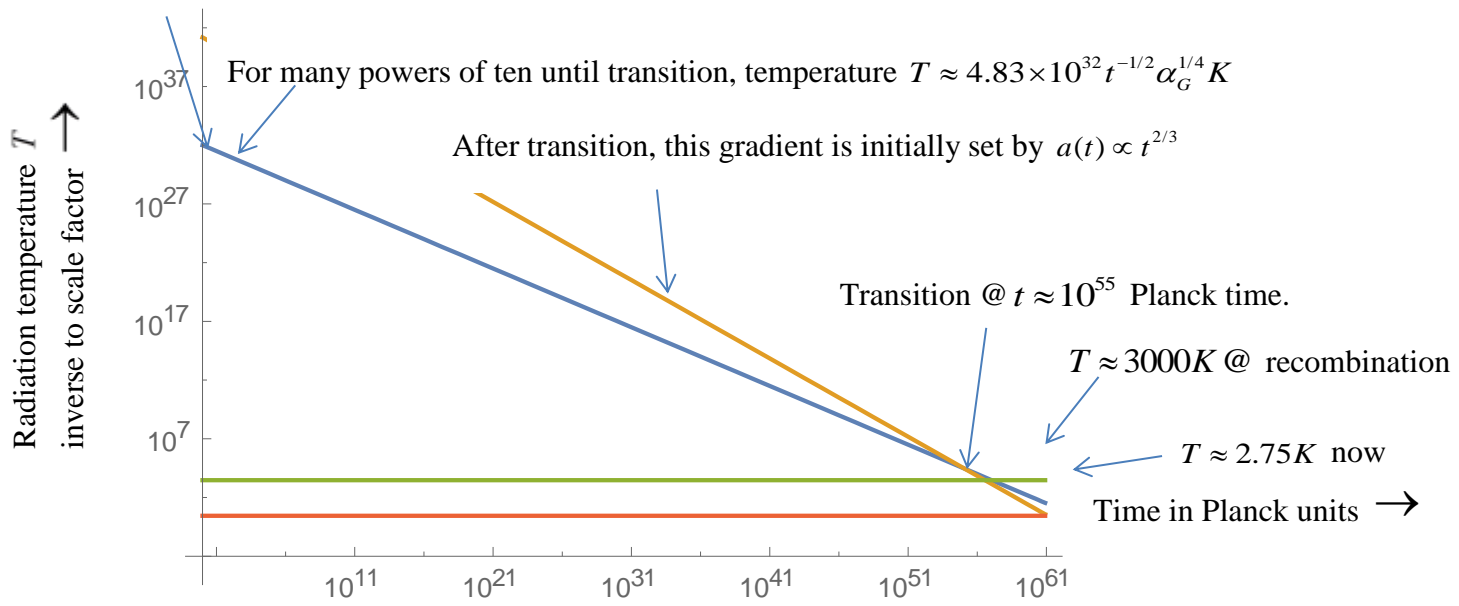
Figure 5.3.2 A logarithmic temperature plot with $\alpha_G = 0.004$ from $t = 1$ Planck units until now.

Figure 5.3.2 plots radiation temperature starting at $T \approx 1.4 \times 10^{32} K @ t \approx 2.92 \alpha_G^{1/2}$ Planck time, dropping to $T \approx 3000K$ at recombination. Equation (5.3.23) controlling this plot is based on Eq. (5.3.18), which this paper agues is true in all flat comoving coordinates and there is no need for a finely tuned critical density to achieve flat space as it is inherent in this model. Of course, we do not know exactly how long after $t = 1$ Planck time all these equations start to apply, but if it happened to be about the same time that inflation is thought to end ($t \approx 10^{10}$ Planck time or $\approx 10^{-33}$ seconds) the causally connected radius would be $R_{OH} \approx 10^{10}$ Planck lengths or $\approx 10^{-25}$ metres with quantum temperature fluctuations (as a fraction of the average) that could be similar to what inflation predicts ($\approx 10^{-5}$), and as observed in the CMB. Nucleosynthesis is virtually identical to the ΛCDM model and there should be less need for inflation as all these equations also apply in regions initially out of causal contact. Section 8.2.2 looks at an acceleration dependant effect on gravity that could effect this early era.

5.4 Non-Comoving Coordinates and Spatial Polarization

To this point we have been working in comoving coordinates for simplicity. Velocities relative to comoving coordinates are called peculiar velocities, so, does all our previous work still apply in non-comoving coordinates with these peculiar velocities? In section 5.1.2 we calculated the density of k_{min} virtual gravitons in comoving coordinates where they are spherically symmetric or time polarized. So at peculiar velocities there can be spatially polarized probability densities of them. However we can apply here the same thinking that Poincare used over a century ago. At that time there were various models of the electron, the Abraham-Lorenz probably being the most well-known [28], [29]. All these models suffered the problem of electromagnetic mass in the field being 4/3 times the relativistic mass, where the extra 1/3 came from the spatially polarized component due to velocity. In 1906 Poincare showed that if the bursting forces due to charge were balanced by stresses (or forces) in the same rest frame as the particle, these would cancel the extra 1/3 figure, restoring covariance

[30] . We can use the same principles here. In comoving coordinates we can think of our time polarized gravitons with their centres of momentum at rest. (See the scalar type interaction example as in section 3.3.2). In section 2.3 we looked at spherically symmetric wavefunctions that build these superpositions around such zero nett momentum centres. They had squared orbital momentums that would generate bursting pressures balanced by zero point forces in the same frame as that centre, which for our time polarized gravitons is at rest in comoving coordinates. These can be thought of as equivalent to the Poincare stresses holding a charged particle together. So in any other frame moving relative to it at a peculiar velocity these zero point balancing forces cancel any extra momentums or energies due to spatially polarized components. Thus spatially polarized virtual gravitons due to peculiar velocities do not add to the zero point energies borrowed from inside the horizon. We can ignore them, and only consider time polarized $k_{\min}$ gravitons in all other frames when equating zero point energies required to build virtual gravitons with that available to be borrowed from the receding horizon. In other words they do not change the metric.

We can think of a box of these $k_{\min}$ gravitons fixed in comoving coordinates. It will have a 3 volume density (or 3 dimensions) $\rho 3D_{Gk\min} = K_{Gk\min} dk_{\min}$ as we have previously calculated where by 3 volume we mean $3V = d^3x = dxdydz$. If we now move relative to it at peculiar velocity ${\color{red}\beta_P}$ (where red symbols will be used from here for peculiar velocities, to distinguish from blue/green metric changes near mass concentrations) it will shrink in size as ${\color{red}\gamma_P^{-1} = (1-\beta_P^2)^{1/2}}$ so that its new 3 volume density $\rho'' 3D_{Gk\min} = K_{Gk\min} dk''_{\min}$, where ${\color{red}dk''_{\min}/dk_{\min} = \gamma_P}$ is the local increase in wavenumber $k_{\min}$. If we repeat our derivations of the background 3 volume density, and the extra emitted by local mass concentrations, we find they also both increase by ${\color{red}dk''_{\min}/dk_{\min} = \gamma_P}$ with no change in the ratio $\Delta\rho/\rho$, so all our logic is unchanged at any peculiar velocity. But all this, is the same as saying that at any peculiar velocity, and in any metric, the 4 volume density of $k_{\min}$ gravitons is invariant at any cosmic time *T,* where 4 Volume is $4V = d^4x = dxdydzdt$ for 4 dimensions. (It is important to note here that we are discussing above the number densities of $k_{\min}$ gravitons which increase as ${\color{red}\gamma_P}$ with peculiar velocity, as distinct from energy densities of $k_{\min}$ gravitons which increase as $\gamma_P^2 = k'^2_{\min}/k^2_{\min}$ with peculiar velocity.)

5.4.1 Invariant 4 volume or 4*D* cosmic wavelength graviton densities

Define $\rho 3D_{Gk\min} = \dfrac{k_{\min}\text{Gravitons}}{3\text{Volume}} = \dfrac{k_{\min}\text{Gravitons}}{\Delta x \Delta y \Delta z}$ and as 4 volume $\Delta x \Delta y \Delta z \Delta t = \Delta x' \Delta y' \Delta z' \Delta t'$

$$\rho 4D_{Gk\min} = \dfrac{k_{\min}\text{Gravitons}}{4\text{Volume}} = \dfrac{k_{\min}\text{Gravitons}}{\Delta x \Delta y \Delta z \Delta t} = \dfrac{k_{\min}\text{Gravitons}}{\Delta x' \Delta y' \Delta z' \Delta t'} \text{ is an invariant.}$$

In flat comoving coordinates only we will define 4 volume $k_{\min}$ graviton density as

4 Volume Density $\rho 4D_{Gk\min}$ = 3 Volume Density $\rho 3D_{Gk\min}$

however $\rho 4D_{Gk\min}$ is invariant in all coordinates and in any metric.

This is equivalent to dividing $k''_{\min}$, in any metric, at any peculiar velocity, by $\gamma_P\gamma_M$ thus returning it to flat space comoving value $k_{\min}$ at any cosmic time T. As both $\rho 4D_{Gk\min}$ & $\Delta\rho 4D_{Gk\min}$ are invariant, their ratio is also invariant in any coordinates, and at any peculiar velocity at any particular cosmic time. But the flat space comoving value of $k_{\min}$ decreases with cosmic time.

5.4.2 Cosmic wavelength graviton and 4 volume or 4*D* action densities

In deriving Eq.   (**5.3.8**) we said that each $k_{\min}$ graviton always borrows a fixed amount of action, where $Action = \Delta E \cdot \Delta T$ per graviton is constant but $\Delta E \propto k_{\min}$. So if four volume (4*D*) $k_{\min}$ graviton density ($\rho 4D_{Gk\min}$) is invariant, the four volume action density required by $k_{\min}$ gravitons must also be invariant.

Our hypothesis is that at any point in spacetime, gravity is determined by the 4 volume $k_{\min}$ action density available from inside the horizon always being equal to the 4 volume $k_{\min}$ action density required by gravitons; with both remaining invariant in any coordinates.

6   Infinitesimal Mass Bosons

6.1   Cosmic Wavelength Superposition Cutoffs

In section 4.2 when we introduced gravity, for the lower limit in our integrals we assumed $k_{\min} = 0$, and then in section 5 showed that there is a lower limit $k_{\min} > 0$. It turns out that for massive $N = 1$ superpositions the effect of this is negligible in comparison to the high frequency cutoff $k_{cutoff} < \infty$, which we showed gravity can address in section 4.2. For infinitesimal rest mass $N = 2$ superpositions we cannot, however, ignore the effect of $k_{\min} > 0$

6.1.1   **Quantifying the approximate effect of $k_{\min} > 0$ on infinite superpositions**

If we look again at section 4.2.1 we can repeat what we did there as follows. Initially to illustrate these effects we will consider only $N = 1$ superpositions where we can say that when $K_{nk\text{Cutoff}} \to \infty$, and (for $N = 1$ only) $K_{nk\min} \to 0$, and thus

$$\left[\frac{-1}{1+K_{nk}^2}\right]_{K_{nk\min}}^{K_{nk}\text{cutoff}} = \frac{1}{1+K_{nk\min}^2} - \frac{1}{1+K_{nk\text{Cutoff}}^2} \approx 1-\left[\frac{1}{K_{nk\text{Cutoff}}^2}+K_{nk\min}^2\right] \approx 1-\varepsilon'' \approx \frac{1}{1+\varepsilon''} \qquad (6.1.1)$$

Our earlier infinitesimal in Eq.(4.2.2) $\varepsilon = \dfrac{1}{K_{nk}^2 \text{cutoff}}$ becomes $\varepsilon'' = \dfrac{1}{K_{nk}^2 \text{cutoff}} + K_{nk\,\text{min}}^2$.

Using section 4.2.1 and 4.2.2 equations, we can show $\dfrac{1}{K_{nk}^2 \text{cutoff}} \approx \dfrac{L_P^2}{\lambdabar_C^2}$ and $K_{nk\,\text{min}}^2 \approx \dfrac{\lambdabar_C^2}{R_{OH}^2}$.

For our purposes here we are ignoring small numerical factors such as $\langle n \rangle^2$ to show in Planck units where $L_P = 1$ that $\varepsilon'' \approx \dfrac{1}{K_{nkCutoff}^2} + K_{nk\,\text{min}}^2 = \varepsilon + \Delta\varepsilon \approx \dfrac{1}{\lambdabar_C^2} + \dfrac{\lambdabar_C^2}{R_{OH}^2}$

$$\text{(6.1.2)}$$

The ratio of the extra contribution $\Delta\varepsilon$ to ε is $\dfrac{\Delta\varepsilon}{\varepsilon} \approx \left[\dfrac{\lambdabar_C^2}{R_{OH}^2} \right]^2$

In Planck units $R_{OH}^2 \approx 10^{122}$ and $\lambdabar_C^4$ for electrons say is $\approx 10^{92}$, so the effect is of order $\Delta\varepsilon / \varepsilon \approx 10^{92}/10^{122} \approx 10^{-30}$ which we have been ignoring. We cannot ignore this, however, in the case of infinitesimal rest masses as we will see.

6.2 Infinitesimal Masses and $N = 2$ Superpositions

Looking again at angular momentum and rest masses discussed in section 3.2 the key factor in our final integrals is in Eq. (6.1.1). Using Eq. (3.1.12) we can rewrite Eq. (6.1.1) as

$$\left[\dfrac{-1}{1+K_{nk}^2} \right]_{K_{nk\,\text{min}}}^{K_{nk}\,\text{cutoff}} = \dfrac{1}{\gamma_{nk\,\text{min}}^2} - \dfrac{1}{\gamma_{nkCutoff}^2} \tag{6.2.1}$$

With massive $N = 1$ superpositions, as above, the difference between $\gamma_{nk\,\text{min}}^2$ & 1 is vanishingly small, i.e. $(\gamma_{nk\,\text{min}}^2 - 1) \to 1/\infty$ and as in section 6.1.1 this first term is of much less significance than the $\gamma_{nkCutoff}^2$ term. Now define an approximate equality between N & $\langle \gamma_{k\text{min}} \rangle^2$ using Eq. (3.1.12) as follows

$$N \approx \left[\langle \gamma_{k\text{min}} \rangle^2 = 1 + \langle K_{k\,\text{min}} \rangle^2 \right] \tag{6.2.2}$$

In section 3.2 we derived angular momentum and rest masses for only massive, or what we called $N = 1$, particles. To get integral angular momentum we had to assume in deriving Eq. (3.2.6) that the minimum value of K_{nk} or $K_{nk\,\text{min}} = 0$. For massive $N = 1$ particles, such as electrons, the error in this assumption (as in section 6.1.1) is $\approx 10^{-30}$ times smaller than ε, which for an electron is already $\varepsilon \approx 10^{-45}$ due to the high frequency cutoff @ $\approx 10^{18.31} GeV$. (We allowed for this $\varepsilon \approx 10^{-45}$ when we included gravity in section 4.2.) From section 6.1.1 above we approximated $K_{nk\,\text{min}}^2$ as $\approx \lambdabar_C^2 / R_{OH}^2$ for all massive particles. So, we can express Eq. (6.2.2) in terms of this approximation for fermions with non-infinitesimal mass

$$N \approx \left[\langle \gamma_{k\text{min}} \rangle^2 = 1 + \dfrac{\lambdabar_C^2}{R_{OH}^2} \approx 1 \right] \quad \text{as} \quad \dfrac{\lambdabar_C^2}{R_{OH}^2} \to 0 \tag{6.2.3}$$

A 10^{-10} eV mass particle has $\dfrac{\lambdabar_C^2}{R_{OH}^2} \approx 10^{-50}$

For the massive particles it appears we can say that $N = 1$. However in section 8.2 we explore the possibility of galaxy halos as spin 2 virtual gravitons of $\approx 10^{-29} eV$ mass where $\langle \gamma_{k\min} \rangle^2 - 1 \approx 10^{-10}$. At this extreme low mass (but still 10^5 larger than infinitesimal masses (which we discuss further below) Equation (6.2.1) shows that we cannot get the correct angular momentum unless something else changes, perhaps by a small change in the actual high frequency cutoff details. So if massive particles are a group with $N = 1$, then it would not seem unreasonable to imagine there could possibly be another group with $N = 2 = 1 + \langle K_{k\min} \rangle^2$ implying that $\langle K_{k\min} \rangle^2 = 1$. Repeating the derivation of Eq. (3.2.6) but with $N = 2 = 1 + \langle K_{k\min} \rangle^2$ and for clarity and simplicity let $K_{nk\text{cutoff}} \to \infty$.

$$\mathbf{L}_z(Total) = s \cdot (N = 2) m\hbar \int_{K_{nk\min}}^{\infty} \frac{K_{nk}^2}{(1 + K_{nk}^2)^2} \frac{dK_{nk}}{K_{nk}} = sm\hbar \left[\frac{-1}{1 + K_{nk}^2} \right]_{K_{nk\min}}^{\infty} \quad (6.2.4)$$

$$\mathbf{L}_z(Total) = sm\hbar \left[\frac{1}{1 + K_{nk\min}^2} \right] = sm\hbar \left[\frac{1}{(N = 2)} \right] = \frac{sm\hbar}{2} \text{ as previously.}$$

Provided we have doubled the probability of superpositions as in Eq. (2.1.4) from $s \cdot (N = 1) dk / k$ to $s \cdot (N = 2) dk / k$, the final angular momentum results in Eqs. (3.2.6) and (6.2.4) are identical. The same is true for rest mass calculations. For multiple integer n infinite superpositions if $N = 2$ then the expectation value $\langle K_{k\min} \rangle^2 = 1$. We thus conjecture:

$$\text{All } N = 2 \text{ infinite superpositions have } \langle K_{k\min} \rangle^2 = 1. \quad (6.2.5)$$

Using Table 4.3.1

$N = 2$ infinitesimal rest mass spin 1 superpositions have $\langle n \rangle \approx 3.98$

$N = 2$ infinitesimal rest mass spin 2 superpositions have $\langle n \rangle \approx 3.29$

Using Eqs. (3.1.11) and Eq. (**5.2.8**)

$$\langle K_{k\min} \rangle^2 = \frac{\langle n \rangle^2 s}{2} \lambda_C^2 k_{\min}^2 \approx \frac{15.82}{2} \lambda_C^2 k_{\min}^2 = 1 \text{ or } \lambda_C \approx 0.355 \frac{R_{OH}}{\Upsilon} \text{ for Spin 1}$$

$$\approx \frac{11.09 \times 2}{2} \lambda_C^2 k_{\min}^2 = 1 \text{ or } \lambda_C \approx 0.300 \frac{R_{OH}}{\Upsilon} \text{ for Spin 2} \quad (6.2.6)$$

From Eq.(**8.2.15**) $\Upsilon \approx 0.17$ and from Table 8.2.1 $R_{OH} \approx 39.3 ly \approx 2.29 \times 10^{61} lp \to$ when $k = 1.9$. Using these values the above equations provide the infinitesimal masses of $N = 2$ photons, gluons and gravitons as in Table 6.2.1 below.

Spin	$\langle n \rangle$	Compton Wavelength λ_c	Infinitesimal Rest Mass
1	3.98	$\approx 2.09 R_{OH}$	$\approx 3.1 \times 10^{-34} eV.$
2	3.33	$\approx 1.77 R_{OH}$	$\approx 2.6 \times 10^{-34} eV.$

Table 6.2.1 Infinitesimal masses and Compton wavelengths of $N = 2$ photons, gluons & gravitons. They limit the range of virtual photons and gravitons to approximately the horizon. The graviton rest masses above are reasonably close to recent proposals for the accelerating expansion of the cosmos [18,19].

6.2.1 Cutoff behaviours for $N = 1$ & $N = 2$ superpositions

Equation (6.2.1) can be written for both $N = 1$ & $N = 2$ superpositions using the results of sections 4.2 & 6.2 and Eq. **(6.2.5)** as follows:

$$\left[\frac{-1}{1+K_{nk}^2}\right]_{K_{nk\,min}}^{K_{nk}\,cutoff} = \frac{1}{\left[\gamma_{nk\,min}^2 = 2\right]} - \frac{1}{\gamma_{nkCutoff}^2} = \frac{1}{2(1+\varepsilon'')} \quad \text{when } N = 2$$

$$\left[\frac{-1}{1+K_{nk}^2}\right]_{K_{nk\,min}}^{K_{nk}\,cutoff} = \frac{1}{\left[\gamma_{nk\,min}^2 \approx 1\right]} - \frac{1}{\gamma_{nkCutoff}^2} = \frac{1}{1+\varepsilon''} \quad \text{when } N = 1$$

(6.2.7)

(We should be using expectation values, but for clarity we simply imply them.) We have shown in section 6.2 that $\langle 1/\gamma_{kmin}^2 \rangle = 1/2$ when $N = 2$, but in reality it is Eq. **(6.2.7)** that must be true. In section 4.2 we showed that for $N = 1$ superpositions the primary coupling of gravity to preons infinitesimally increased the interaction probability by ε' to $(1+\varepsilon')$ where

from Eq. (4.2.4) $\quad \varepsilon' = \dfrac{m_0^2 \chi_G' \cdot G}{2s\hbar c(8+8\sqrt{\alpha_{EMP}})^2} = \varepsilon = \dfrac{1}{K_{nk}^2 cutoff} = \dfrac{2m_0^2 c^2}{sn^2\hbar^2 (k_{cutoff})^2}$.

In the $N = 1$ case this meant that any deficits due to a non-infinite cutoff were exactly balanced by the contribution from gravity, but in the $N = 2$ case this infinitesimal correction is out by a factor of two. However Eq. (6.2.7) says that exactness can be maintained in the $N = 2$ case by an infinitesimal change from $\langle 1/\gamma_{k\,min}^2 \rangle = 1/2$ to $\langle 1/\gamma_{k\,min}^2 \rangle \approx 1/2$. Thus both $N = 1$ & $N = 2$ superpositions can cutoff at Planck energy as in section 4.2.2. The low frequency cutoff for all superpositions must be at $k_{min} \approx \Upsilon / R_{OH}$ if they are to affect gravity.

6.2.2 An exponential cutoff at cosmic wavelengths for infinite superpositions

We used a square cutoff above for k_{min} but an exponential cutoff is more likely.
Going over what we did in Eq.(6.2.4) and using Eq.**(6.2.5)**

Putting $x = \dfrac{k}{k_{min}} = \dfrac{K_{nk}}{K_{nk\,min}}$ then using $\displaystyle\int_{x=1}^{x=\infty} \frac{x\,dx}{(1+x^2)^2} = 0.25 \approx \int_{x=0}^{x=\infty} \frac{(1-e^{-0.65x})x\,dx}{(1+x^2)^2} \approx 0.2505$

An exponential cutoff $(1-e^{-0.65x})$ @ k_{min} is $\approx$ the same as a square cutoff @ k_{min} (6.2.8)
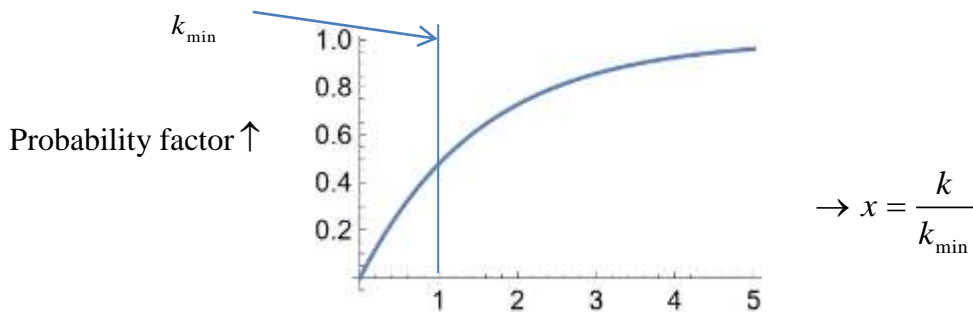
Figure 6.2.1 A simple $e^{-0.65x}$ exponential cutoff for all infinite superpositions that gives the correct angular momentum for $N = 2$, spins 1 & 2 infinitesimal mass bosons.

6.2.3 Virtual particle pairs from the vacuum and spacetime curvature

For almost a century it has been a puzzle why spacetime appears to be flat on average and not massively curved by Planck scale zero point energy densities. In section 5.1.1 we conjectured that virtual particles are just single wavenumber k superposition members, whereas real particles are full infinite superpositions of all wavenumbers k from $k_{\min}$ to k_{Planck}. We assumed this was true in all of section 5. If this is the actual difference between virtual and real particles, then only full infinite superpositions (representing that particle) have real properties that can be measured (such as measured mass/energy) rather than implied. If $k_{\min}$ virtual gravitons are such single members they can couple to $k_{\min}$ members of full infinite superpositions. On the other hand, virtual particles out of the vacuum, are mainly short lived high k single value members that will not couple to $k_{\min}$, if our conjectures are true.

The density of $k_{\min}$ virtual pairs from the vacuum based on the Lorentz invariant supply of local zero point fields is virtually zero and the supply from expanding space is consumed by $k_{\min}$ gravitons as in section 5.2 , (see sections 6.2.4 & 6.2.5 below). But this is not the full story. The virtual particles that dress electrons and quarks for example add mass to the real particles. As these short lived virtual particles are emited and reabsorbed they impart momentum and kinetic energy increasing the effective mass of the real long lived paricles. In fact, the majority of the proton and neutron mass is due to the virtual gluons interacting between quarks.

6.2.4 Zero point energy from the horizon behaves differently to local

As we said above local zero point energies are Lorentz invariant. At high frequencies there is no shortage locally to build the high frequency components of full infinite superpositions. But as we have shown this is not so as we approach cosmic wavelengths. If there were no supply from expanding space there would be only a few modes of the local supply of $k_{\min} \approx 1/R_{OU}$ quanta inside the horizon. Because preons are born with zero momentum and infinite wavelength they can absorb $k_{\min} \approx 1/R_{OU}$ quanta from space expansion inside the horizon as we have discussed. This $k_{\min}$ quanta supply behaves differently to normal Lorentz invariant zero point local fields. It is only available to zero spin preons that are born with zero momentum, or infinite wavelength, in the rest frame in which infinite superpositions are built.

6.2.5 Revisiting the building of infinite superpositions

In section 2 we developed equations to determine the probability of each mode of a superposition using local zero point fields. In section 5 when we found the cosmic wavelength supply inadequate, we used quanta from space expansion. So how do we justify our use of the local zero point fields to determine mode probabilities and behaviours? As we noted above there is a plentiful supply of high frequency local zero point fields. This local supply is adequate for high densities of superpositions for all modes from the Planck energy $k \approx 1$ high energy mode cutoffs to somewhere around $k \approx 10^{-17}$, or near the Higgs boson energy. The coupling to local zero point fields in this high frequency region determines the behaviour of

all the SM particles. There is, however, a gradual transition to absorbing quanta from the expanding space supply as the wavelength increases. Because this supply of $k_{\min}$ quanta behaves as the invariants $K_{Qk\min}$ or $K_{Gk\min}$ above, and entirely differently to Lorentz invariant local zero point fields, spacetime has to warp around mass concentrations and the universe has to expand.

6.2.6 The primary to secondary graviton coupling ratio χ_G

In Eq. (4.2.12) we found $\chi'_G \approx 318.3$ as the ratio between the primary graviton coupling to a bare Planck mass and the normal measured gravitational constant G. Equation (5.1.7) defined graviton coupling between Planck masses and equation (8.2.16) finds $\alpha_G \approx 0.004$ so that the primary to secondary graviton coupling ratio (as for colour and electromagnetism in Eq. (3.3.2) is:

$$\chi_G = \alpha_G^{-1}\chi'_G \approx 318.3 \times 250 \approx 79,500 \qquad (6.2.9)$$

To solve graviton superpositions we can use Eq. (3.3.14), which is the *gravitational interaction probability* between fermions, and we can now put on the RHS the coupling ratio $\chi_G \approx 20,352$ in the same way as we did for Eq. (3.3.19). This $c_{4c}*c_{4c}(1-c_{4c}*c_{4c})$ we are going to calculate here is for spin 2 & $N=2$. It is different to the double combination of $(N=2)\times(\text{Spin 1})$ or $(N=1)\times(\text{Spin 2})$ for $4c_{4b}*c_{4b}(1-c_{4b}*c_{4b})$ we derived in Eq. (4.4.1).

$$\frac{[2s_{1/2}N_1 c_{6a}*c_{6a}(1-c_{6a}*c_{6a})]^2 [2s_2 N_2 c_{4c}*c_{4c}(1-c_{4c}*c_{4c})]^2}{q^4} = \frac{4(\chi_G^{-1})^2}{q^4}$$

$2s_{1/2}=1, N_1=1, \& 2s_2=4, N_2=2$ so $[c_{6a}*c_{6a}(1-c_{6a}*c_{6a})][8c_{4c}*c_{4c}(1-c_{4c}*c_{4c})]=2\chi_G^{-1}=2/79,500$

$$\text{or} \quad c_{4c}*c_{4c}(1-c_{4c}*c_{4c}) \approx \left[\frac{1}{40,000}\right]\frac{1}{8[c_{6a}*c_{6a}(1-c_{6a}*c_{6a})]}$$

But from Eq. (4.4.1) $c_{6a}*c_{6a}(1-c_{6a}*c_{6a}) = \sqrt{2/\chi_C} \approx \sqrt{2/50.4053} \approx 0.199194$

$$\text{So} \quad c_{4c}*c_{4c}(1-c_{4c}*c_{4c}) \approx \frac{1}{4\times40,000\times0.199194} \approx 0.00003 \approx \frac{1}{32,000}.$$

Using Eq.(4.4.3), $\sum c_n*c_n \cdot n^4 \approx 170.95$ for spin 2, $N=2$ we get the infinitesimal mass graviton superposition values in Table 4.3.1.

6.2.7 Massive bosons and the Higg's mechanism

In the SM the Higg's mechanism adds mass to zero mass photons but here we say it adds mass to infinitesimal mass photons to convert them to massive photons. But additionally, it converts them from $N=2$ to $N=1$, and also from $n=3,4,5$ to $n=4,5,6$ superpositions. Section 0 looks at possible connections with the Higgs field further.

7 Virtual Gravitons and Mass Interacting with Itself

7.1 Do we have to take account of $\psi_m * \psi_m$ on $k$min Densities?

In section 5 we began by finding the average $k_{\min}$ graviton probability density in a uniform universe. We then placed a mass concentration in it, and calculated the extra probability density of $k_{\min}$ gravitons (before the dilution due to local space expansion) due to the amplitude of this mass multiplied by the amplitude of the rest of the mass in the universe. This ended up being proportional to $2m/r$ in Planck units. Apparently ignoring the $\psi_m * \psi_m$ term we got $\Delta\rho_{Gk\min} = (\psi_{\text{Universe}} * \psi_m) + (\psi_m * \psi_{\text{Universe}}) \propto 2m/r$ as in Eq.(5.2.5).

However, we approximated by assuming that our concentrated mass $m <<< M$ did not change the rest of the mass in the cosmos. If we subtract the mass m from the cosmic mass M and look at how our concentrated mass m interacts with this reduced value we have $(M - m)m = Mm - m^2$, if we now add the interaction term of the mass interacting with itself m^2 we then have $(M - m)m + m^2 = Mm$ which is our original approximation.

In other words by not subtracting our small concentrated mass m from the larger cosmic mass M we have effectively already included the local gravitons emitted by this local mass interacting with itself.

8 An Infinitesimal Change to Einstein's Equations

8.1 An Infinitesimal change to General Relativity at Cosmic Scale

Let us review how we have tried to connect gravity with our infinite superpositions in the second half of this paper. We started out with the hypothesis that $g_{00} = g_{rr}^{-1} = 1$ everywhere when there are no mass concentrations, assuming that uniform densities don't curve spacetime. We introduced mass concentrations and spacetime had to curve around them so as to keep 4 volume $k_{\min}$ action densities, required and available, invariant. But what do we mean by a mass concentration? If we think of the mass in the universe as a dust of density ρ_U and consider a small sphere of volume $V = \int dv$ enclosing this dust, its mass will be $m' = \int \rho_U dv = \rho_U V$, but our hypothesis says it will have zero effect on the spacetime curvature surrounding it. If we now increase this density to ρ by bringing dust from far away into this sphere its mass will increase to $m = \int \rho dv$, and the effect on spacetime curvature is now proportional to the increase in the enclosed mass $\Delta m = m - m' = \int (\rho - \rho_U)dv = \int \Delta\rho dv$.

Using similar reasoning, if instead of increasing the density we now remove the original enclosed dust the effect on the spacetime curvature is $\propto -m' = \int -\rho_U dv = -\rho_U V$ and spacetime curvature is of opposite sign to that surrounding positive mass. Relooking at Eq.(**5.2.7**), but instead of a mass concentration m, we replace it with mass dilution $-m$, Eq.(**5.2.7**) becomes:

$$\frac{\Delta\rho_{Gk\min}}{\rho_{Gk\min}} \approx 1.725 \frac{k_{\min}^2}{\rho_U} \frac{-m}{r} \approx \frac{-m}{r} \qquad (8.1.1)$$

If this dust is essentially at rest in comoving coordinates we can define a tensor $T_{\mu\nu}(\text{Cosmos})$. In comoving coordinates $T_{\mu\nu}(\text{Cosmos})$ has only one significant non zero term $T_{00}(\text{Cosmos}) = \rho_U$, a density of only a few atoms per cubic metre. In any other coordinates this same $T_{\mu\nu}(\text{Cosmos})$ tensor is transformed by the usual tensor transformations that apply in GR. If these coordinates move at peculiar velocity β_P then $T_{00}'''(\text{Cosmos}) = \gamma_P^2 \rho_U = \gamma_P^2 T_{00}(\text{Cosmos})$. The same transformation happens in any metric but with $\gamma_M^2 \rho_U$. We argue that Equ.(**5.2.7**) is consistent with the infinitesimally modified Einstein field equations

$$\text{Modified Einstein } G_{\mu\nu} \equiv R_{\mu\nu} - \frac{1}{2} g_{\mu\nu} R = \frac{8\pi G}{c^4} \Big[T_{\mu\nu}(\text{Local}) - T_{\mu\nu}(\text{Cosmos}) \Big] \tag{8.1.2}$$

Einstein had always wanted his theory of gravity in curved spacetime to be similar to the Gauss/Poison equation $\nabla^2 \phi = \rho$ the electric charge density. But this charge density is in reality the local difference in the normally very accurately (on average) balanced positive and negative charge densities. We can express this difference as follows:

$$\text{Poisson/Gauss } \quad \nabla^2 \phi = \big[\rho(\text{positive}) - \rho(\text{negative}) \big] = \rho(\text{nett charge}) \tag{8.1.3}$$
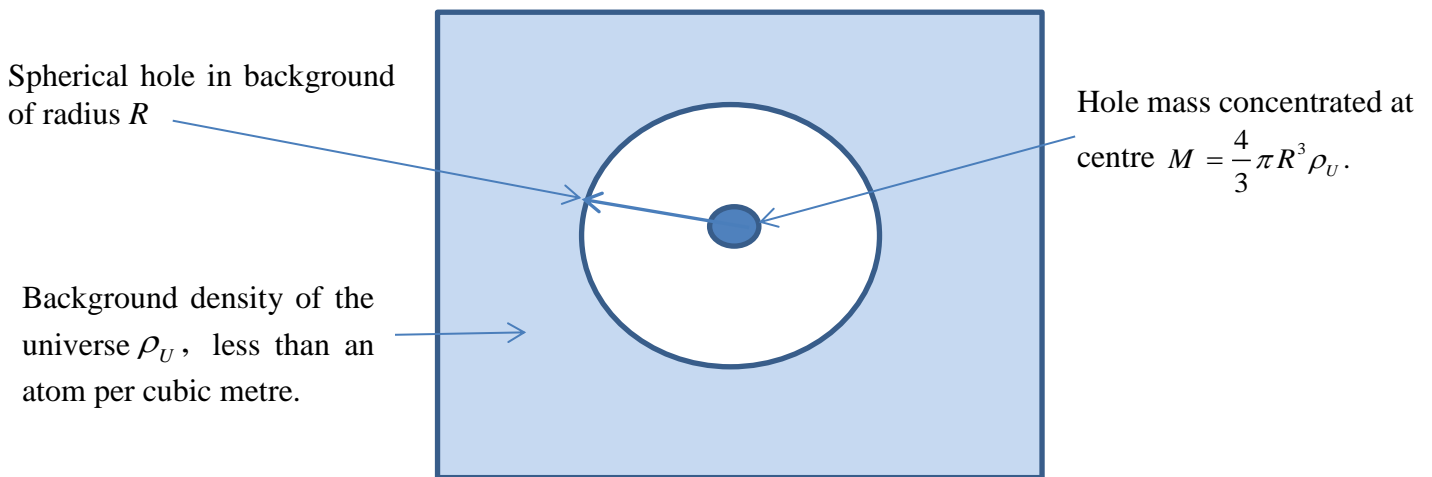
If we write the electric charge equation this way we can see that our modified Einstein tensor equation above is perhaps not too different, and hopefully Einstein might have approved. Equation (**8.1.2**) has some parallels to, but is not the same as, the Λ term he introduced to stabilize the cosmos. The red terms are zero if $T_{\mu\nu}(\text{Local}) = T_{\mu\nu}(\text{Cosmos})$ and $\rho(\text{positive}) = \rho(\text{negative})$. Just as the average value over the whole universe of $\rho(\text{positive})$ is the same as that of $\rho(\text{negative})$, the same is also true for the average value of $T_{\mu\nu}(\text{Local})$ which has to be $T_{\mu\nu}(\text{Cosmos})$. This forces the average values of $g_{00} = g_{rr}^{-1}$ to be very close to one. It also means that there is no nett gravitational attraction of matter over any large cosmic sphere. (We will look at what this means for the FLRW metric in the next section) Thus this infinitesimal modification is most relevant in the extreme case as $T_{\mu\nu}(\text{Local})$ approaches $T_{\mu\nu}(\text{Cosmos})$. Far from mass concentrations $T_{\mu\nu} \leq T_{\mu\nu}(\text{Cosmos})$, spacetime curvature in these remote voids is of the opposite sign to that surrounding positive mass, but the causally connected universe is always flat regardless of the value of Ω. (See section 8.1.2) Equation (**8.1.2**) is also consistent at all cosmic times with Eq. (**5.2.9**) $\rho_{Gk\min} = K_{Gk\min} dk_{\min}$. The effect of our modified Einstein equation at large scale can be seen with a very oversimplified (for illustrative purposes) example. Consider a very large spherical hole of radius R in an otherwise homogenous background of the cosmos with average density ρ_U, where the matter that was inside this spherical hole has now collapsed into a central concentrated mass $M = \frac{4}{3}\pi R^3 \rho_U$. Providing everything is spherically symmetric we can use our modified Einstein Eq.(**8.1.2**) to get $T_{00}(\text{Local}) - T_{00}(\text{Background}) = 0 - \rho_U = -\rho_U$ with the

hole having an effective negative density of ρ_U and a negative effective mass inside any particular radius r of $-m = -\frac{4}{3}\pi r^3 \rho_U$ or $\frac{m}{M} = \frac{r^3}{R^3}$, where we define this bubble radius as:

Galactic bubble radius with galactic mass $M = \frac{4}{3}\pi R^3_{Bubble}\rho_U$.

(8.1.4)

In weak gravitational fields Newton and Einstein are approximately the same, with Newton predicting that provided both the negative hole mass and the concentrated central mass are spherically symmetric, at the outside radius R they must cancel each other, with no gravitational acceleration at this radius. (Provided the mass of the background dust outside radius R is spherically symmetric it has no effect on this.) The effect of all this can be summarized as in Equ's.(**8.1.5**):

Effective total mass inside bubble $\qquad M'(r) = M\,(1 - \dfrac{r^3}{R^3_{Bubble}})$

(8.1.5)

Effective gravitational attraction inside bubble $\quad F'(r) = \dfrac{M}{r^2}(1 - \dfrac{r^3}{R^3_{Bubble}})$

Spherical hole in background
of radius R

Hole mass concentrated at
centre $M = \dfrac{4}{3}\pi R^3 \rho_U$.

Background density of the
universe ρ_U, less than an
atom per cubic metre.

Figure 8.1.1 An illustration of an oversimplified example of a spherical hole in the background density of the universe that has collapsed into a central mass.

$\dfrac{\text{Modified gravitation attraction}}{\text{General Relativity attraction}}$ ↑

$\dfrac{r}{R} \to$
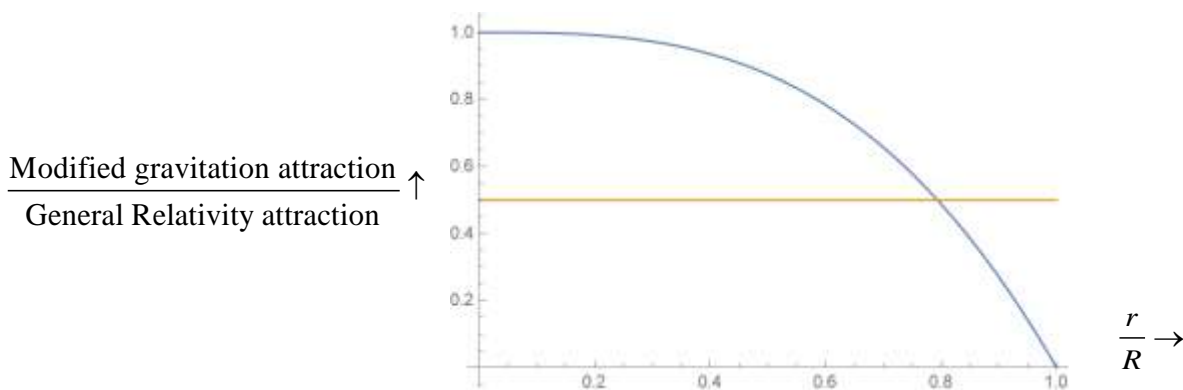
Figure 8.1.2 An illustration of an oversimplified example of a spherical hole in the background density of the universe that has collapsed into a central mass.

We can integrate these forces from radius $r_1 \to R_{Bubble}$ to get the usual GR or Newtonian change in potential but the negative mass effect gives a potential change of the opposite sign.

$$\text{Newtonian potential change } \Delta V = \frac{M}{r_1} - \frac{M}{R_{Bubble}}$$

(8.1.6)

$$\text{Negative mass potential change } \Delta V' = + \frac{M}{2R_{Bubble}}$$

If there are very approximately 10^{12} galaxies and the radius of the cosmos is currently $\approx 10^{61}$ Planck lengths the average bubble radius is $\approx 10^{57}$ Planck lengths. If the average galaxy mass is $M \approx 10^{49}$ Planck masses the change in the potential due to this negative mass effect is $\Delta V' \approx 10^{-8}$ Planck energy units which is a very small change. Figure 8.1.2 plots the effects of Equ's. **(8.1.5)**. A galaxy of say 10^{12} solar masses is roughly the same mass as a background sphere of $\approx 4 \times 10^6$ light years. At this radius the attraction has dropped to zero, but it is roughly halved at $\approx 3.2 \times 10^6$ light years, or about 80% of the bubble radius. Our example is quite unrealistic as the transition will not be abrupt, but it does illustrate something that has been observed in recent surveys of the universe where the rate at which matter is falling into denser regions of the universe appears to be less than predicted by **GR[32]**

8.1.1 This infinitesimal change does not effect most gravitational fields

Equation **(8.1.2)** only modifies Einstein when the local mass density $\rho_{Local} \to \rho_U$ where ρ_U is a few atoms per cubic metre which is extremely low. The Milky Way has a disk diameter of $\approx 100,000 ly$ and to keep things simple, if we assume a spherically symmetric distribution of the total galaxy mass inside a sphere of this radius. the average mass density is about $10^5 \rho_U$ so Einstein's GR is still very accurate. The same should apply inside the solar system. In Section 5 we tried to show in Eq. **(5.2.12)** that the Schwarzchild metric relates with Eq.**(8.1.2)** We have not attempted to do the same with the Kerr metric which is an exact solution to Einstein's equations. Provided $\rho_{Local} >>>>> \rho_U$ we will assume there is no change, however, when there is angular momentum there may well be circularly polarized gravitons emitted with an $\frac{\alpha^2}{r^2} \cos^2 \theta$ angular distribution about the spin axis. This could possibly be why the determinant of the Kerr metric can be written as $|g_{\mu\nu}| = r^4 \sin^2(1 + \frac{\alpha^2}{r^2} \cos^2 \theta)^2$. We will look more carefully at galaxy behaviour in Section 8.2. The only regions where $\rho_{Local} \to \rho_U$ are what are normally referred to as the galaxy free voids.

8.1.2 Friedmann-Lemaitre-Robertson-Walker Metrics and Friedmann's Equations

The FLRW metric and Freidmann equations have been the bedrock of cosmology for nearly a century, a cosmology that in its current ΛCDM form has been recently showing some cracks. (See Reiss **[33]** and New Physics required due to Hubble tensions). It is an exact solution to the 00 component of GR so how can it possibly be questioned? If we relook at our infinitesimally modified Einstein Eq. **(8.1.2)** and re express it as follows

Writing $T'_{\mu\upsilon} = T_{\mu\upsilon}(\text{Local}) - T_{\mu\upsilon}(\text{Cosmos})$ (8.1.7)

Infinitesimally Modified Einstein becomes $G_{\mu\upsilon} \equiv R_{\mu\upsilon} - \dfrac{1}{2} g_{\mu\upsilon} R = \dfrac{8\pi G}{c^4} T'_{\mu v}$

Over large homogenous and isotropic regions of space the average values of all 16 components of $T_{\mu\upsilon}(\text{Local})$ are the same as $T_{\mu\upsilon}(\text{Cosmos})$ and this is true for all large volumes inside the horizon.

All 16 components of both $G_{\mu\upsilon}$ & $T'_{\mu v}$ average zero in large regions (8.1.8)

If the components of the Freidmann equations average zero it cannot control cosmic expansion and we argue that QM does. We will consequently continue to use the following metric.

FLRW flat space metric with no KE or gravitation effects $ds^2 = -c^2 dt^2 + a(t)^2 dr^2$ (8.1.9)

8.2 Massive Spin 2 Virtual Gravitons and Dark Matter Halos

Table 4.3.1 listed theortically possible infinite superpositions and included a possible spin 2 massive boson that we called a massive graviton to partner with infinitesimal mass gravitons. Pairs of these spin 2 gravitons have some parallels with massive and infinitesimal mass spin 1 photons that are also bosons. The photon mediates electrical charge with three different massive photons for $-1, 0, +1$ charge, and they all have masses in the $\approx 100 GeV$ range. The spin 2 graviton on the other hand, mediates changes in the metric where no charge is involved, consequently only one massive graviton appears to be necessary. Its mass however might behave very differently to massive photons. Just as infinitesimal mass bosons have a mass of $k_{\min} \approx R_{OH}^{-1}$ or $\approx 10^{-34} eV$ (at the current time) and always approximately inverse to the horizon radius, we are going to speculate that massive spin 2 gravitons are always somewhere between $10^4 \rightarrow 10^6$ times as massive as infinitesimal mass gravitons. This would mean that at the current cosmic time they would be $\approx 10^{-29} eV$ with Compton wavelength halos of $\approx 100,000 \rightarrow 200,000 ly$ radius around the galaxy cores emitting these virtual massive gravitons. While this very low mass appears at first sight to be far too small to behave like dark matter, infinitesimal mass gravitons couple between Planck masses and there are about 10^{19} protons per Planck mass. If protons or quarks exchanged massive gravitons the coupling constant between them only needs to be less than one and as we will see below it does not need to be very large. Also if these massive gravitons are time polarized their spherical symmetry gives an inverse radius squared mass density just as dark matter is supposed to have to give galaxies their flat orbital velocities.

8.2.1 Massive gravitons generating MOND-like galaxy behaviour

The approach we are going to take in this section appears to only work if the mass of massive gravitons $m_G = b \cdot k_{\min}$, where the mass ratio of massive to infinitesimal mass b is a constant. We are thus going to assume that the mass of massive spin 2 gravitons is always $m_G = b \cdot k_{\min}$ where $b >>> 1$ and this mass is vastly greater than that of infinitesimal mass gravitons.
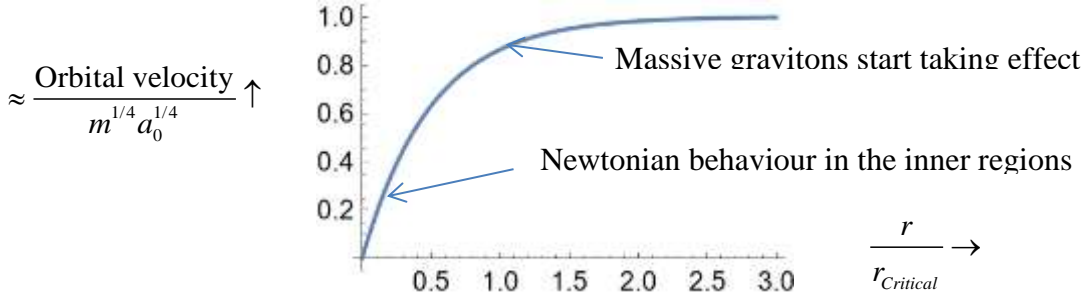
Using Eq. (5.1.4) at wavenumber k_{min} let $k'_{Gk\,min} = \sqrt{k^2_{min} + b^2 k^2_{min}} \approx b k_{min} \approx m_G$ if $b >>> 1$,

$$\text{with wavefunction } \psi_{Gk\,min} = \sqrt{\frac{2k'_{Gk\,min}}{4\pi}}\, \frac{e^{-k'_{Gk\,min}r + i k_{min}r}}{r} \qquad \approx \sqrt{\frac{2m_G}{4\pi}}\, \frac{e^{-m_G r + i k_{min}r}}{r}$$

$$\psi_{Gk\,min}*\psi_{Gk\,min} \approx \frac{2m_G}{4\pi r^2} e^{-2m_G r} \text{ with radial probability } R_{Gk\,min}*R_{Gk\,min} \approx 2m_G e^{-2m_G r} \qquad (8.2.1)$$

To give galaxies their observed orbital velocity behaviour they are thought to have a ratio of dark matter to baryonic of 9:1. Assume a coupling constant between baryonic Planck masses of α_{MG} for massive gravitons, also assume an average galactic baryonic mass of 10^{48} Planck masses. If massive gravitons are $\approx 10^{-29}eV$ or $\approx 10^{-56}$ Planck masses in this cosmic era, their total mass will be $\approx (10^{48})^2 \alpha_{MG} 10^{-56} \approx 10^{40} \alpha_{MG}$ and if $\alpha_{MG} \approx 10^{9}$ this is 10^{49} Planck masses of massive gravitons which is about what is needed. This coupling constant could be a realisticly small number, much less than one if it is between neutrons/protons/quarks, or some baryonic particles. If we imagine as an unrealistic example a hollow sphere of baryonic matter where there are no gravitons or massive gravitons inside it. But on the outside, the radial mass density of massive gravitons is inverse to the radius sqared as in Eq. (**8.2.1**) within the Compton wavelength approximately. If we plot the orbital velocity with radius, it will follow Newtonian predictions in the inner core region and exponentially transition into the flat velocities observed. This Newtonian gravity will thus be concentrated around the peak radial baryonic mass densities (as in Renzo's rule). A very hypothetical plot of this is shown in Figure 8.1.3.

$\approx \dfrac{\text{Orbital velocity}}{m^{1/4} a_0^{1/4}} \uparrow$

Massive gravitons start taking effect

Newtonian behaviour in the inner regions

$\dfrac{r}{r_{Critical}} \rightarrow$

Figure 8.1.3 Plot of a very hypothetical orbital velocity radial profile assuming the peak radial mass densities, where the massive gravitons originate, are somewhere greater than one Milgom critical radius. This behaviour has many parallels to MOND predictions.

8.2.2 Accelerating cosmic expansion

If the mass of massive gravitons is always $m_G = b \cdot k_{min}$ then as $k_{min} \approx R_{OH}^{-1}$, and in the initial stages at least, R_{OH} is proportional to cosmic time, then we can say that $m_G \approx \propto t^{-1}$. If all cosmic matter had clustered into galaxies, and as the ratio of dark to baryonic is currently 9:1, we can say that the mass of massive gravitons is $\approx \propto 9t^{-1}$ at any cosmic time. But this clustering will happen exponentially. We can thus speculate that the total cosmic mass density may have an exponential form such as:

$$\text{Cosmic mass density } \rho_U \approx \rho_{Baryonic}\left[1 + 9t^{-1}(1 - Exp[-f(t)])\right] \qquad (8.2.2)$$

This implies large extra mass in the early eras when supermassive black holes appear to have formed more rapidly than expected. But we first need to find an exponential function that makes sense logically and also fits with observations. The radius of the Compton wavelength halo $r_{Halo} \approx \propto t$, so the volume inside this halo is $v_{Halo} \approx \propto t^3$

$$\text{(a) Compton wavelength radius halo volume } v_{Halo} \approx \propto t^3 \qquad (8.2.3)$$

At any cosmic time the density of the background supply is $\propto R_{OH}^{-2} \propto t^{-2}$. If we take the Milky Way as an example, and assume a Compton wavelength of about 10^{56} Planck lengths, the average density inside this radius is about 10^4 times the cosmic average density. We are going to assume that at all cosmic time the halo density is proportional to the background density

$$\text{(b) Average baryonic density in this halo volume } \rho_{B\,halo} \approx \propto R_{OH}^{-2} \propto t^{-2} \qquad (8.2.4)$$

The baryonic mass inside the halo is $v_{Halo} \approx \propto t^3$ times t^{-2}, or

$$\text{(c) The baryonic mass inside the halo is } M_{Baryonic\,Halo} \approx \propto t^3 \times t^{-2} \propto t. \qquad (8.2.5)$$

The number of massive gravitons emitted is proportional to this baryonic mass squared:

$$\text{(d) The number of massive gravitons emitted is } \propto M_{Baryonic\,Halo}^2 \propto t^2 \qquad (8.2.6)$$

At large volumes of space we need to multiply by the average density of galaxies. From Eq. (**8.1.7**) when mass is initially distributed evenly the local mass density is equal to the cosmic average and there is no tendency to cluster, but it is unstable. We can think of this instability as similar to the top of a hill with a slope proportional to the horizontal distance from the central top point. This is equivalent to a $y = kx^2$ curve with slope $\dot{y} = kx$.

In terms of the rate of individual galaxy formation this is equivalent to:

$$\text{(e) Rate of individual galaxy formation } \propto t^2 \text{ per unit time.} \qquad (8.2.7)$$

At any early cosmic time the integrated total number of galaxies is

$$\text{(f) Total average density of galaxies is } \propto t^3. \qquad (8.2.8)$$

Multiplying factors (d) and (f) together we can say that in a very large volume of space the total number of massive gravitons emitted is:

$$\text{Total number of massive gravitons } \propto (d) \times (f) \propto t^2 \times t^3 \propto t^5. \qquad (8.2.9)$$

Now $1 - Exp[-t]^5 \approx t^5$ when $t <<< 1$ so we will conjecture that Eq. (**8.2.2**) becomes

$$\text{Cosmic mass density } \rho_U \approx \rho_{Baryonic} X(t)$$

In the matter dominated era
$$\text{where } X(t) \approx \left[1 + 9t^{-1}(1 - Exp[-\frac{t}{k}]^5) \right] \qquad (8.2.10)$$

$$\text{Baryonic mass density } \rho_{Baryonic} \approx \frac{\rho_U}{X(t)}$$

The approximations we have used here depend on how linear the horizon radius is with time. As we will see, the radius starts at $r = 3t$ but ends up in the region of $r \approx 3.2t$, so these approximations reduce the accuracy of our equations, but they maybe a reasonable guide for future possible paths. As in section 5 we assume that all *infinitesimal* mass superpositions borrow their mass from the time mode zero-point energy coming from the horizon (as in Figure 5.3.1) time modes of zero-point fields. In Eq.(5.3.16) we put $\dfrac{\Upsilon^2 V'}{4\pi} \approx 1.84\alpha_G$, and if we relook at the way we derived Eq. (**5.3.8**) we had included ρ_U^2 as the probability factor for graviton emission. As in Eq. (**8.2.10**) $\rho_U \approx \rho_B X(t)$ with $\rho_U^2 \approx \rho_B^2 X(t)^2$ and we can put $\Upsilon^2 V' \propto \rho_B^2 X(t)^2 \alpha_G$ and $\Upsilon\sqrt{V'} \propto \rho_B X(t)\sqrt{\alpha_G}$. At any cosmic time in the matter dominated era, there is some baryonic density ρ_B, and if we imagine it to be fixed while we increase the clustering ratio, the factor $X(t)$ changes, implying $\Upsilon\sqrt{V'} \propto X(t)$, or that:

$$\Upsilon^2 \propto \frac{X(t)^2}{V'} \tag{8.2.11}$$

Using this equation we can use Eq. (**5.2.8**) to imply:

$$\text{The average density of the universe } \rho_U \approx 1.725 k_{\min}^2 \propto \frac{\Upsilon^2}{R_{OU}^2} \propto \frac{X(t)^2}{R_{OU}^2 V'} \tag{8.2.12}$$

Conjecturing the scale factor cubed is inversely proportional to baryonic mass density ρ_B^{-1} :

$$a(t)^3 \propto \rho_B^{-1} \propto \frac{X(t)}{\rho_U} \propto \frac{R_{OU}^2 V' X(t)}{X(t)^2} \propto \frac{R_{OU}^2 V'}{X(t)} \tag{8.2.13}$$

In flat space we can use Eq.(**5.3.19**) ($R_{OH} = \int V dt$ where $V = \dfrac{dR}{dt}$ is only true in flat space), and using the relation $HR_{OH} = V'$ or $H = V' R_{OH}^{-1}$ we can get the DE:

$$\frac{V'}{R_{OH}} = \frac{\dot{R}(t)-1}{R(t)} = \frac{\dot{a}(t)}{a(t)} \tag{8.2.14}$$

With appropriate boundary conditions assuming $H_0 = 73 km / \sec / Mps$, Table 8.2.1 shows four combinations of parameter k in Eq.(8.2.14). Caramena and Marra [**20**] using 2020 Pantheon data, measured deceleration at $q_0 = -1.08 \pm 0.29$ in line with the $k = 1.9$ value. The radius and age are a bit small compared to ΛCDM values but, as we mentioned above, our approximations limit assuracy as the non linearity of $R(t)$ increases. The following graphs assume that central $q_0 = -1.08 \pm 0.29$, or $k = 1.9$ solution.

| Parameter k.	Horizon radius	Cosmic age	Deceleration	Redshift
$k = 1.9$	$\approx 39.3 \times 10^9 ly.$	$\approx 12.3 \times 10^9 y.$	$q_0 = -1.09$	$z_t \approx 0.38$
$k = 1.85$	$\approx 41 \times 10^9 ly.$	$\approx 12.7 \times 10^9 y.$	$q_0 = -1.19$	$z_t \approx 0.43$
$k = 1.8$	$\approx 43 \times 10^9 ly.$	$\approx 13.4 \times 10^9 y.$	$q_0 = -1.3$	$z_t \approx 0.48$
$k = 1.75$	$\approx 46 \times 10^9 ly.$	$\approx 14 \times 10^9 y.$	$q_0 = -1.4$	$z_t \approx 0.52$

**Table 8.2.1** Four possible solutions of Eq. assuming $H_0 = 73 km / \sec / Mps$.
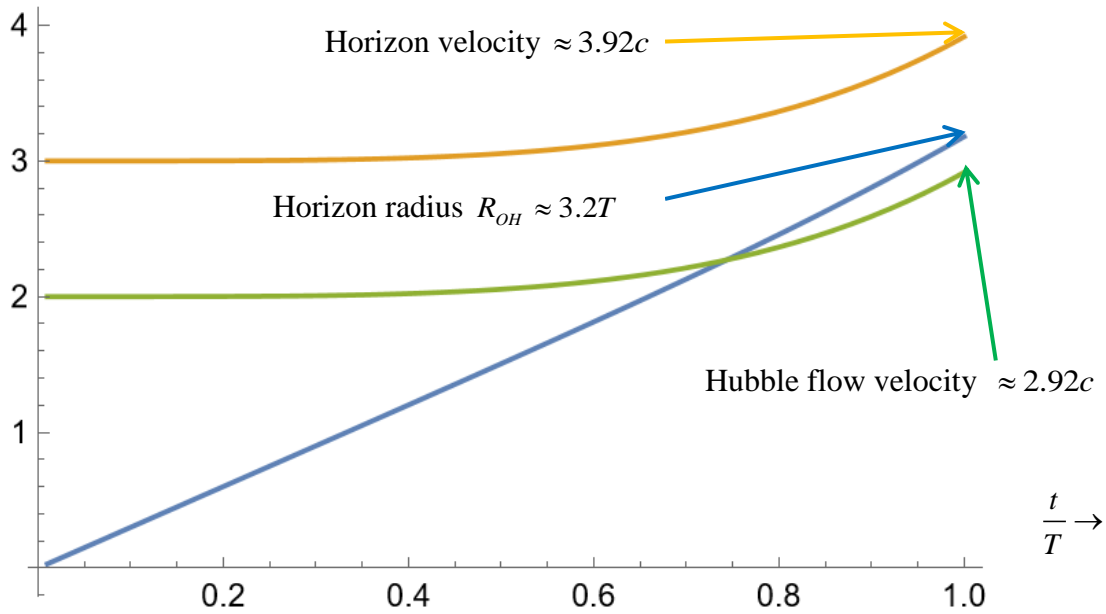
Figure 8.2.1 A plot of the $k = 1.9$ solution of Eq. (8.2.14) with $H_0 = 73 km/\sec/Mps$.
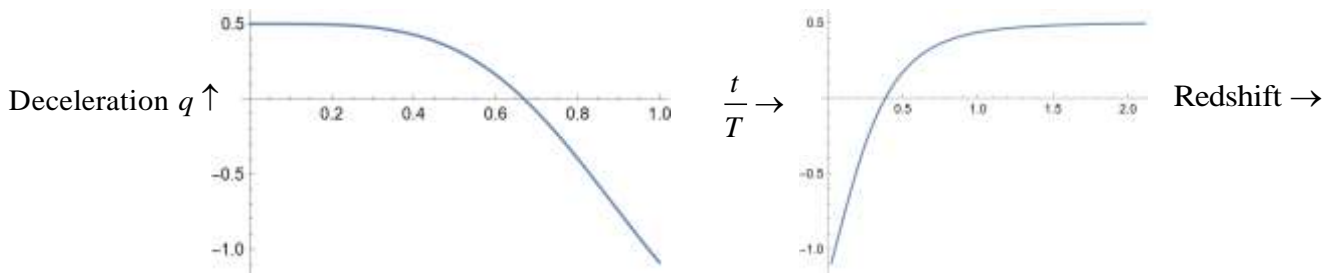

Figure 8.2.2 A plot of deceleration parameter q versus time on the left, and versus redshift z on the right. Transition, when $k = 1.9$ was about 4.1 billion years ago.
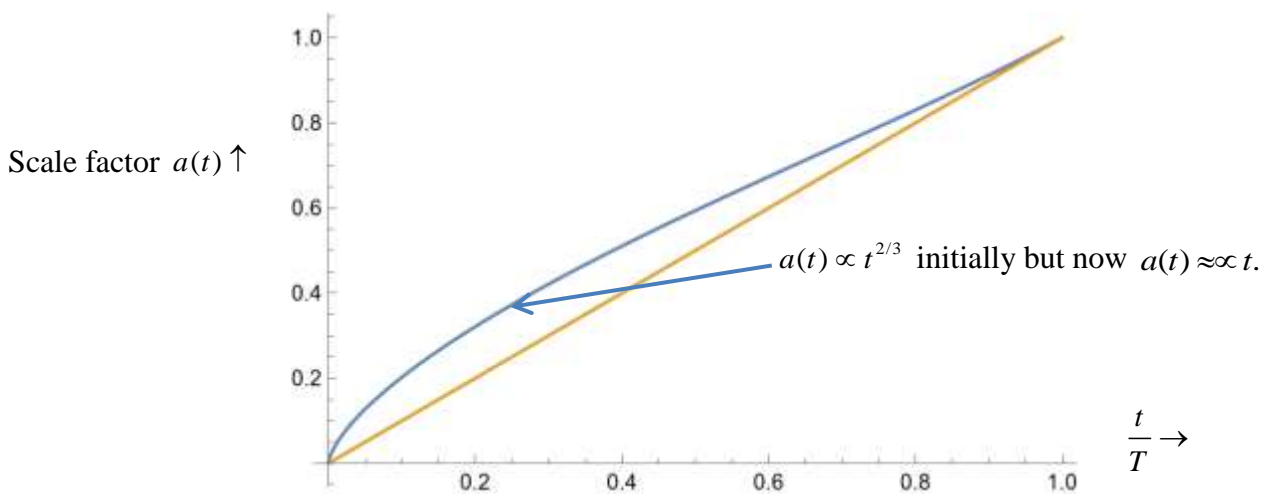
Figure 8.2.3 A plot of the scale factor with $k = 1.9$ showing similar behaviour to the Lambda-CDM. All the solutions in Table 8.2.1 show very similar scale factor behaviour.
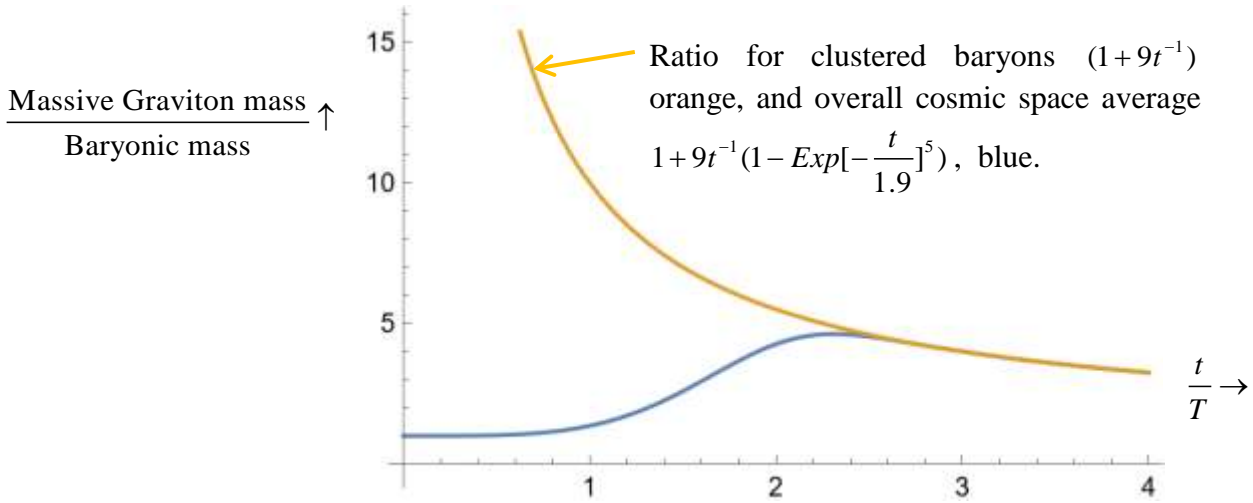
Figure 8.2.4 A plot of Eq.(8.2.10) of the ratio of the mass of massive gravitons to baryonic mass, for both clustered galaxies and the overall cosmic average versus cosmic time. Both curves have an inverse time factor as massive graviton mass is inverse to cosmic time,
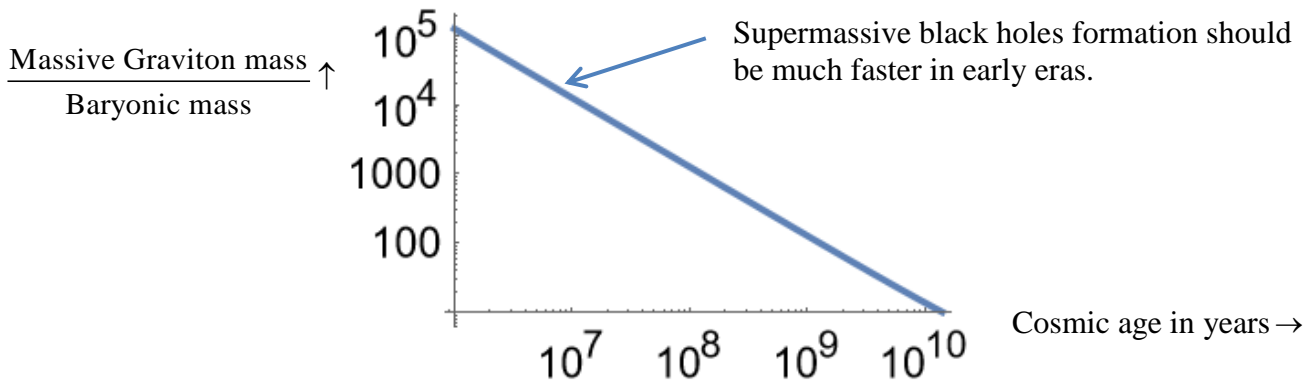
Figure 8.2.5 A logarithmic plot of the mass ratio for clustered baryonic mass versus cosmic time in years.

8.2.3   Baryonic density for this solution

One kg/m^3 is $\approx \dfrac{1}{0.516 \times 10^{97}}$ Planck units and current observations measure 0.2 to 0.25 atoms per cubic metre. Proton mass is $1.67 \times 10^{-27} kg$, $\rho_{Baryonic} \approx 0.225 \times 1.67 \times 10^{-27} \approx 0.375 \times 10^{-27} kg/m^3$

$\approx \dfrac{0.375 \times 10^{-27}}{0.516 \times 10^{97}} \approx 7.3 \times 10^{-125}$ Planck units. When $k = 1.9 \,\& \, t = 1$, $\left[1 + 9t^{-1}(1 - Exp[-\dfrac{t}{1.9}]^5)\right] \approx 1.35$

Eq. **(8.2.10)** $\rho_U \approx \rho_{Baryonic}\left[1 + 9t^{-1}(1 - Exp[-\dfrac{t}{1.9}]^5)\right] \approx 7.3 \times 10^{-125} \times 1.35 \approx 9.86 \times 10^{-125}$

Eq. **(5.2.8)** $\rho_U \approx 1.725 k_{min}^2 \approx 1.725 \Upsilon^2 R_{OH}^{-2}$ so that $1.725 \Upsilon^2 R_{OH}^{-2} \approx 9.86 \times 10^{-125}$,

Thus $\Upsilon^2 \approx \dfrac{9.86 \times 10^{-125} R_{OH}^2}{1.725}$. At $39.3 \times 10^9 ly$, $R_{OH} \approx 2.29 \times 10^{61} lp \rightarrow R_{OH}^2 \approx 5.24 \times 10^{122} lp^2$.

$$\Upsilon^2 \approx \frac{9.86 \times 10^{-125} \times 5.24 \times 10^{122}}{1.725} \approx 3 \times 10^{-2} \rightarrow \Upsilon \approx 0.173 \tag{8.2.15}$$

In Eq.(5.3.16) we put $\dfrac{\Upsilon^2 V'}{4\pi} \approx 1.84\alpha_G$ so that:

$$\alpha_G \approx \frac{\Upsilon^2 V'}{4\pi \times 1.84} \approx \frac{3 \times 10^{-2} \times (V' = 2.92)}{4\pi \times 1.84} \approx 0.004. \tag{8.2.16}$$

8.2.4 The Higgs boson

It is not clear whether the Higgs boson is a spin zero superposition as in Table **2.2.1**. However, if it is, it would be a superposition of two infinite superpositions (one spin up and one spin down) with a total angular momentum vector summing to zero, just as two spin ½ fermion superpositions can for example.

9   Further Issues not Already Covered.

9.1.1 Preferred frames

It might seem that we have been arguing in earlier sections for a preferred frame. But there is really no difference in what we are proposing compared to current physics. In comoving frames the cosmic microwave background is isotropic. At peculiar velocity β_P it is no longer isotropic, and the average background temperature increases by γ_P, exactly the same increase as k_{min} to $k'_{min} = \gamma_P k_{min}$; that is if we could measure it, which is most unlikely. We have frequently talked in this paper about local observers measuring k_{min}, but only as a thought experiment, and the average (over all directions) background temperature can be used to measure either $\gamma_{peculiar}$ or γ_{metric} at any particular cosmic time, provided we already know its value in flat comoving coordinates, which from Eq.(**8.2.15**) is $k_{min} \approx 0.17 R_{OH}^{-1}$ There are no other changes in physics in this comoving frame; it is exactly as Einstein originally postulated, an important experimentally verified feature of GR. If we think in terms of four volume, or $4D$ k_{min} action density invariance, whether we are in a non-comoving frame, or in a non-flat metric, it makes no difference.

9.1.2 Gravitational waves and 4 volume invariance

We showed in section 5.4.1 that the 4 volume k_{min} graviton density at any cosmic time $\rho 4D_{Gk\,min}$ is invariant in all coordinates and in any metric. But the metric can oscillate and not change this invariance, with such disturbances travelling at the speed of light. We can imagine extra gravitons around a mass concentration and the background gravitons (if there is accelerating mass as in binary pairs) generating real transversely polarized $m = \pm 2$, gravitons. We can also show from Eqs.(5.1.9) that most of these gravitons are close to the locally

measured value of the k_{min} wavenumber, about 96% are between k_{min} & $5\,k_{min}$. Thus, most of this radiated energy is near k_{min}. The frequency of the radiated wave is twice the orbital frequency of the binary pair source, typically hundreds of orbits per second. Typical wavelengths are in the thousands of kilometres or roughly 10^{41} Planck lengths. As most of the energy in the wave is in quanta near k_{min} there is no connection with the frequency of the radiated wave as in spin 1 photons and electromagnetism. The wavelength of k_{min} gravitons is $1/k_{min} \approx 1.2 R_{OU} \approx 3.2 \times 10^{63}$ Planck lengths, with the ratio between these two wavelengths of the order of $\approx 10^{22}$. This ratio is inverse to the binary pair orbital frequency. It could only approach one if the binary orbital period is approximately twice the age of the universe.

9.1.3   Constancy of fundamental charge

It has always been fundamental that the electromagnetic charge of protons and electrons is precisely equal and opposite to get a neutral universe. In section 4.2 we showed that the probability of superpositions was $sN \cdot dk(1+\varepsilon)/k$ where the infinitesimal ε is proportional to rest mass squared and thus different for various particles. We used this probability to determine interaction coupling strengths in section 3.3. This suggests that the probability of virtual photon emission is also proportional to the probability $sN \cdot dk(1+\varepsilon)/k$ of each superposition, and would not be precisely equal for electrons and protons due to small variations in ε of the order of $\approx 10^{-45}$ between electrons and quarks. If, however, we look closely at Eq.(4.2.3) and the following equations, by adding the amplitude for gravity at right angles we effectively added the probabilities of spin 2 gravity generated superpositions to those of spin 1 colour and electromagnetic superpositions. If, somehow, only those superpositions generated by spin 1 electromagnetic and colour interact with spin 1 photons, this would cancel any minute difference in charge. If this is not so, then there are infinitesimal differences in charge of the order of $\approx 10^{-45}$ which would surely have shown up in some form by now, unless there are minute differences in the total number of electrons and protons.

9.1.4   Superpositions, Feynman's strings and possible resonances

For over a century there have been models of the electron with the Abraham-Lorenz probably the best known [28], [29] but all of them suffered from electromagnetic mass in the field being 4/3 times the relativistic mass. Poincare showed that bursting forces due to charge balanced by stresses (or forces) in the same rest frame as the particle could cancel the extra 1/3 figure, and restore covariance [30].   In chapter 29 Volume II of his famous lectures on physics, Feynman, probably jokingly, suggested that if the electron is held together by strings, their resonances could explain the muon mass [38]. He just may have been right. The dominant $n = 6$ mode of the electron family of superpositions is held in orbit by a squared vector potential $Q^2 A^2 = 16\hbar^2 k^4 r^2$. The bursting force is a scalar potential of order α_{EM}, a small perturbation in comparison. Perhaps we could imagine some sort of cubic equation with three solutions for rest mass, and something similar for quarks, but with larger perturbing forces.

10   Discussion

This paper set out to form the fundamental particles from infinite superpositions. There are several significant consequences of this proposal, including the hypothesis that the four volume density of cosmic wavelength (or k_{min}) gravitons inside the observable horizon is invariant at any cosmic time. The density of matter, is approximately proportional to the inverse horizon area, but also proportional to the inverse of the Hubble flow velocity $(\rho_U \propto 1/(R_{OH}^2 V'))$, suggesting that QM controls the expansion of space.

When mass is distributed evenly as a dust there is a uniform three volume (spatial) density throughout a sphere of radius R_{OH} and space and spacetime is flat everywhere. If any of this mass is concentrated in a central location it increases the three volume density of k_{min} gravitons around this mass and space has to expand locally in agreement with Einstein's equations, apart from an infinitesimal difference that becomes larger at large cosmic radii.

Of course, QM can only control the density and expansion rate of the cosmos in the manner described here unless there is something wrong with the Friedmann equations. We have argued, however, that our infinitesimally modified Einstein equations, over very large homogenous and isotropic regions of space, make all components of these modified tensors average zero. This nullifies their effect in the Friedmann equations.

Perhaps the most significant consequence of this proposal is that, just like spin 1 photons, spin 2 gravitons have a massive member as well as one with what we describe as having infinitesimal mass. However, in the case of gravitons the massive member has a mass that is always approximately proportional to the inverse horizon radius ($\propto R_{OH}^{-1}$), and is currently about $10^{-29} eV$, having a Compton wavelength similar to galaxy halos. The spherically symmetric wavefunctions of these $10^{-29} eV$ massive gravitons, with inverse radius squared probability, give galaxies their MOND-like properties we observe. In other words. provided their Compton wavelength is long enough, they behave just like a form of dark matter that decreases in density with radius as r^{-2}.

Our approach suggests a modified GR complying with both quantum mechanics and SR, but the domain in which GR is accurate is always retricted to a location in space. It proposes a very different method for forming fundamental particles which does not unite the fundamental forces at high energy but agrees with the most basic version of the SM apart from infinitesimal mass bosons. Like Einstein, as in Figure 3.3.3, it looks at gravity not as a force, but purely as a consequence of warped spacetime, or invariant four volume (4D) k_{min} graviton densities with particles following geodesics.

It is common practice in cosmology to put the scale factor $a(t) \propto t^p$, and the QM approach in this paper controls the scale factor in the radiation era at $p = 1/2$ with a horizon velocity $V = 2$. In the matter era massive gravitons, with a mass that is always approximately inverse to the horizon radius, control the scale factor initially at $p = 2/3$ and the horizon velocity at $V = 3$ as in current cosmology if $\Omega = 1$, but with no dark energy. We proposed an extremely

simple mathematical model of this which demonstrates that the generation of massive gravitons can accelerate the expansion of space. As cosmic time progresses p is $> 2/3$ and V is > 3, where the actual time history of this change, tracks this massive graviton generation inside galaxy halos. As the mass of massive gravitons is approximately inverse to cosmic time they were very massive in the early eras which must have significantly effected the rate at which supermassive black holes could form.

As noted in our introduction, Merritt points out that dark energy responsible for accelerating expansion in the ΛCDM is an auxiliary hypothesis, added to the model around 1998. However, since that time astronomers have adjusted its properties, as needed, to match whatever new observational data relating to the universe's large scale structure becomes available, under the assumptions that Einstein's theory of gravity is correct. (D. Merritt, personal communication with the author's brother, October 20, 2018). And in this regard, the Reiss team claim their latest figures for the Hubble parameter provide *"stronger evidence for physics beyond the ΛCDM "* (Reiss *et al.,* 2019 p.1) **[33]**

On a final note, the primary interactions involved in forming the fundamental particles are simple, allowing simple mathematics. Indeed, we have purposely avoided exotic mathematics throughout this paper in the belief that, while powerful and elegant, it can hide the wood for the trees so to speak. The theoretical physicist Hossenfelder expresses a similar sentiment in the title of her recent book **[3]** *Lost in Math: How Beauty Leads Physics Astray*. If "Mother Nature" can be described simply, why not do so?

The ideas presented, although radical, at a fundamental level are also very simple. Superpositions are a signature component of quantum mechanics and we have merely extended them to building the fundamental particles. The proposals form a consistent package conforming with both quantum mechanics and SR. They also suggest new physics that may facilitate progress in a field considered by many to be in difficulty, or even in crisis **[1-5].**

11 Conclusions

If the fundamental particles are built from infinite superpositions as we propose, they must have at least an infinitesimal mass that is approximately inversely proportional to the horizon radius multiplied by the the Hubble flow velocity. And this may have some very significant consequences:

- Because cosmic wavelength gravitons vastly outnumber all other particles, the invariance of the action quanta they borrow from the expanding space inside the horizon directly relates with infinitesimally modified Einstein field equations.

- This infinitesimal modification limits the range of GR to much smaller than horizon scale and also makes the Einstein equations average zero over isotropic and homogeneous regions.

- The Freidman equation components must also average zero over large regions of space and space is flat. QM controls the expansion of space regardless of Ω, with or without inflation.

- In the matter era, the inverse radius squared probability of massive gravitons behave just like dark matter, giving galaxies and galaxy clusters their observed MOND-like behaviour.

- Because the mass of massive gravitons is approximately inverse to cosmic time, it was very large in early eras and should have sped up supermassive black hole generation

- The holographic principle is seen as a property of quantum gravity, and this paper builds on that principle. It includes gravity at horizon scale wavelengths, but not near Planck energy as in most papers including gravity with the other forces.

- Space has to be always flat, spacetime is distorted locally, and the domain of accuracy of GR is restricted to a location in space.

- Because spin 2 polarization vectors rotate at twice the rate of spin 1 polarization vectors, they can not transmit momentum or force. Thus, gravity cannot unite with the other fundamental forces, which is exactly what Einstein told us over a century ago. It is an emergent property of QM as is accelerating expansion.

Acknowledgements

12 References

[1]. J. Baggott, (2013). Farewell to Reality: *How Modern Physics Has Betrayed the Search for Scientific Truth* (Constable).

[2] L. Smolin, (2006). *The Trouble with Physics: The Rise of String Theory, the Fall of a Science, and What Comes Next.* (Houghton Mifflin Harcourt, USA.)

[3] S. Hossenfelder, (2018). *Lost in Math: How Beauty Leads Physics Astray.* (Basic Books, USA,)

[4] A. Unzicker, S. Jones, (2013). *Bankrupting Physics: How Today's Top Scientists are Gambling Away Their Credibility*. (St. Martin's Press, USA.).

[5] P. Woit, (2006). *Not Even Wrong: The Failure of String Theory & the Continuing Challenge to Unify the Laws of Physics*. (Basic Books, USA.)

[6] R. Penrose, (2004). *The Road to Reality: A Complete Guide to the Laws of the Universe*. (London: Vintage Books.)

[7] R. Dawid, (2009). On the conflicting assessments of the current status of string theory. Philosophy of Science 76, 5.

[8] 3:AM magazine interview with Dawid http://www.3ammagazine.com/3am/string-theory-and-post-empiricism/

[9] G. Ellis, J. Silk, (2014). Scientific method: Defend the integrity of physics. *Nature 516.*

[10] Backreaction interview with Hossenfelder (2014),

http://backreaction.blogspot.com/2014/07/post-empirical-science-is-oxymoron.html

[11] D. Merritt, (2017). Cosmology and convention. Studies in History and Philosophy of *Modern Physics*, 57 1.

[12] P. Steinardt, (2015). Big Bang blunder bursts the multiverse bubble. *Nature 510, 9.*

[13] F. Wilczek, (2018). Has elegance betrayed physics? *Physics Today 71 57,*

https://doi.org/10.1063/PT.3.4022

[14] J.C. Pati, A. Salam, (1974). *Phys. Rev.* **D10,** 275.
[15] See for example H. Terazawa, K. Akama, (1980). *Phys. Lett.* **B96,** 276 and references therein.
[16] H. Harari, (1979). *Phys. Lett.* **B86**, 83.
[17] M. Shupe, (1979). *Phys. Lett.* **B86**, 87.
[18] De Rham, C., Gabadadze, G. & Tolley, (2011). A.J. *Phys. Rev. Lett.* **106,** 231101.
[19] De Rham, C., Gabadadze, G., Heisenberg, L. & Pirtskhalava, (2011). D. *Phys. Rev.***D83,** 103516.
[20] David Camarena and Valerio Marra (2020). Local determination of the Hubble constant and the deceleration parameter. https://doi.org/10.1103/PhysRevResearch.2.013028

[21] See for example S. Schweber, (1994). *QED and the Men Who Made It,* (Princeton University Press,
[22] I. Aitchison, A. Hey, (1989). *Gauge Theories in Particle Physics, 2nd edition*, (Institute of Physics Publishing, Bristol.
[23] A. Rae, (1992). *Quantum Mechanics 3rd edition,* (Institute of Physics Publishing, Bristol,
[24] R. Feynman, (1964). *The Feynman Lectures on Physics.* Volume III. (Addison Wesley, Reading, Massachusetts.
[25] W. Greiner, B. Muller, (1995). *Gauge Theory of Weak Interactions,* 2nd edition. (Springer-Verlag, New York.
[26] M. Peskin, (1997). *Beyond the Standard Model.* SLAC [SLAC-PUB-7479].

[27] J. Maldacena (1998). The Large N Limit of Superconformal Field Theories and Supergravity arXiv:hep-th/971120

[28] M. Abraham, (1903). Prinzipien der Dynamik des Elektrons, *Ann. der Phys. 10*, 105 Die *Grundhypothesen der Elektrontheorie.* Phys. Z. 5, 576.

[29] H. A. Lorentz, (1916). *The theory of elect rons.* Leipzig: Tuebner

[30] H. Poincare, (1906). *Sur la dynamique de l'electron.* Rend. Circ.Matem. Palermo 21, 129.

[31] L. Susskind (1995) *The World as a Hologram.* Journal of Mathematical Physics *36 (11): 6377–6396.* arXiv:hep-th/9409089. Bibcode:1995JMP....36.6377S. doi:10.1063/1.531249. S2CID 17316840

[32] Giblin, Heymans, Asgari & the KiDS collaboration et al.: KiDS-1000 Shear Catalogues (2020) Weak gravitational lensing shear measurements.**[arxiv.org/2007.01845].**

[33] Reiss A.G., Casertano S., Yuan W., Macri L.M., Scolnic A. (2019). Large Megallanic Cloud Cepheid Standards Provide a 1% Foundation for the Determination of the Hubble Constant and Stronger Evidence for Physics Beyond the ΛCDM.
https://arxiv.org/abs/1903.07603v2

[34] D. Marolf and J. Polchinski. (2013). *Phys. Rev. Lett.* **111,** 171301

[35] A. Almheiri, D. Marolf, J. Polchinski, and J. Sully. (2013). *Journal of High Energy Physics.* **2013, No.** 2, 063

[36] K. Papadodimas and S. Raju. (2012). An infalling Observer in AdS/CFT arXiv:1211.6767

[37] Bousso, (2013). Frozen Vacuum arXiv:1308.3697

[38] R. Feynman, (1964). *The Feynman Lectures on Physics,* Chapter 28, Volume II. (Addison Wesley, Reading, Massachusetts.)